NOTICE

The quality of this microform is heavily dependent upon the quality of the original thesis submitted for microfilming. Every effort has been made to ensure the highest quality of reproduction possible.

If pages are missing, contact the university which granted the degree.

Some pages may have indistinct print especially if the original pages were typed with a poor typewriter ribbon or if the university sent us an inferior photocopy.

Reproduction in full or in part of this microform is governed by the Canadian Copyright Act, R.S.C. 1970, c. C-30, and subsequent amendments.

AVIS

La qualité de cette microforme dépend grandement de la qualité de la thèse soumise au microfilmage. Nous avons tout fait pour assurer une qualité supérieure de reproduction.

S'il manque des pages, veuillez communiquer avec l'université qui a conféré le grade.

La qualité d'impression de certaines pages peut laisser à désirer, surtout si les pages originales ont été dactylographiées à l'aide d'un ruban usé ou si l'université nous a fait parvenir une photocopie de qualité inférieure.

La reproduction, même partielle, de cette microforme est soumise à la Loi canadienne sur le droit d'auteur, SRC 1970, c. C-30, et ses amendements subséquents.

MINERALOGY AND GEOCHEMISTRY OF THE MURDOCK CREEK INTRUSION, KIRKLAND LAKE, ONTARIO.

STEPHEN MICHAEL ROWINS

Thesis submitted to
the School of Graduate Studies and Research
in partial fulfillment of the requirements for the M.Sc.
degree in Geology

Ottawa-Carleton Geoscience Centre and
Université d'Ottawa/University of Ottawa

ISBN 0-315-60058-6

UNIVERSITÉ D'OTTAWA
UNIVERSITY OF OTTAWA

ABSTRACT

The Murdock Creek intrusion, immediately southwest of Kirkland Lake, Ontario, in the southern part of the Abitibi belt, is a member of a suite of late Archean (≈ 2680 Ma) syenitic intrusions located within and adjacent to the Kirkland Lake-Larder Lake fault zone (KLF), which host virtually all of the gold mineralization in the Kirkland Lake camp. It intrudes komatiitic meta-basalts of the Larder Lake Group, and is composed of six plutonic units which define a continuous compositional spectrum (SiO_2≈ 42-59 wt.%). An early crystallizing mafic margin consisting of clinopyroxenite, meladiorite, melamonzodiorite, and melasyenite encloses an extensive felsic core of alkali-feldspar syenite. A coeval hornblendite unit with lamprophyric affinities, intrudes throughout the pluton and most closely approximates the mantle-derived liquids which differentiated to produce the suite of syenitic intrusions and possibly potassic alkaline extrusive rocks of the Timiskaming Group. Clinopyroxene and biotite in this wide range of rock types have consistently low Fe/(Fe+Mg) and high $Fe^{3+}/(Fe^{2+}+Fe^{3+})$ ratios indicating a deficiency of Fe^{2+} in the magma during crystallization. Together with the presence of abundant, early-formed magnetite and titanite, this is interpreted to result from an intrinsically high magmatic oxygen fugacity (f_{O_2}), which remained constant during pluton evolution ($f_{O_2} \approx 10^{-12}$ bars). The intrinsically oxidized nature of the pluton suggests a genetic link with gold mineralization in the Kirkland Lake camp, because hydrothermal fluids which carried

gold also had unusually high f_{O_2}.

Major and trace element variation over the range of rock types support the mineralogical, petrographic, and field evidence for fractional crystallization as the dominant process controlling magma evolution, with incompatible elements (LILE's and LREE's) and the ratios K/Rb, La/Yb increasing (from the mafic marginal rocks to the felsic core), compatible elements (Sc, V, Cr, Co, Ni) and Ca/Y decreasing, and coherent ratios such as Th/U, Zr/Hf, Cr/Ni, and the standard LILE ratios K/Sr, K/Ba, Rb/Sr, Rb/Ba showing relatively little change. Enhanced K_2O, LILE, and LREE contents, and depletions in Ti-group elements (Nb, Ta, Ti) are notable geochemical characteristics of all units.

A model for pluton petrogenesis begins with partial melting of metasomatically LILE- and LREE-enriched upper mantle, the fusion initiated by mantle upwelling via lithosphere extension along the KLF. This lead to a pulse of potassic mafic alkaline magma which, utilizing the KLF as a magmatic conduit, differentiated at depth and during ascent to mid-crustal levels. Upon final emplacement, the evolved rock compositions were generated principally by <u>in situ</u> crystal fractionation of clinopyroxene, biotite, plagioclase, and K-feldspar.

SOMMAIRE

L'intrusion Murdock Creek, située immédiatement au sud-ouest de Kirkland Lake, Ontario, dans le sud de la ceinture de l'Abitibi, fait partie d'une suite d'intrusions syénitiques tardi-archéennes mises en place à l'intérieur, ou tout près de la zone de faille Kirkland Lake-Larder Lake. Cette zone de faille encaisse la quasi-totalité de toute la minéralisation aurifère de la région minière de Kirkland Lake. L'intrusion recoupe les métabasaltes komatiiques du Groupe de Larder Lake et est composée de six unités plutoniques définissant une suite compositionelle continue ($SiO_2 \approx$ 42 à 59 %pds). La cristallisation de l'intrusion fut amorcée par une bordure mafique composée de clinopyroxénite, méladiorite, mélamonzodiorite et mélasyénite autour d'un centre de syénite à feldspath alcalin. Un unité contemporaine de hornblendite de caractère lamprophyrique recoupe l'intrusion et représente le mieux les liquides mantéliques desquels sont dérivés ces syénites et possiblement les laves potassiques alcalines du Groupe Timiskaming avoisinant. Tous les clinopyroxènes et les biotites de ces roches ont des rapports Fe/(Fe+Mg) bas et des valeurs $Fe^{3+}/(Fe^{2+}+Fe^{3+})$ élevées, indiquant une déficience en Fe^{2+} durant la cristallisation de ces magmas. Ce chimisme ainsi que l'abondance de magnétite et de titanite primaires sont les résultats d'une haute fugacité d'oxygène (fO_2) dans le magma qui fut aussi maintenue constante pendant l'évolution de l'intrusion ($fO_2 \approx 10^{-22}$ bars). Le caractère intrinsèquement oxydé de ce pluton suggère un lien génétique avec

la minéralisation aurifère de la région car les fluides hydrothermaux transporteurs de l'or avaient, eux-aussi, une fugacité d'oxygène très élevée.

Les variations des éléments majeurs et traces en travers les unités corroborent les indications minéralogiques, pétrographiques et de terrain en faveur d'une cristallisation fractionnée. Ainsi on observe de la bordure mafique au centre felsique, un accroissement des éléments incompatibles (éléments lithophiles à grand rayon et terres rares légères), des rapports K/Rb et La/Yb, une décroissance des éléments compatibles (Sc, V, Cr, Co, Ni) et du rapport Ca/Y. Les rapports cohérents tels que Th/U, Zr/Hf, Cr/Ni au encore K/Sr, K/Ba, Rb/Sr et Rb/Ba laissent entrevoir peut de changement. L'enrichissement en éléments lithophiles de grand rayon et en terres rares légères ainsi que l'appauvrissement en Nb, Ta, et Ti sont des caractéristiques importantes de toute l'intrusion.

Le modèle pétrogénétique du pluton débute par l'anatexie d'un manteau supérieur métasomatisé et enrichi en éléments lithophiles de grand rayon et en terres rares légères, suivit d'un soulèvement mantélique et d'une extension lithosphérique le long de la faille Kirkland Lake-Larder Lake. Ceci donne lieu à des liquides mafiques potassiques et alcalins qui fûrent différentiés lors de leur ascension le long de la zone de faille. Lors de l'emplacement final de ces liquides mafiques, à un niveau moyen, les compositions observées fûrent obtenues principalement par une cristallisation fractionnée <u>in situ</u> de clinopyroxène, biotite, plagioclase et feldspath alcalin.

ACKNOWLEDGEMENTS

This study has benefited from the interest and support of a number of people.

Drs. Eion Cameron and André Lalonde deserve high praise in their capacity as thesis advisors. Their enthusiasm for the project, and willingness to let this student pursue his own particular interests were invaluable. I am especially grateful for their encouragement in writing this thesis in its present publishable format.

Drs. Keiko Hattori (University of Ottawa) and Bob Garrett (Geological Survey of Canada) are thanked for reviewing Paper 1.

Dr. Gerry Czamanske (United States Geological Survey, Menlo Park) is warmly thanked for a careful review of Paper 2.

Dr. N.M.S. Rock (University of Western Australia) provided valuable comment on the nature of the hornblendite-lampropyhre association discussed in Paper 3.

R. Hartree (University of Ottawa) and members of the Geochemistry Subdivision of the Geological Survey of Canada are thanked for carrying out much of the analytical work. The assistance of J. Loop in the University of Ottawa Geochemistry Laboratory is gratefully acknowledged. J-F. Tardif is thanked for the preparation of thin sections.

I would like to thank my fellow graduate students at the much-celebrated Ottawa-Carleton Geoscience Centre for their helpful discussions over the course of this study.

To my parents, I express my gratitude for their continued

encouragement throughout my academic endeavours.

I would like to thank Carolyn for her patience and understanding during the past two and half years.

This research was funded by an NSERC grant to Dr. Eion Cameron.

TABLE OF CONTENTS

TABLE OF CONTENTS - Continued

TABLE OF CONTENTS - continued

LIST OF FIGURES

LIST OF FIGURES - Continued

PAPER 3

LIST OF TABLES

LIST OF APPENDICES

GENERAL INTRODUCTION

Late Archean syenitic intrusions (≈ 2680 Ma) near Kirkland Lake, Ontario, in the southern part of the ≈ 2.7 Ga Abitibi belt show a strong spatial association with gold mineralization, a feature commonly observed in many Archean greenstone terranes. This has led to the suggestion of possible temporal and genetic links between felsic (syenitic) magmas and lode gold deposits (Colvine et al. 1984, 1988; Cameron and Carrigan 1987; Cameron and Hattori 1987). This hypothesis has, however, been hampered by a lack of evidence documenting the evolution of the felsic magmas from which the intrusions were derived. This study presents the results of a petrological investigation of one of these syenitic plutons, the Murdock Creek intrusion. Field work was primarily undertaken in the summers of 1987 and 1988 while employed by the Geological Survey of Canada under the supervision of Dr. E.M. Cameron.

The results of this study are presented in three complementary papers. The first paper describes the results of field work and petrographic studies carried out on the Murdock Creek intrusion in 1987-88. Field relations between the various plutonic units are discussed and petrographic evidence allows for preliminary estimates of some intensive parameters, including oxygen fugacity (f_{O_2}), during primary crystallization of the pluton.

The second paper documents the oxidation state of the Murdock Creek magma throughout its evolution, using the compositions of

primary and secondary ferromagnesian silicates. Results are then discussed in terms of possible genetic links between alkaline magma generation, CO_2 represented by carbonatization, and gold-bearing fluids.

The third paper presents whole-rock geochemical data which, in combination with earlier reported mineralogical and petrographic data, allows for the development of a petrogenetic model for the evolution of the Murdock Creek intrusion which attributes magma generation to low-degree partial melting of metasomatically-enriched upper mantle during lithosphere extension and mantle upwelling.

GEOLOGY OF THE ARCHEAN MURDOCK CREEK INTRUSION, KIRKLAND LAKE, ONTARIO

STEPHEN M. ROWINS, ANDRÉ E. LALONDE, AND EION M. CAMERON[1]

Ottawa-Carleton Geoscience Centre, Department of Geology, University of Ottawa, Ottawa, Ontario, K1N 6N5, Canada.

[1]Geological Survey of Canada, Ottawa, Ontario, K1A OE8, Canada, and Ottawa-Carleton Geoscience Centre, Department of Geology, University of Ottawa, Ottawa, Ontario, K1N 6N5, Canada.

Published in Current Research, Part C, Geological Survey of Canada, Paper 89-1C, p. 313-323, 1989.

ABSTRACT

The Murdock Creek intrusion, immediately southwest of Kirkland Lake, Ontario, in the Abitibi belt, is a composite syenitic pluton, of presumed late Archean age, consisting of six distinct units. It is a member of a suite of late-tectonic syenitic intrusions located within and adjacent to the Kirkland Lake-Larder Lake fault zone, which host virtually all of the gold mineralization in the Kirkland Lake camp. Field relationships between the various rock types and preliminary petrographic evidence indicate that the Murdock Creek intrusion evolved from a single pulse of relatively anhydrous and oxidized syenitic magma which crystallized and differentiated *in situ*. Recent studies have shown that the gold deposits in the Kirkland Lake mining camp were derived from oxidized hydrothermal fluids; one possibility is that such fluids evolved from oxidized felsic magmas. The oxidized nature of the Murdock Creek magma suggests that a genetic connection between magma and ore fluids should be further examined. The absence of either a distinct metamorphic contact aureole or a peripheral cataclastic zone produced during plutonic emplacement, suggest that intrusion occurred at mesozonal depths.

SOMMAIRE

L'intrusion Murdock Creek, sise immédiatement au sud-ouest de Kirkland Lake dans la ceinture Abitibi, est composée de six unités plutoniques distinctes, tous présumées d'âge archéenne. Elle est membre d'une suite d'intrusions syn- à tardi-tectoniques que l'on retrouve à l'intérieur ou en bordure de la zone faillée de Kirkland Lake-Larder Lake. Ces intrusions encaissent pratiquement tous les gîtes d'or du camp minier de Kirkland Lake. Les relations temporelles ainsi que la pétrographie indiquent que l'intrusion provient de la solidification et de la différenciation in situ d'une unique impulsion de magma anhydre et oxidé. Des études récentes démontrent que les gîtes d'or de la région de Kirkland Lake sont dérivés de fluides hydrothermaux oxidés; il est possible que ces fluides aient eux-mêmes évolués à partir de magmas felsiques oxidés. La nature oxidée du magma de Murdock Creek encourage une étude plus approfondie du lien génétique possible entre magma et fluides minéralisants. L'absence d'une auréole thermique distincte ou encore d'une zone cataclastique périphérique au pluton indiquent un emplacement dans la mésozone.

INTRODUCTION

The Murdock Creek intrusion is a composite syenitic pluton, of presumed late Archean age, immediately southwest of Kirkland Lake, Ontario, in the southern part of the ≈ 2.7 Ga Abitibi belt in the Superior Structural Province (fig. 1). The pluton is one of a suite of late-tectonic (Colvine et al. 1988) syenitic intrusions within and adjacent to the Kirkland Lake-Larder Lake fault zone. The intrusions host ≈ 97% of the gold mineralization in the camp (Hodgson 1986). A close spatial association between felsic intrusions and lode gold deposits in Archean greenstone terranes has long been recognized; possible temporal and genetic links between the two are the topics of considerable study (Hodgson 1983; Cameron and Carrigan 1987; Cameron and Hattori 1987; Colvine et al. 1988). The acceptance of any genetic model has, however, been hampered by a lack of evidence documenting the evolution of the felsic magmas from which the intrusions were derived. This is, in part, due to the extensive alteration around major gold deposits, which destroys the primary igneous minerals of the intrusion used to document magmatic evolution (e.g., Czamanske and Wones 1973). An investigation of the Murdock Creek intrusion commencing in 1987 showed that the western portion of the pluton is unaffected by the shearing, quartz-veining and carbonatization which have extensively modified the rest of the pluton. This provides an opportunity to estimate the intensive parameters (P, T, P_{H_2O}, P_{O_2}) and to evaluate the relative oxidation state of the magma(s). Cameron and Hattori (1987) found

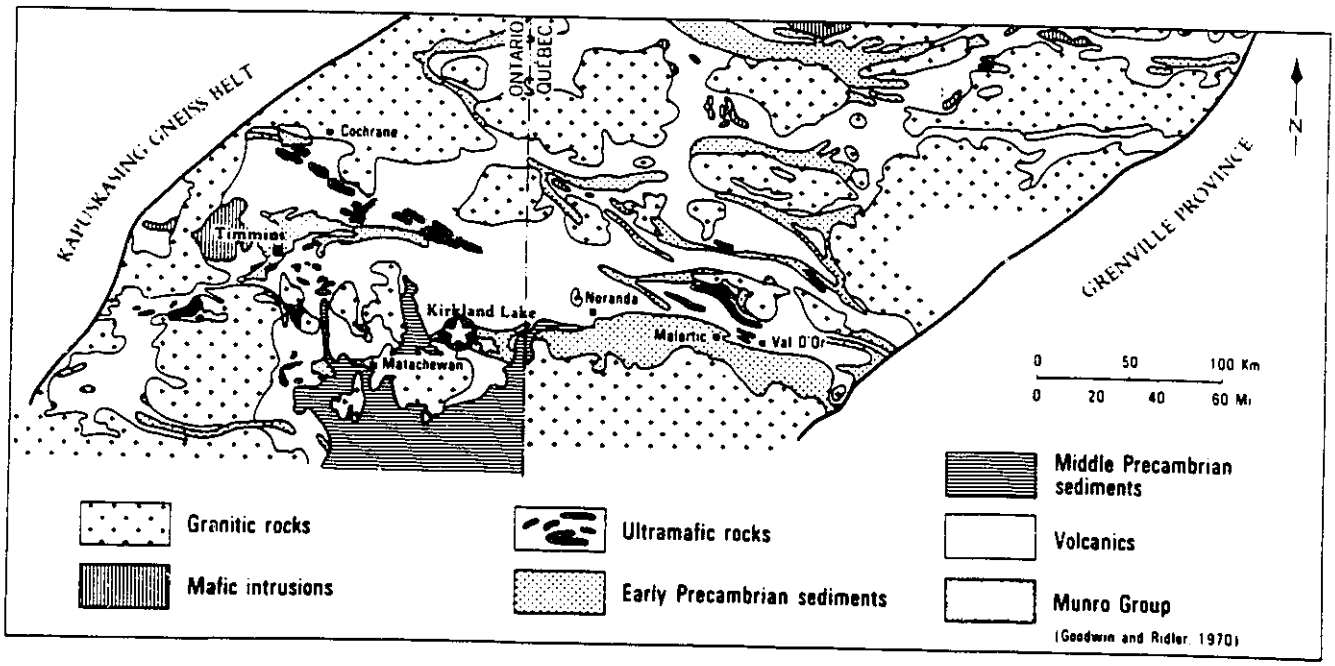

Fig. 1. Geology of the Abitibi belt (after Goodwin and Ridler 1970).

that sulphide minerals from the Kirkland Lake gold ores were depleted in ^{34}S, indicating isotopic fractionation in the ore fluids between sulphate and sulphide phases. This evidence for relatively oxidized fluids is supported by the occurrence of sulphate minerals and hematite with the gold mineralization. Cameron and Hattori (1987) suggested that such fluids could have been derived from an oxidized felsic magma. Documenting the oxidation state of the Murdock Creek magma is an initial step in testing this hypothesis. This paper describes the results of field work and preliminary petrographic studies carried out in 1987-88.

GEOLOGICAL SETTING

The volcanic, sedimentary, and related intrusive rocks of the Kirkland Lake district form the southern limb of an elongate, east-plunging synclinorium (fig. 2). Note that all rocks in the region have been metamorphosed, but the prefix "meta" is omitted in the text. The supracrustal rocks have been divided into two successions, representing two cycles of volcanism, referred to by Jensen (1980) as the Lower and Upper Supergroups. Each cycle was initiated by komatiitic volcanism, followed by tholeiitic, calc-alkaline, and finally alkalic. The two cycles are separated by sedimentary units comprising argillite, conglomerate, greywacke, chert, and iron formation. The dominant structural feature of the area is the major east-west trending Kirkland Lake-Larder Lake fault zone, a narrow sinuous belt approximately

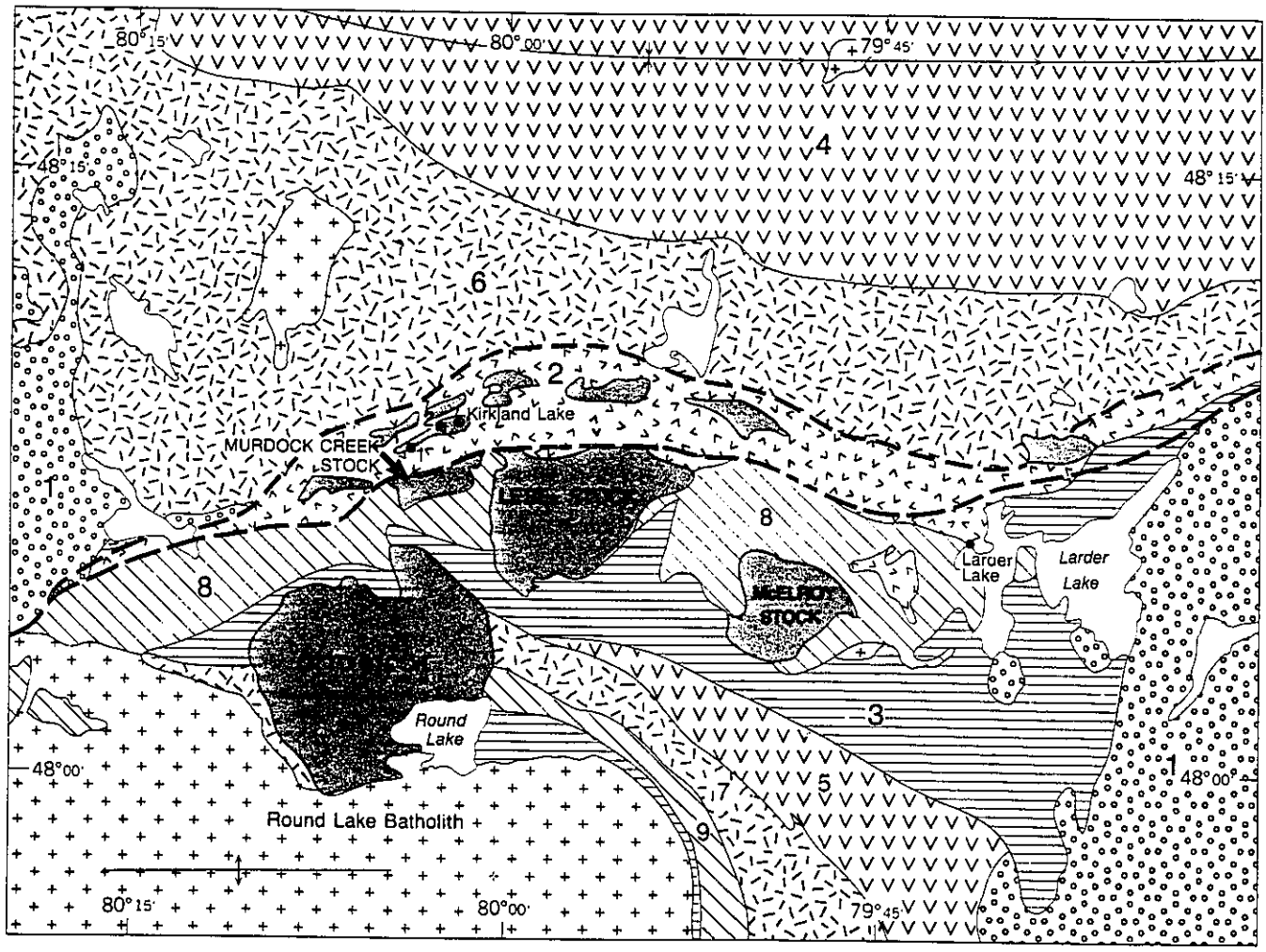

Fig. 2. Geology of the Kirkland Lake area (modified from Jensen 1978).

60 km long and up to 5 km wide, that extends from Matachewan in the west through Noranda towards Val d'Or in the east. Displacements along this fault and the Porcupine-Destor fault, major faults in the Abitibi belt, have been interpreted to be dominantly strike-slip (Hubert et al. 1984) or normal-slip (Dimroth et al. 1983). Subsequent reactivation of the existing structures, predominantly as reverse faults (Sibson et al. 1988), has resulted in a complicated structural zone in which gold mineralization and late felsic plutonism have been focused.

The Murdock Creek intrusion is emplaced within the mafic and ultramafic lava flows of the Larder Lake Group (Jensen 1980). To the north, the pluton is in fault-contact with the greywacke and tuffaceous conglomeratic sediments of the Timiskaming Group (Thomson 1950).

DESCRIPTION OF THE FIELD UNITS

All plutonic rocks described in this paper are classified according to the IUGS nomenclature (Streckeisen 1976). The following study is based primarily on rock units forming the western part of the intrusion where the primary mineralogy and igneous textures largely escaped deformation and alteration.

At the present level of erosion, the Murdock Creek intrusion is exposed as a crudely elliptical body, elongated in an east-west direction parallel to the Larder Lake-Kirkland Lake fault zone. A thin, heterogeneous mafic margin encloses an extensive alkali-feldspar syenite core. The intrusion is a

composite body consisting of six mappable units: 1) clinopyroxenite, 2) meladiorite, 3) hornblendite, 4) melamonzodiorite, 5) melasyenite, and 6) alkali-feldspar syenite (fig. 3). With the exception of hornblendite, these units typically exhibit regular and gradational contacts in the field; abrupt contacts sometimes observed result from the movement of unconsolidated magma intruding into earlier solidified rock units. Textural and mineralogical evidence given below suggest that the units are from a single pulse of syenitic magma which crystallized and differentiated in situ. The following is a description of the six units, beginning with the oldest.

1) Clinopyroxenite.-Clinopyroxenite is massive, homogeneous and medium-grained. It is dark greenish-black but may weather brownish-grey. It outcrops as a thin (10-300 m thick), discontinuous marginal unit at the western periphery of the intrusion, where it comes in contact with basalts of the Larder Lake Group and fluvial sediments of the Timiskaming Group. The clinopyroxenite is typically fresh, except near contacts with the country rock or where intruded by pink alkali-feldspar syenite dykes. In the field, a fine-grained textural variant of clinopyroxenite may be difficult to distinguish from basalt; however, close examination reveals that the basalts possess a metamorphic fabric defined by the segregation of felsic (plagioclase and quartz) and mafic (amphibole) minerals into discrete bands, 0.1 to 1 mm wide. This imparts a "streaked" appearance to the rock. In addition, the older intruded basalts

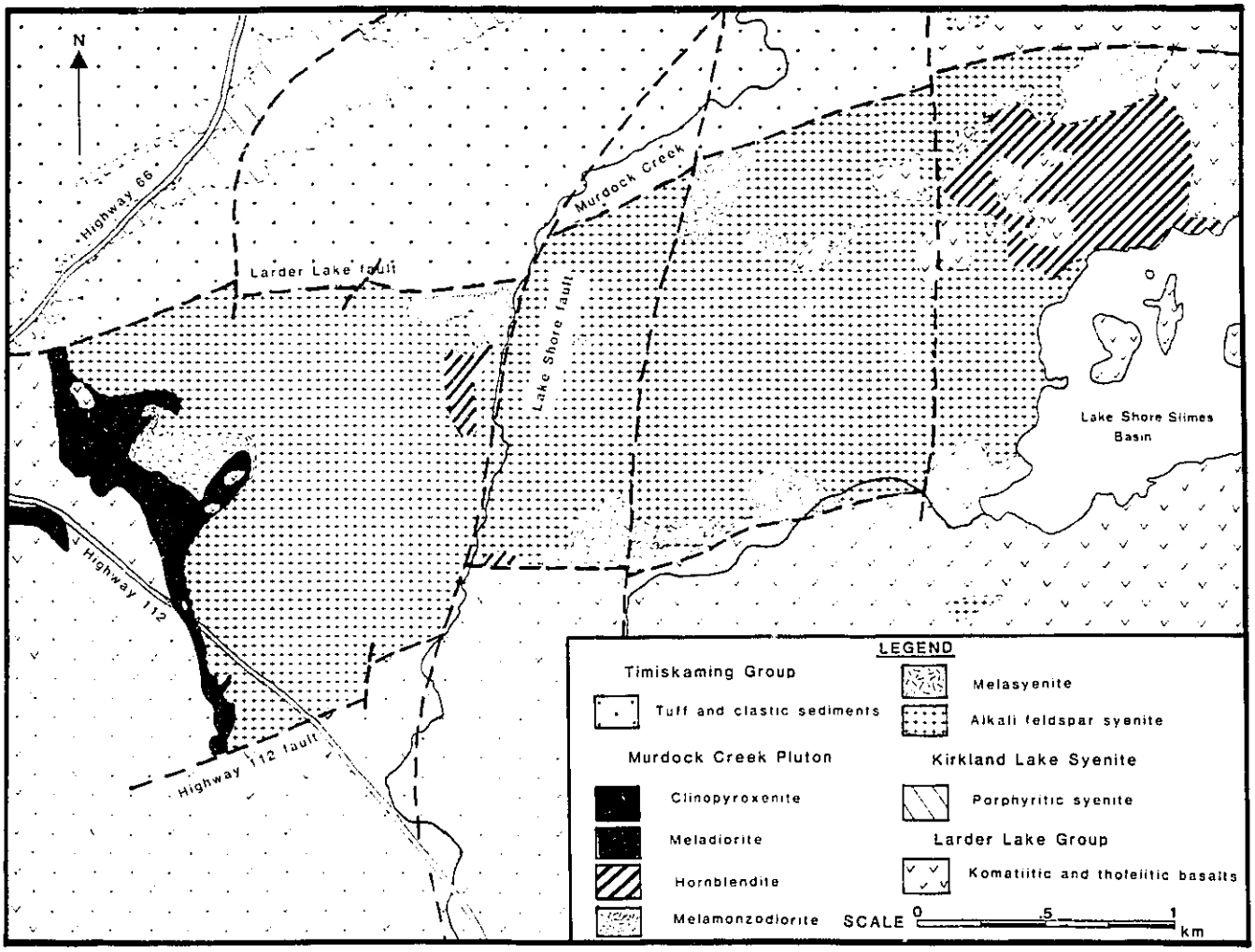

Fig. 3. Geology of the Murdock Creek intrusion (Thomson 1950 and this paper).

are usually more altered than the clinopyroxenite, with abundant epidote, calcite, and quartz veins.

2) Meladiorite.-Meladiorite is a dark green, medium-grained rock that may be either massive or foliated. It is a minor unit that occurs as a thin (0-50 m thick), discontinuous unit in the northwest mafic margin of the intrusion. The rock has a distinctive spotted appearance in the field produced by greenish-white plagioclase laths set in a dark green matrix of clinopyroxene and biotite. Meladiorite may be slightly porphyritic with plagioclase phenocrysts up to 1 cm in length. The preferential alignment of these plagioclase laths may yield a weak to moderate primary foliation, however the rock's texture is usually massive.

3) Hornblendite.-Hornblendite is a texturally heterogeneous rock recognized by its greenish-black colour, coarse euhedral hornblende crystals (0.5-10 mm across) and rough, knobby-weathered surface (fig. 4). Considerable variation in grain size occurs, with medium- and coarse-grained variants in the same outcrop. Hornblendite intrudes sporadically throughout the mafic margin, except in the northeastern extremity of the intrusion where it forms an extensive (500-700 m) peripheral body. Pink alkali-feldspar syenite dykes and xenoliths of basalt are common.

4) Melamonzodiorite.-Melamonzodiorite is a minor unit, transitional between meladiorite and melasyenite. This unit is quite heterogeneous varying from fine- to medium-grained, and

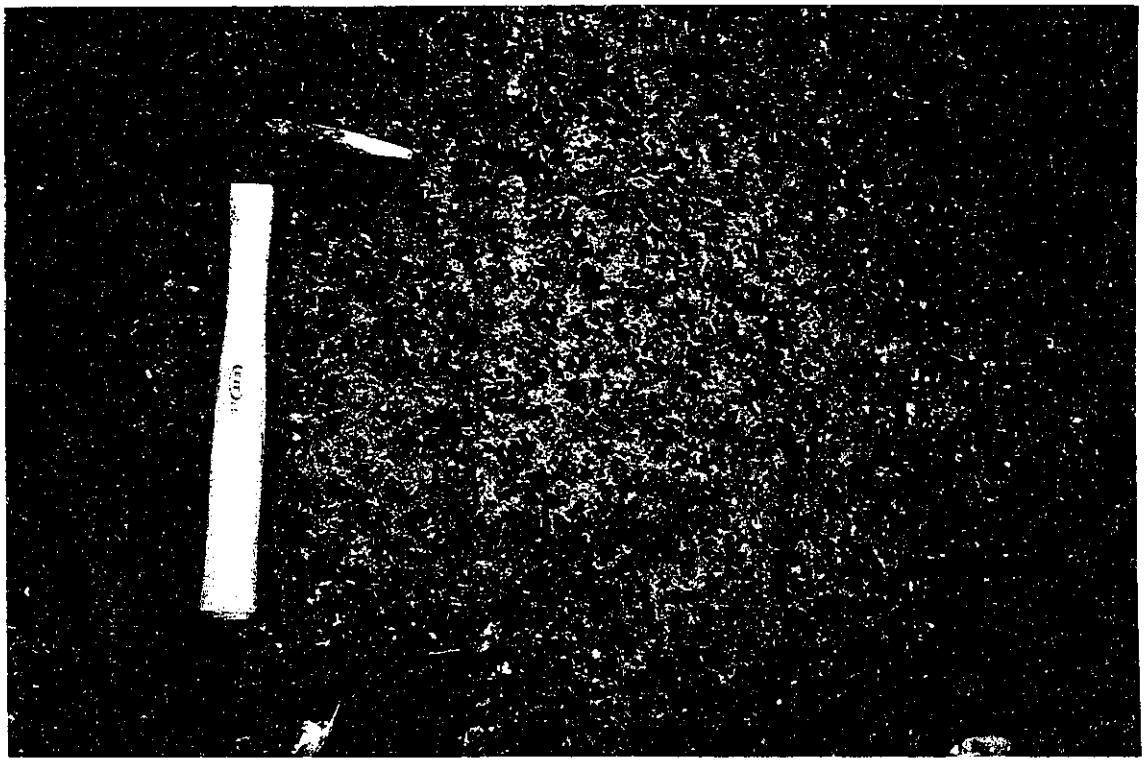

Fig. 4. Rough, knobby-weathering surface of hornblendite.

Fig. 5. Resistant late dykes of pegmatitic alkali-feldspar syenite in medium-grained alkali-feldspar syenite.

from syenitic to clinopyroxene-rich, over tens of centimeters. Melamonzodiorite is massive and greyish-green when fresh, but becomes light brownish-grey upon weathering. Variable proportions of pale yellowish-green perthite and plagioclase irregularly distributed throughout a dark greenish-black matrix of clinopyroxene and biotite, results in a mottled appearance. Pink alkali-feldspar syenite dykes intrude the melamonzodiorite in the northwestern part of the intrusion.

5) Melasyenite.-Melasyenite is a transitional unit which becomes increasingly leucocratic towards the core of the intrusion, away from the mafic margin. The rock is medium-grained, massive to trachytic, with pale orange-pink perthite crystals set in a slightly finer-grained matrix of dark green clinopyroxene, biotite and occasional secondary amphibole. Mafic varieties can appear slightly porphyritic with coarse subhedral perthite laths contrasting with a medium-grained mafic groundmass, imparting a spotted appearance similar to that exhibited by the meladiorite. The coarse-grained perthite crystals (10-15 mm across) commonly exhibit colour zoning in which a pink core is enclosed by a greyish-white rim. Plagioclase crystals are smaller (1-4 mm across) and possess a milky-white luster. As the rock becomes more leucocratic its textures and mineral distributions become increasingly homogeneous, the spotted appearance giving way to a more evenly coloured pink syenite. Based on the highly mafic composition of this unit (≈ 40-50 vol.% mafic minerals) with respect to the alkali-feldspar

syenite (≈ 10-20 vol.%), the melasyenite is interpreted to be the last mafic unit to crystallize. This is consistent with its location along the interior contact of the mafic margin with the extensive alkali-feldspar syenite core.

6) Alkali-feldspar syenite.-Reddish-pink alkali-feldspar syenite is the most extensive rock unit of the pluton. It occupies the central core of the intrusion. The unit is heterogeneous, medium- to coarse-grained, massive or well-foliated, in which case the foliation is defined by the parallel alignment of reddish perthite laths and dark green, columnar mafic minerals (predominantly clinopyroxene). This trachytic alignment is generally concordant with the internal contacts between the various plutonic units, however, it is locally discordant. The most intense red colouration of the feldspars coincides with the most strongly altered mafic silicates, both adjacent to faults and small shear zones within the intrusion. A coarse-grained variant with pinkish-grey, subhedral perthite crystals ranging up to 3 cm in length crops out in the west-central part of the intrusion as small irregular bodies, tens of metres across. This coarse textural variant grades subtly over several metres back into the much more common, medium-grained alkali-feldspar syenite.

FIELD RELATIONSHIPS

The Murdock Creek intrusion may be subdivided into two separate domains on the basis of degree of alteration and

deformation. West of the north-trending Lake Shore fault (Thomson 1950), syenitic units are fresh with only minor shearing and attendant alteration. East of this fault, the rock is intensely sheared and altered (fig. 3). Features distinctive of deformation and the attendant flow of hydrothermal fluids are areas of low relief, such as along stream beds (i.e., Lake Shore fault, Highway 112 fault); sheared and carbonated rock; silicification and resultant quartz-veining; chloritization and pyritization of mafic minerals; intense reddening of the feldspars; and the development of mylonitic or cataclastic rock textures.

Dykes and cognate inclusions are distributed throughout the intrusion, with an anomalous concentration of basaltic xenoliths in the northeastern corner of the pluton. These large (20-200 m diameter) basaltic xenoliths are possibly roof pendants. Late, fine- to medium-grained alkali-feldspar syenite dykes frequently cut both the crystallized mafic margin and its enclosed basaltic xenoliths without any preferred orientation. Basaltic xenoliths not contained in the mafic margin but in the younger alkali-feldspar syenite core, are also intruded by pink alkali-feldspar syenite dykes which have been derived directly from the enclosing syenitic melt. Small angular xenoliths of the intruded rock frequently occur within these dykes.

Dykes of bright red, pegmatitic alkali-feldspar syenite (1-30 cm wide) occurring either singly or together in small swarms intrude medium-grained alkali-feldspar syenite. These coarse leucocratic pegmatites weather-out as resistant ridges against

the finer-grained, less resistant, alkali-feldspar syenite (fig. 5). These late pegmatite dykes are also frequently associated with small shear zones in the intrusion.

Along the western edge of the intrusion, the contact between the clinopyroxenite and the Larder Lake basalts consists of a heterogeneous 200 m wide zone of intermingled altered clinopyroxenite and basalt. Numerous lime-green epidote veins and pale pink calcite veins with euhedral green amphibole needles (2-15 mm long) occur throughout this zone. Dark lime-green epidote pods with anastomosing alteration selvages, found within this zone, may give the appearance of pillow basalts, however, this feature is not primary but results from alteration. Late, quartz-bearing, whitish-grey felsic dykes intrude this heterogeneous contact zone. These dykes are not related to the syenitic magma of the Murdock Creek intrusion, since primary quartz is absent in rock units forming the intrusion. However, small salmon-pink coloured alkali-feldspar syenite dykes, distinctly different from the quartz-bearing variety do appear directly equivalent to the Murdock Creek plutonic unit. Since these two dyke varieties are not exposed together, their relative ages are not known.

PETROGRAPHY OF THE UNITS

Clinopyroxenite.-This fine- to medium-grained ultramafic unit consists almost entirely of pale green, moderately pleochroic diopsidic pyroxene (as determined by preliminary microprobe

analysis), with subordinate amounts of biotite and secondary amphibole. Euhedral to subhedral pyroxene crystals (0.3 mm to 3 mm in length) produce a cumulate texture, although gravitational crystal settling (Irvine 1982) is not implied. Typical inclusions in clinopyroxene include apatite, zircon, titanite, and opaque oxide and sulphide minerals. A notable feature in some pyroxene crystals is the presence of tiny acicular inclusions encircling the crystal core (fig. 6). These "rods" or "needles" are ≈ 0.01 mm long and are dark brownish-black at high magnification. Similar acicular inclusions have been noted in amphibole by Gorbatschev (1960) and have been interpreted as possible "exsolution" needles of titanite.

Uralitization of pyroxene is widespread and highly pleochroic greenish-brown hastingsitic amphibole occurs as irregular patches throughout primary pyroxene. Fibrous, pale bluish-green and faintly pleochroic actinolite replaces both primary pyroxene and secondary amphibole, beginning along crystal margins and proceeding inwards along fractures and cleavage planes. Both varieties of amphibole are deuteric. Subhedral, brown biotite flakes are commonly interstitial between the larger pyroxene crystals and also in irregular aggregate clusters with magnetite, apatite, and titanite. The titanite may occur as discrete subhedral wedges or as an exsolution corona around magnetite, the latter being the product of sphenitization, commonly attributed to subsolidus oxidation (Carmichael and Nicholls 1967).

Plagioclase, along with biotite, is interstitial to the

Fig. 6. Acicular needles (titanite ?) encircling the core of a clinopyroxene crystal, which also contains biotite inclusions (B).

Fig. 7. Crystals of hornblende (H) with mutually interfering grain boundaries producing a cumulate texture. Intercumulus groundmass consists of saussuritized plagioclase (P), clinopyroxene (C), and biotite (B).

pyroxene. Usually it is intensely saussuritized and sericitized, though faint albite twinning may still be discernable. Minor secondary phases include epidote, calcite, and quartz. Primary accessories include zircon, pyrite, and chalcopyrite. In this rock, pyroxene crystallized first followed by the primary accessory phases, biotite, and plagioclase.

Meladiorite.-Mineralogically and texturally, meladiorite is very similar to the marginal clinopyroxenite unit, except that plagioclase is now a significant phase (colour index (CI) after Streckeisen (1976) = 55±15). Pale green, unzoned diopsidic pyroxene is the dominant mafic silicate; primary brown biotite and secondary amphibole are minor constituents. Pyroxene grains are equant and subhedral, ranging from 0.5 to 5 mm in diameter; actinolitic alteration along crystal faces is common. Tiny exsolution needles of titanite (?) similar to those in pyroxene from the clinopyroxenite unit also occur in meladiorite pyroxene. Unzoned plagioclase (An_{30-34}) laths, 0.7 to 8 mm in length, are typically altered to sericite, calcite, and epidote. In some foliated variants, these aligned laths are weaved, along with subhedral biotite, into foliation bands which wrap around and partially replace pyroxene, indicating a period of post-crystalline flattening.

Opaque minerals (predominantly magnetite) may account for up to 2% of the rock. Magnetite and apatite occur together in the foliated biotite bands. Minor sulphide phases are present and include chalcopyrite, bornite and covellite. These occur together

in small, rounded composite grains. Under reflected light, brass-yellow chalcopyrite forms sharp, straight criss-crossing exsolution lamellae in a purple bornite host, producing a distinctive basketweave exsolution texture (Ramdohr 1969). Along grain boundaries and fractures, both chalcopyrite and bornite are altered to blue covellite. Other minor phases in meladiorite include K-feldspar, calcite, epidote, and rutile. In the meladiorite unit, pyroxene, biotite, and plagioclase crystallized simultaneously. Rock texture is best described as hypidiomorphic-granular.

Hornblendite.-Hornblendite shows wide diversity in textures and mineral proportions. Hornblende constitutes 50-70% of the rock with subordinate diopsidic pyroxene and greenish-brown biotite. Equant, twinned, moderately pleochroic crystals of yellowish-green to greenish-brown hornblende (3-15 mm across) produce a cumulate texture, although once again, gravitational crystal settling is not necessarily implied (fig. 7). Common inclusions in hornblende include diopside, biotite, apatite, and magnetite. Faint optical zonation is present in some hornblende crystals, where pale green actinolitic hornblende is preferentially developed along grain margins. Colourless secondary tremolite may also replace hornblende. The intercumulus groundmass consists principally of saussuritized anhedral plagioclase (An_{10-15}) together with subhedral clinopyroxene, biotite, and magnetite. Anhedral K-feldspar displaying microcline grid-twinning is rare. Late alteration of the primary mafic

silicates to chlorite and calcite is minor. Notable accessory phases include titanite, zircon, rutile, pyrite, and chalcopyrite.

Melamonzodiorite.-Melamonzodiorite (CI = 50±10) is distinctive by variable proportions of feldspar minerals and a wide diversity of mineral textures. Coarse- to medium-grained plagioclase and perthite laths (0.4-6 mm long) are extensively saussuritized and sericitized. Ragged and sutured crystal margins are indicative of minor recrystallization, although specific foliation is absent. Mafic minerals tend to occur in lenticular clots (0.5-6 mm in long dimension) along with apatite and titanite. Pale green diopsidic pyroxene crystals (1-3 mm across) are frequently uralitized and altered to greenish-brown biotite. Uralite pseudomorphs after pyroxene may subsequently undergo patchy alteration to fibrous, pale bluish-green actinolite. Apatite is the most common inclusion in biotite.

Secondary titanite and rutile commonly occur as minute grains clustered around biotite and as late exsolution coronas mantling magnetite. Melamonzodiorite is a hypidiomorphic-granular rock.

Melasyenite.-The predominance of perthitic alkali-feldspar over plagioclase is the main distinguishing feature of melasyenite (CI = 40±10). In most other respects, the melasyenite resembles the melamonzodiorite unit. Perthite crystals are typically Carlsbad twinned, subrounded laths ranging from 0.5 to 8 mm in length; perthitic intergrowths are of the vein and bleb varieties. This wide range in perthite crystal size is believed

to have resulted from the movement of primary perthite laths in a viscous, partially crystallized syenitic magma or crystal-mush, producing substantial granulation of crystal edges. Sericitic alteration of perthite is widespread and strongest along fractures and cleavages. Plagioclase (An_{15-18}) is rare and usually saussuritized.

Diopsidic pyroxene, brown biotite, magnetite, and apatite tend to occur in mafic clots (1-8 mm across) interstitial to the larger perthite laths (fig. 8). Pyroxene is similar to that found in other units of the intrusion and may occasionally have inclusions of the tiny dark brownish-black "needles". Prominant accessory phases include titanite and zircon.

Alkali-feldspar syenite.-Alkali-feldspar syenite (CI = 20±15) consists principally of subhedral, perthitic feldspar crystals (75-90%) which vary from fine- to coarse-grained. Carlsbad twinning is common and exsolution intergrowths include vein, bleb, patch, and interlocking varieties. Turbidity in perthite is heterogeneously distributed, being most intense along thin fractures. In some instances, sodic domains are sufficiently coarse to permit identification of albite twinning, and are more turbid than the potassic domains which display the characteristic grid-twinning of microcline. In the trachytic-textured alkali-feldspar syenite, perthite grains have ragged crystal margins rimmed by a fine-grained mass of polygonal albite. Where granulation of perthite crystal margins is less severe, only recrystallized films of clear albite form on the crystal edges.

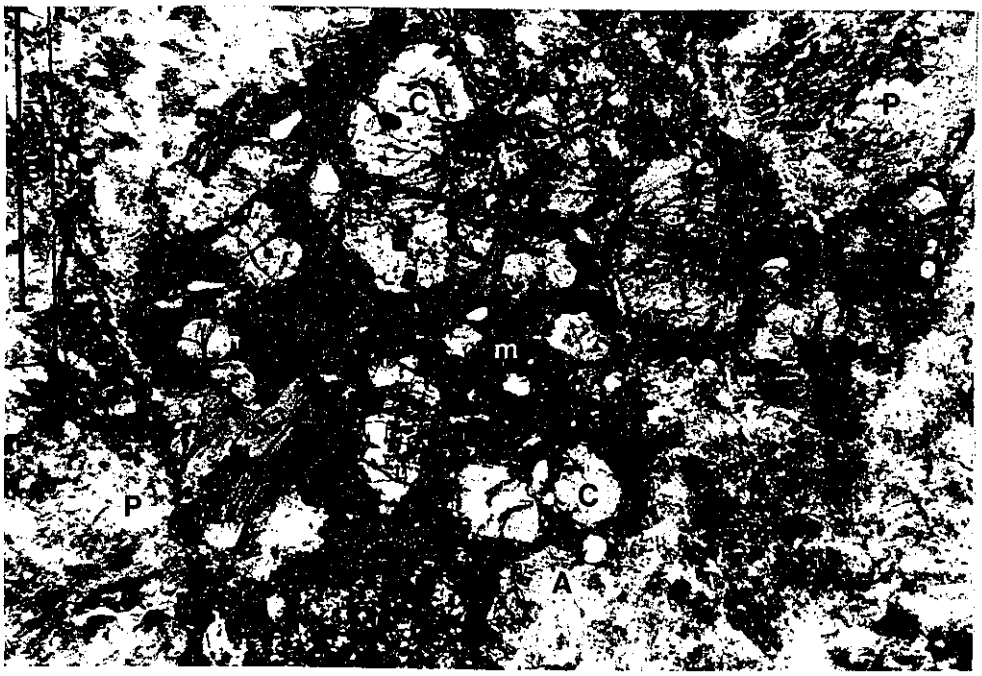

Fig. 8. Clinopyroxene (C), biotite (B), magnetite (M), and apatite (A) in mafic clots interstitial to perthitic feldspar (P).

Fig. 9. Zoned clinopyroxene with aegirine-augite rims (A) and diopside cores (DS), surrounded by turbid perthite.

Plagioclase is usually absent, but when present, occurs as small sericitized masses, interstitial to the larger perthite laths.

Equant, subhedral to euhedral, pyroxene crystals (0.3-10 mm in diameter) are slightly pleochroic and compositionally zoned, with bright green aegirine-augite rims and pale green diopside cores (fig. 9). Alteration of pyroxene is variable, with uralitic replacement most common. In more altered alkali-feldspar syenite, pale bluish-green actinolite may completely pseudomorph pre-existing pyroxene. Less commonly, there is complete pseudomorphous replacement of pyroxene by very pale green tremolite. Deuteric amphibole is itself frequently retrograded to greenish-brown biotite containing minute rutile crystals. Both primary and secondary biotite may display incipient alteration to chlorite.

Titanite is a prominent accessory in alkali-feldspar syenite and is of two distinct generations: 1) large (1-6 mm long) euhedral, wedge-shaped crystals are an early primary phase, randomly distributed throughout the unit (fig. 10), and 2) a much later generation forms coronas or partial coronas around anhedral magnetite grains, the result of subsolidus oxidation (sphenitization) of titaniferous magnetite. Other late alteration features include quartz-calcite and biotite-chlorite veinlets which cut and replace feldspar and pyroxene along fractures and cleavages. Small anhedral sulphide masses composed of pyrite, chalcopyrite, bornite and covellite are present in trace amounts. Chalcopyrite, bornite and covellite occur together and display

Fig. 10. Euhedral wedges of primary titanite in perthite.

Fig. 11. Quartz veins cutting intensely sheared and carbonated rock.

the same "basketweave" texture which was observed in the meladiorite unit. The overall rock texture is best termed hypidiomorphic-granular.

STRUCTURE

The northern periphery of the Murdock Creek intrusion is truncated by the east-trending Larder Lake fault. This dips to the south at ≈ 60° (Thomson 1950) and delineates the southern boundary of the Kirkland Lake-Larder Lake fault zone. Along the fault and extending approximately 100-200 m out on either side is a zone of intense carbonatization overprinting both the syenitic rock and sedimentary units of the Timiskaming Group. Calcite and dolomite are the principal carbonate minerals. Shearing and mylonitization may be so intense that recognition of the protolith is impossible. Later periods of brittle deformation lead to the development of quartz veins throughout the carbonated rock (fig. 11).

A previously unrecognized fault has been identified trending in an easterly direction along the southern edge of the pluton at the intrusive contact with basalts of the Larder Lake Group. This is a zone of weakness due the difference in mechanical competency between the two lithologies and would thus localize any faulting due to changes in the regional stress regime. The east-trending southern fault, informally referred to as the "Highway 112 fault", is a complex mylonitic and cataclastic brecciated zone outlined by green carbonatized (fuchsite-bearing) rocks. Several

north-trending post-ore faults, later than the east-west shear zones, may record significant lateral and vertical displacement (Thomson 1950).

Within the alkali-feldspar syenite core of the intrusion there are numerous small shear zones, several metres wide, associated with alkali-feldspar syenite pegmatite dykes. Shearing produced a cataclastic texture, where intensely reddened feldspars are fragmented and blue riebeckitic amphibole replace the earlier mafic silicates (fig. 12). The occurrence of the shears exclusively within the alkali-feldspar syenite, in association with alkali amphibole and pegmatite, suggests that they acted as pressure-release conduits along which late-magmatic, volatile-rich fluids were forcefully expelled during the final stages of magma solidification. In the alteration zones adjacent to the major faults, alkali-feldspar syenite commonly contains numerous thin and parallel (0.5-2 mm wide) cleavage surfaces or slip shears coated with dark green chlorite. These are interpreted as pressure-solution surfaces related to local stresses during faulting (fig. 13).

METAMORPHISM

Volcanic rocks in the Kirkland Lake area underwent regional burial metamorphism to prehnite-pumpellyite grade at pressures of about 1 kb according to Jolly (1974). Subsequent overprinting of the regional metamorphism is common where plutonic bodies have intruded into the supracrustal rocks generating contact aureoles

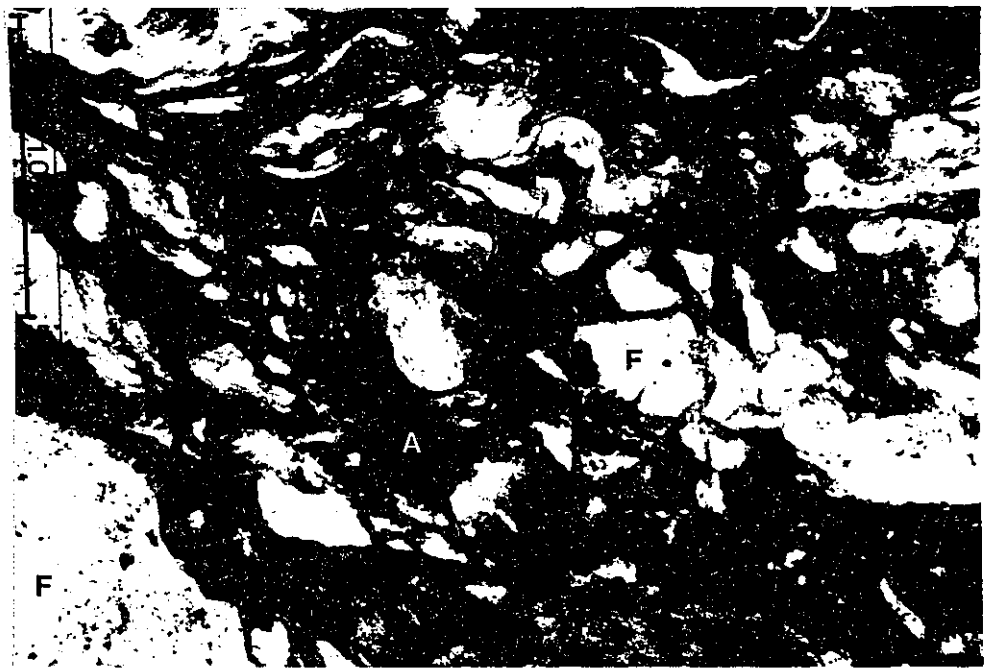

Fig. 12. Fragmented feldspar (F) and fibrous riebeckitic amphibole (A) define a cataclastic texture, produced during minor shearing and alteration of alkali-feldspar syenite.

Fig. 13. Alkali-feldspar syenite with thin, parallel cleavage surfaces or slip shears (S) coated with dark green chlorite.

of variable size and grade. However, unlike several other syenitic intrusions in the area (Otto stock, Lebel stock), the Murdock Creek intrusion has not generated a significant metamorphic aureole or a fine-grained chilled-margin.

EVIDENCE OF MAGMATIC OXIDATION IN THE MURDOCK CREEK INTRUSION

In the introduction it was briefly noted that Cameron and Hattori (1987) identified the ore fluids at Kirkland Lake as being relatively oxidized, since they contained a significant proportion of their total S content as sulphate. A number of smaller deposits in the Timmins-Kirkland Lake area were also shown to have been derived from oxidized fluids, as well as major deposits, such as Hemlo, Ontario, and Kalgoorlie, Australia. There are only two realistic sources for these fluids: oxidized felsic magmas (Cameron and Hattori 1987) and fluids derived during oxidative metamorphism of the lower crust (Cameron 1988). For the Kirkland Lake camp the close spatial relationship between syenitic intrusions and gold suggests that this association be tested. There are presently no data to precisely identify the temporal relationship between the intrusions and the gold. Since the veins cut the syenites, they clearly post-date the exposed portions of these intrusions. However, whether there was a sufficiently long interval to exclude the syenite magma as a source for the gold is unknown. To obtain more precise geochronological information is one of the objectives of this project.

Oxidized fluids of magmatic origin must have equilibrated with a similarly oxidized magma. Petrographic evidence from the Murdock Creek intrusion suggests that oxidizing conditions prevailed during crystallization of some of the rock units. Evidence of this includes, Mg-rich clinopyroxene, abundant primary titanite, and the predominance of magnetite over ilmenite. Alkali-feldspar which is intensely reddened by hematite reflects post-magmatic oxidation, possibly inherited from the late magmatic stage. Magnesium enrichment in pyroxene reflects oxidizing conditions during crystallization, when Fe, as Fe^{2+} and Fe^{3+} partitioned into magnetite. Under these conditions, Mg^{2+} substitutes for Fe^{2+} in pyroxene (Czamanske and Wones 1973). Verhoogen (1962) showed that primary titanite required relatively oxidizing conditions for its formation and Carmichael and Nicholls (1967) calculated limits in f_{O_2}-temperature space. Cameron and Carrigan (1987) noted the abundance of primary titanite in various felsic intrusions spatially associated with gold mineralization in the Abitibi belt. The dominance of magnetite over ilmenite has been used by Chappell and White (1974) and Ishihara (1977) to separate the more "oxidized" I-type (magnetite series) granitoids from the "reduced" S-type (ilmenite series). All rock types from the Murdock Creek intrusion contain magnetite but lack ilmenite, and thus broadly correspond to the oxidized I-type granitoids. Finally, the presence of turbid red feldspar in most of the units may indicate that oxidizing conditions were maintained throughout the crystallization of the

intrusion and continued into the post-magmatic stage, when late, oxidizing fluids produced the turbidity in the feldspars. The red colouration is due to the presence of finely divided hematite flakes lining the walls of fluid inclusions in the alkali-feldspar. This hematite results from the dissolution of nearby ferromagnesian minerals (Boone 1969).

These preliminary observations of magmatic oxidation will be followed by estimation of the oxygen fugacity during the different stages of magmatic crystallization.

SUMMARY

The continuous compositional spectrum shown by the units forming the Murdock Creek intrusion, along with the gradational nature of their contacts, indicate that the pluton formed from a single pulse of relatively anhydrous and oxidized syenitic magma which crystallized and differentiated in situ. Internal dykes related to the specific plutonic units and observed flow foliations suggest that movement of magma continued after the earlier units had solidified. The lack of miarolitic cavities and porphyritic textures suggest vesiculation of the melt did not occur. Furthermore, the absence of either a distinct contact aureole or a peripheral cataclastic zone produced during plutonic emplacement suggests that intrusion occurred at mesozonal depths. Late reactivations of the Larder Lake and Highway 112 faults has resulted in post-emplacement shearing and alteration along the northern and southern margins of the intrusion. The lack of

either primary quartz or feldpathoid minerals indicates that the magma(s) were just silica saturated. The minor exposure of the mafic margin of the intrusion indicates that the bulk of the magma was relatively felsic.

The crystallization sequence in the Murdock Creek intrusion is clinopyroxene, biotite, apatite, magnetite, titanite, plagioclase (andesine to oligoclase), and alkali-feldspar. An exception to this sequence occurs in hornblendite where igneous hornblende precedes clinopyroxene. Zircon is a notable accessory phase in the more felsic rock types. Amphibole (except in hornblendite), coronitic titanite, and some greenish-brown biotite are secondary reaction products around clinopyroxene and magnetite, related to deuteric effects rather than to later prograde metamorphism.

Petrographic evidence and preliminary electron microprobe analyses of the ferromagnesian silicates indicate that the plutonic units from the Murdock Creek intrusion crystallized under relatively oxidizing conditions. Turbid red feldspars reflect post-magmatic oxidation which may be inherited from the late magmatic stage.

Ongoing research includes a detailed study of the mineral chemistry and the whole rock geochemistry which characterizes the individual rock types. In addition, U-Pb zircon, titanite and rutile radiometric age determinations of the extensive alkali-feldspar syenite and an adjacent carbonated and sheared melasyenite hosting hydrothermal gold mineralization is underway

to establish the relationship between emplacement of the Murdock Creek intrusion and gold mineralization in the Kirkland Lake camp.

ACKNOWLEDGEMENTS

We are grateful to Mike Dyment and Jocelyn Kidston for pointing out several interesting field exposures in the Kirkland Lake area. Bob Garrett (Geological Survey of Canada) and Keiko Hattori (University of Ottawa) kindly reviewed the manuscript.

REFERENCES

Boone, G.M., 1969, Origin of clouded red feldspars: petrologic contrasts in a granitic porphyry intrusion: Amer. Jour. Sci., v. 267, p. 633-668.

Cameron, E.M., 1988, Archean gold: relation to granulite formation and redox zoning in the crust: Geology, v. 16, p. 109-112.

_____, and Carrigan, W.J., 1987, Oxygen fugacity of Archean felsic magmas: relationship to gold mineralization, in Current research. Part A: Geol. Surv. Can. Pap. 87-1A, p. 281-298.

_____, and Hattori, K., 1987, Archean gold mineralization and oxidized hydrothermal fluids: Econ. Geol., v. 82, p. 1177-1191.

Carmichael, I.S.E., and Nicholls, J., 1967, Iron-titanium oxides and oxygen fugacities in volcanic rocks: Jour. Geophys. Res., v. 72, p. 4665-4687.

Chappell, B.W., and White, A.J.R., 1974, Two contrasting granite types: Pacific Geology, v. 8, p. 173-174.

Colvine, A.C., Fyon, J.A., Heather, K.B., Marmont, S., Smith, P.M., and Troop, D.G., 1988, Archean lode gold deposits in Ontario: Ont. Geol. Surv. Misc. Pap. 139, 136 p.

Czamanske, G.K., and Wones, D.R., 1973, Oxidation during magmatic differentiation, Finnmarka complex, Oslo area, Norway; 2, The mafic silicates: Jour. Petrol., v. 14, p. 349-380.

Dimroth, E., Imreh, L., Goulet, N., and Rocheleau, M., 1983,

Evolution of the south-central segment of the Archean Abitibi belt, Quebec. Part II: Tectonic evolution and geomechanical model: Can. Jour. Earth Sci., v. 20, p. 1355-1373.

Goodwin, A.M., and Ridler, R.H., 1970, The Abitibi orogenic belt: Geol. Surv. Can. Pap. 70-40, p. 1-30.

Gorbatschev, R., 1960, On the alkali rocks of Almunge. A preliminary report on a new survey: Geol. Inst. Univ. Uppsala Bull., v. 39, p. 1-69.

Hodgson, C.J., 1983, Preliminary report on the Timmins-Kirkland Lake area gold deposits file: Ont. Geol. Surv. Open File Report 5467, 160 p.

_____ 1986, Place of gold ore formation in the geological development of the Abitibi greenstone belt, Ontario, Canada: Trans. Inst. Min. Metal. (Sec. B: Appl. Earth Sci.), v. 95, p. B183-B194.

Hubert, C., Trudel, P., and Gelinas, L., 1984, Archean wrench fault tectonics and structural evolution of the Blake River Group, Abitibi belt, Quebec: Can. Jour. Earth Sci., v. 21, p. 1024-1032.

Irvine, T.N., Terminology for layered intrusions: Jour. Petrol., v. 23, p. 127-162.

Ishihara, S., 1977, The magnetite-series and ilmenite-series granitic rocks: Mining Geol. (Japan), v. 267, p. 633-668.

Jensen, L.S., 1978, Archean komatiitic, tholeiitic, calc-alkalic and alkalic volcanic sequences in the Kirkland Lake area, in Currie, A.L., and Mackasey, W.O., eds., Toronto '78 field

trips guidebook: Geol. Assoc. Can., p. 327-359.

_____ 1980: Kirkland Lake-Larder Lake synoptic mapping projects, Districts of Cochrane and Timiskaming, in V.G. Milne et al., eds., Summary of field work: Ont. Geol. Surv. Misc. Pap. 96, p. 55-60.

Jolly, W.T., 1974, Regional metamorphic zonation as an aid in the study of Archean terrains: Abitibi regions, Ontario: Can. Mineral., v. 12, p. 499-508.

Philpotts, A.R., 1967, Origin of certain iron-titanium oxide and apatite rocks: Econ. Geol., v. 62, p. 303-315.

_____ 1981, A model for the generation of Massif-type anorthosites: Can. Mineral., v. 19, p. 233-253.

Ramdohr, P., 1969, The ore minerals and their intergrowths: London, Pergamon, 1207 p.

Sibson, R.H., Robert, F., and Poulson, K.H., 1988, High-angle reverse faults, fluid pressure cycling, and mesothermal gold-quartz deposits: Geology, v. 16, p. 551-555.

Streckeisen, A., 1976, To each plutonic rock its proper name: Earth Sci. Rev., v. 12, p. 1-33.

Thomson, J.E., 1950, Geology of Teck Township and the Kenogami Lake area, Kirkland Lake gold belt: Ont. Dept. Mines Ann. Rep. 1948, v. 57, pt. 5, p. 1-53.

Verhoogen, J., 1962, Distribution of titanium between silicates and oxides in igneous rocks: Amer. Jour. Sci., v. 260, p. 211-220.

MAGMATIC OXIDATION IN THE SYENITIC MURDOCK CREEK INTRUSION, KIRKLAND LAKE, ONTARIO: EVIDENCE FROM THE FERROMAGNESIAN SILICATES

STEPHEN M. ROWINS, ANDRÉ E. LALONDE, AND EION M. CAMERON[1]

Ottawa-Carleton Geoscience Centre, Department of Geology, University of Ottawa, Ottawa, Ontario, K1N 6N5, Canada.

[1]Geological Survey of Canada, Ottawa, Ontario, K1A 0E8, Canada, and Ottawa-Carleton Geoscience Centre, Department of Geology, University of Ottawa, Ottawa, Ontario, KIN 6N5, Canada.

Accepted for publication by The Journal of Geology, February, 1990.

ABSTRACT

The syenitic Murdock Creek intrusion, of late Archean age, lies within one of the major lode gold camps of the world, at Kirkland Lake. There is a strong spatial association between syenitic intrusions, gold mineralization, and carbonatization. Hydrothermal fluids that carried the gold had an unusually high oxygen fugacity (f_{O_2}). Notwithstanding a wide range in rock compositions within the intrusion, from clinopyroxenite to alkali-feldspar syenite, clinopyroxene and biotite have consistently low Fe/(Fe+Mg) and high $Fe^{3+}/(Fe^{2+}+Fe^{3+})$ ratios. These compositional features indicate a deficiency of Fe^{2+} in the magma during crystallization. Together with the presence of abundant, early-formed magnetite and titanite, this is interpreted to result from an intrinsically high magmatic f_{O_2} which remained constant during pluton evolution ($f_{O_2} \approx 10^{-12}$ bars). Mineral compositions, proportions of crystallizing mineral phases, and textural features indicate that the pluton formed from a single pulse of already evolved syenitic magma that fractionally crystallized in situ under low water pressure at mid-crustal depths. The intrinsically oxidized nature of the pluton implies an oxidized source region such as metasomatized upper mantle where partial melting occurred. CO_2-rich fluid or melt was the likely agent for metasomatism. Dissolution and transport of gold is favoured by high f_{O_2} in the fluid phase. The high f_{O_2} of the syenitic magma suggests a common genetic link between magma generation, CO_2 represented by carbonatization, and

gold-bearing fluids.

INTRODUCTION

The Murdock Creek intrusion is a composite syenitic pluton, near Kirkland Lake, Ontario, within the late Archean Abitibi belt of the Superior Structural Province (fig. 1). It is a member of a suite of late-tectonic syenitic intrusions emplaced at ≈ 2680 Ma (Marmont and Corfu 1988; Smith and Sutcliffe 1988), within and adjacent to the Kirkland Lake-Larder Lake fault zone (KLF). Syenitic intrusions within the KLF host virtually all gold mineralization at Kirkland Lake (Thomson et al. 1950). The camp is an example of the long recognized spatial association of felsic intrusions, gold mineralization, and shear zones in Archean greenstone terranes.

This study was primarily undertaken to document the oxidation state of the syenitic Murdock Creek magma throughout its evolution. Study of gold mineralization at Kirkland Lake (Cameron and Hattori 1987) suggests formation from hydrothermal fluids that were intrinsically oxidized. This is shown by the presence in the veins of sulfate minerals, hematite, and sulfide minerals strongly depleted in ^{34}S. The oxidized nature of the fluids helps constrain their source. Several recent studies of Archean gold mineralization have called upon fluids expelled during prograde metamorphism of greenstones at greenschist and amphibolite grade (Groves and Phillips 1987; Kerrich 1987, 1989). However, these fluids were unlikely to have been sufficiently oxidized, since they would have been in equilibrium with mafic volcanic rocks characterized by low $Fe^{3+}/(Fe^{2+} + Fe^{3+})$ and with graphite in the

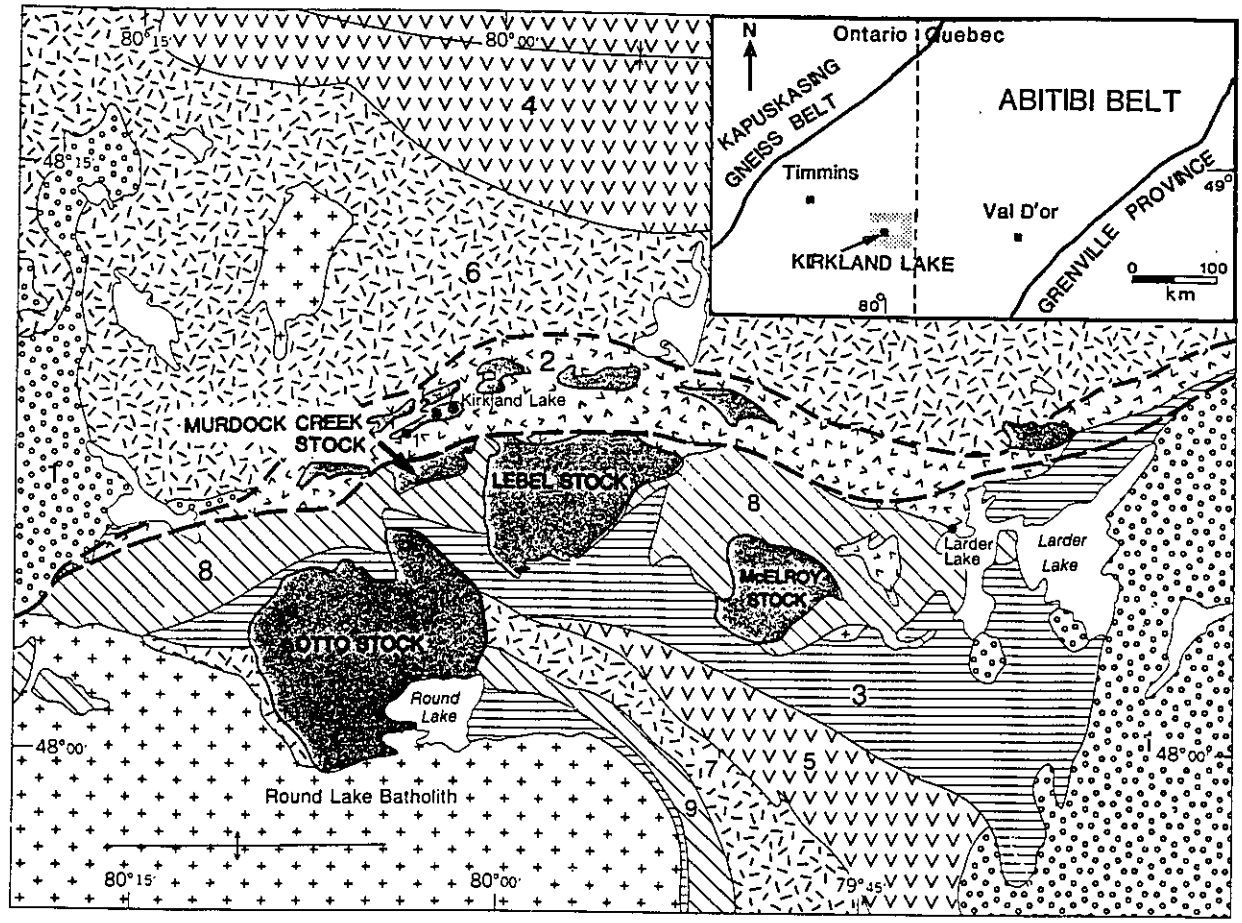

1. *COBALT GROUP*

Syenitic rocks

Trondhjemitic rocks

2. *TIMISKAMING GROUP*
Alkalic volcanic rocks and associated sedimentary rocks

3. *LARDER LAKE GROUP*
Intercycle sedimentary rocks, calc-alkalic tuffs, komatiitic volcanic flows, and ultramafic intrusive rocks

4. *BLAKE RIVER GROUP*
5. *SKEAD GROUP*
Calc-alkalic volcanic rocks

6. *KINOJEVIS GROUP*
7. *CATHARINE GROUP*
Tholeiitic volcanic rocks

8. *LARDER LAKE GROUP*
9. *WABEWAWA GROUP*
Komatiitic volcanic rocks

Kirkland Lake-Larder Lake Fault Zone
Anticline
Syncline
Macassa Mine 1
Lake Shore Mine 2

km
0 10

GSC

Fig. 1.-Geology of the Kirkland Lake area (modified from Jensen 1978).

sedimentary succession. A preliminary examination of syenites within the camp (Cameron and Carrigan 1987) showed that they were derived from oxidized magma and thus represent a possible source for the gold-bearing fluids.

The link between oxidation and gold is revealed by the chemistry of the metal. Its dissolution and transport is favoured in solutions with high f_{O_2}:

$Au^0 + O_2 + ligand \rightarrow Au^+ligand$ (soluble complex).

In this, dissolution of metallic gold, Au^0, requires oxidation (i.e., an electron donor) to Au^+, which is then bound to a ligand to form a soluble complex. Bisulfide is the most common ligand for gold in hydrothermal fluids. The dissolution of sulfide minerals from rocks to produce a bisulfide-rich fluid is also favoured in fluids with high f_{O_2}. Thus oxidized fluids are excellent carriers for gold because they support the reaction $Au^0 \rightarrow Au^+$ and because they dissolve the most common ligand for gold. Lode gold deposits of Archean age were almost invariably formed from CO_2-rich fluid. In the deep crust and mantle the highest f_{O_2}'s are attained by CO_2-rich fluids (Woermann and Rosenhauer 1985).

There are at least two possible reasons for the association between relatively oxidized alkaline magmas and gold. In the first, most simply, the fluids are derived at depth from the magma as CO_2 is released (Cameron and Hattori 1987). In the second, both the magmas and CO_2-rich fluids are released from the source regions. The CO_2-rich fluids stream upwards through

ductile shear zones, extracting gold from the shear zones, which can be highly permeable if deformation takes place under high differential stress. This second scenario has been investigated by Cameron (1988, 1989a) prompted by the work of Newton (1986), who showed that charnockites from south India that are believed to have formed during CO_2-streaming through the lower crust, equilibrated at high f_{O_2}.

These concepts linking oxidation and gold mineralization lack documentation on the nature and cause of oxidation in magmas that are spatially associated with ore. Syenitic rocks within the KLF were mostly altered by fluids moving along this major crustal fracture, hindering petrological study. The northern margin of the Murdock Creek intrusion is a fault-contact with the KLF. The western part of the intrusion has not been significantly altered by shear zone fluids and it was from this portion that the samples described here were collected. This is the first detailed study of the intrusion since it was mapped by Burrows and Hopkins (1923) and later by Thomson (1950). Outlines of the geology and structure of the pluton are given by Rowins et al. (1989a, 1989b).

GEOLOGICAL SETTING

The Abitibi belt is one of the largest and best preserved Archean greenstone terranes in the world, with gold production in excess of 137 million ounces (Hodgson and MacGeehan 1982). Rocks in the Kirkland Lake region mainly comprise a thick sequence of

komatiitic, tholeiitic, and calc-alkaline basalt, with lesser amounts of sedimentary rocks, belonging to the Larder Lake, Kinojevis, and Blake River Groups. These form the southern limb of an elongate, east-plunging synclinorium (fig. 1) metamorphosed to sub-greenschist and greenschist grade at low pressure (Jolly 1974). Zircon U-Pb ages of 2703±2 Ma have been obtained for calc-alkaline rocks in the upper part of this sequence (Nunes and Jensen 1980).

The outstanding structural feature of the district is the major east-trending Kirkland Lake-Larder Lake fault zone (KLF), a narrow sinuous belt approximately 60 km long and up to 5 km wide that forms the western part of a regional strike-slip fault, the Larder Lake-Cadillac fault (Hubert et al. 1984). The KLF is largely occupied by the Timiskaming Group: a thick sequence of weakly metamorphosed clastic sedimentary rocks, alkaline flows, and pyroclastic rocks unconformably overlying rocks of the Larder Lake and Kinojevis Groups. Syenitic plutons within the KLF intrude the Timiskaming sequence. Intrusion of the syenites preceded the introduction of gold by an unknown interval, since the gold-bearing structures cut the syenites. In addition to the spatial association between gold and syenite, there is a strong association with carbonatization. Indeed, carbonatization within the KLF is so extensive that some zones were earlier described as sedimentary carbonate. The southern boundary of the KLF brings the Timiskaming Group into fault contact with Larder Lake rocks, while the north boundary is mostly an unconformity of the

Timiskaming Group over earlier basalts. The Murdock Creek pluton is intruded into komatiitic basalts of the Larder Lake Group (Jensen and Langford 1985) immediately south of the KLF.

GENERAL GEOLOGY OF THE MURDOCK CREEK INTRUSION

The Murdock Creek intrusion is a crudely elliptical body, elongated in an east-west direction parallel to the KLF. Six plutonic units are defined using the IUGS classification scheme (Streckeisen 1976). A thin, early crystallizing mafic margin consists of (oldest to youngest) clinopyroxenite, meladiorite, melamonzodiorite, melasyenite and melanocratic alkali-feldspar syenite. This encloses an extensive felsic core of alkali-feldspar syenite (fig. 2). In figure 2, melanocratic alkali-feldspar syenite is not distinguished from normal alkali-feldspar syenite as the two units are intergradational. A cumulate-textured hornblendite unit outcrops sporadically throughout the pluton, except in the northeastern extremity of the intrusion where it forms an extensive (700 x 500 m) peripheral body. Because the hornblendite intrusions are cut by late alkali-feldspar syenite dykes, their emplacement is interpreted to be coeval with the intrusion and crystallization of the Murdock Creek pluton. With the exception of this hornblendite unit, all rock types exhibit gradational contacts in the field. These relationships, supported by earlier petrography (Rowins et al. 1989a) and by the mineralogical studies presented herein, confirm the hypothesis by Rowins et al. (1989a) that the

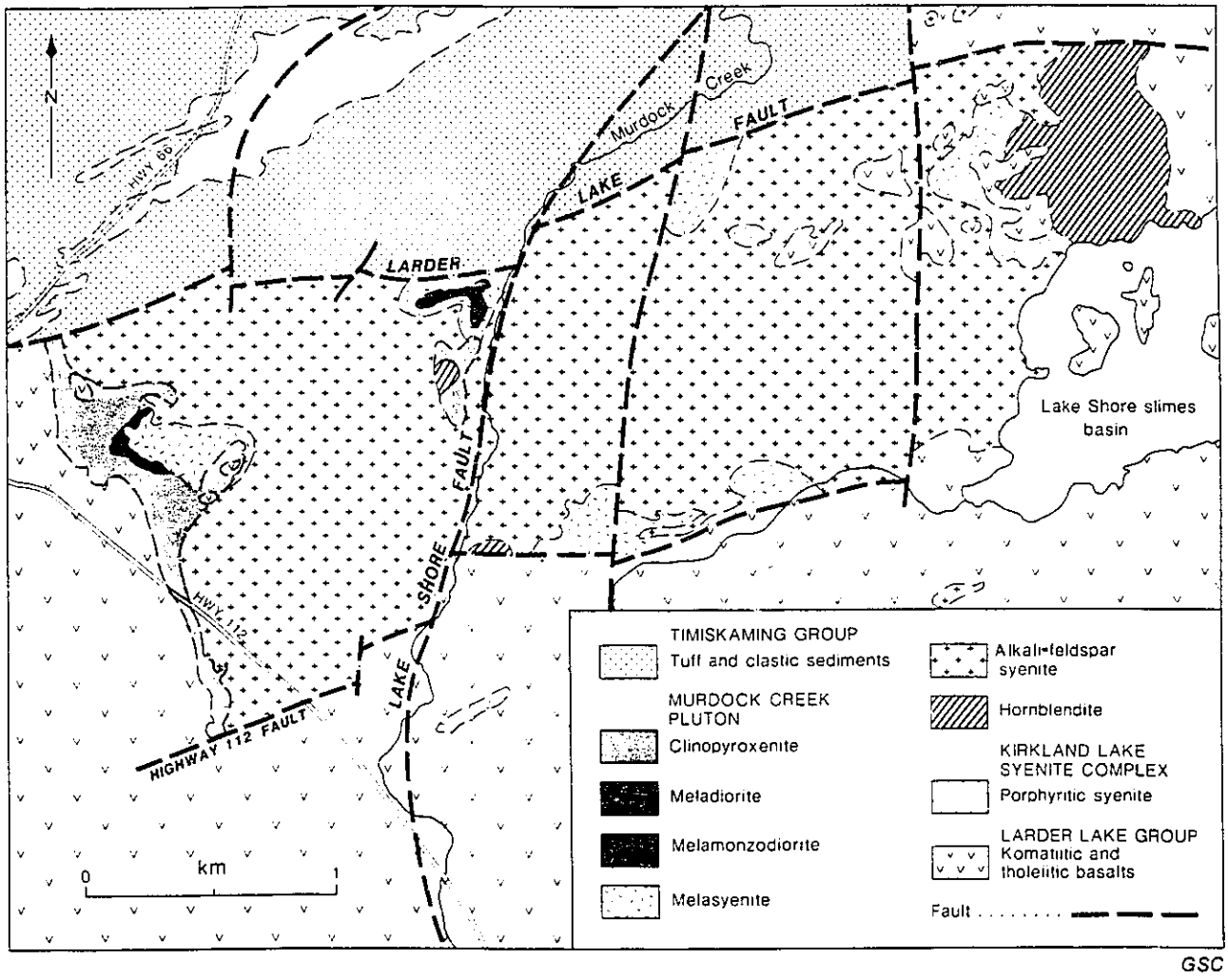

Fig. 2.-Geology of the Murdock Creek intrusion (Thomson 1950; Rowins et al. 1989a and this paper).

compositional variation exhibited by the pluton resulted from the differentiation, at depth, of a single pulse of mafic magma (probably potassic basalt). Differentiation is believed to have occurred at depth because the mafic cumulates expected to have formed from this process are scarce at the present erosional level. The less dense, felsic products of fractionation moved upwards. Upon final emplacement at its present level in the crust, the syenitic magma further differentiated in situ, hence the frequent gradational contacts between units.

The spectrum of rock types defining the margin-to-core differentiation sequence is not present at any one location, although along the western periphery of the intrusion five of the six units were mapped. Abrupt contacts sometimes observed between units are produced by movement of unconsolidated magma intruding into earlier solidified rock units.

Rocks of the mafic margin are composed predominantly of diopside with varying proportions of plagioclase and perthite; biotite, the only primary hydrous ferromagnesian mineral, is a minor constituent. Magnetite, titanite, apatite and zircon are all common accessory phases. Primary quartz and nepheline were not observed in any rock unit, nor, excluding the intrusive hornblendite unit, was primary amphibole although secondary amphibole occurs in small amounts. Clinopyroxene decreases in abundance from the mafic margin towards the center of the intrusion, as the total feldspar content rises rapidly. Plagioclase (An_{30-34}) crystallized first and increased in

abundance until the onset of alkali-feldspar crystallization, whereupon the proportion of plagioclase gradually decreased and its composition became more sodic (An_{10-10}) and alkali-feldspar contents continued to rise. At the stage where plagioclase crystallization ceased and the only feldspar crystallizing was perthite, alkali-feldspar syenite was produced and alkali-feldspar succeeded clinopyroxene as the dominant crystallizing mineral phase.

Dykes of various compositions are randomly distributed throughout the pluton and most are directly equivalent to Murdock Creek plutonic units. Pegmatitic dykes of alkali-feldspar syenite are rare, but when found, are frequently associated with small shear zones (several metres wide) within the alkali-feldspar syenite core of the intrusion. These shears are distinct from those associated with the gold-bearing, quartz-carbonate veins in the eastern part of the intrusion and are interpreted as pressure-release conduits along which late-magmatic, volatile-rich fluids were forcefully expelled during the final stages of magma solidification.

Two types of enclave are found near the margin of the intrusion: basaltic xenoliths, which presumably represent stoped fragments of country rock; and igneous textured autoliths, which probably represent fragments of older differentiates that have fallen back into the fractionating magma. The intrusion lacks a significant thermal aureole or a fine-grained chilled-margin. Instead, there is a heterogeneous zone consisting of intermingled

clinopyroxenite and basaltic country rock. Along the northern and southern perimeters of the intrusion, this contact zone is generally absent or obscured by post-emplacement faulting and alteration.

OCCURRENCE AND TEXTURAL CHARACTERISTICS OF THE FERROMAGNESIAN AND IRON-TITANIUM OXIDE MINERALS

Clinopyroxene.-Pale green, slightly pleochroic diopside occurs in all units of the intrusion. Grains are subhedral to euhedral, equant (0.2 to 5 mm across) or columnar (up to 10 mm long) and commonly display compositional zoning; bright green aegirine-augite is preferentially developed in crystal margins and along cleavages and fractures (fig. 3a). Typical inclusions found in diopside include anhedral grains of magnetite, euhedral apatite and titanite, subhedral flakes of biotite, and prismatic zircon. A notable feature of some clinopyroxene grains from rocks of the mafic margin is the presence of tiny acicular inclusions (0.01 to 0.02 mm long) forming a well-defined ring around the crystal core, that were identified by scanning electron microscopy as Cr-rich magnetite (fig. 3b). The orientation of these "needles" at approximately 90° to one another produces a distinctive grid pattern.

Although clinopyroxene from the various rock types is optically indistinguishable, there are recognizable differences in mode of occurrence. In clinopyroxenite, the diopside crystals produce a cumulate-textured rock, although gravitational crystal

Fig. 3 (Next page).-Photomicrographs (transmitted light, uncrossed polars) of ferromagnesian mineral textures. A. Preferential development of aegirine-augite (A) along crystal margins, fractures, and cleavages in primary diopside (D). B. Perpendicularly oriented "needles" of Cr-rich magnetite encircling the core of a diopside crystal which also contains biotite inclusions (B). C. Clinopyroxene (C), biotite (B), magnetite (M), apatite (A) and titanite (T) in mafic clots interstitial to larger perthite laths (P). D. Simultaneous replacement of diopside (D) and perthite (P) to form magnesian hastingsite (H). E. Fibrous magnesio-riebeckite (R) weaving around fragmented grains of perthite (P). F. Primary hornblende (H) with mutually interfering grain boundaries defining a cumulate texture. Intercumulus groundmass consists mainly of saussuritized plagioclase (Pl), diopside (D), and biotite (B).

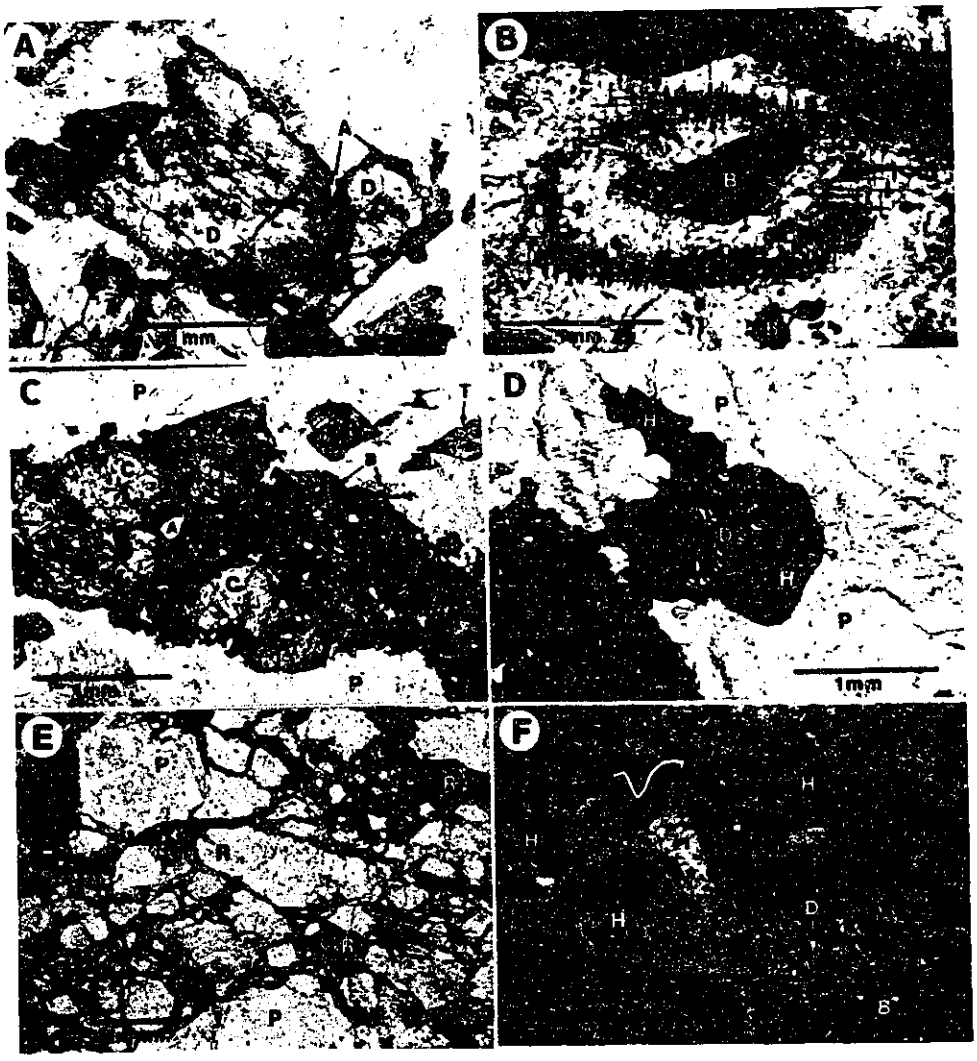
A
D
D
mm
B
B
C
P
T
C
C
P
D
H
P
D
H
P
1mm
E
P
R
R
P
F
H
H
H
D
B

settling (Irvine 1982) is not implied. Clinopyroxene from the transitional mafic rocks (meladiorite, melamonzodiorite, and melasyenite) coexists with subequal proportions of plagioclase and alkali-feldspar producing a hypidiomorphic-granular to -inequigranular rock texture. Finally, in the highly evolved alkali-feldspar syenite, diopside characteristically occurs with biotite, magnetite, apatite, and titanite in irregular mafic clots (1 to 8 mm across) interstitial to larger alkali-feldspar laths (fig. 3c).

Clinopyroxene from the intrusive hornblendite unit is weakly pleochroic, pale green to colourless diopside and strongly resembles the diopside found in the other rock types of the Murdock Creek intrusion. The diopside occurs either as partially resorbed inclusions in coarse-grained cumulus hornblende, or more commonly, as small anhedral to subhedral grains (0.1 to 1.0 mm across) in a hypidiomorphic intercumulus groundmass which also contains biotite, plagioclase, and rare alkali-feldspar.

Biotite.-Biotite is a minor but ubiquitous phase in all rock types, usually occurring as subhedral flakes with ragged terminations. These flakes are highly pleochroic, light tan to dark brown, and up to 5 mm in long dimension. Euhedral apatite crystals are the commonest inclusions; fine-grained titanite or rutile may be present, especially at grain boundaries. Alteration to chlorite along cleavages is poorly developed. Where present, hydration of biotite to chlorite liberated secondary magnetite which forms minute granules arranged in clusters along fractures

and cleavages. The mode of occurrence of brown biotite is similar throughout all units of the intrusion. It occurs in the mafic clots along with diopside, magnetite, and apatite as described earlier, or it may simply form individual flakes interstitial to larger mineral phases. These two distinct modes of occurrence, together with the textural features described above, indicate that this brown biotite is primary.

Secondary biotite is not abundant, but a strongly pleochroic greenish-brown variety is most commonly associated with primary magnetite; randomly oriented tabular sheaths may enclose and partially consume the magnetite or alternatively, and much less frequently, small ragged biotite flakes grow in an outward radiating pattern, roughly perpendicular to the magnetite grain edge which they are replacing. The secondary greenish-brown biotite also cuts across primary biotite and in some cases partly replaces the feldspar and clinopyroxene.

Subhedral flakes of strongly pleochroic greenish-brown to light tan biotite are found in hornblendite and are of primary origin. They occur either as inclusions in hornblende or as a major component of the intercumulus groundmass.

Amphibole.-Fibrous, pale bluish-green and faintly pleochroic actinolite replaces diopside, beginning along crystal margins and proceeding inwards along fractures and cleavage planes. Occasionally, an entire diopside grain is pseudomorphed by actinolite, or much less commonly, by very pale green to colourless tremolite. Actinolite is also associated with calcite

in sinuous veinlets which cut and replace various primary and secondary mafic silicates.

A highly pleochroic, light yellow-brown to deep bluish-green magnesian hastingsite irregularly mantles diopside; crystal habit is variable, ranging from anhedral aggregates to discrete euhedral prisms. With reference to replaced grain boundaries, magnesian hastingsite frequently extends into adjacent perthite or plagioclase, indicating the simultaneous replacement of both diopside and feldspar (fig. 3d). Less commonly, magnesian hastingsite overgrows and partially consumes primary flakes of biotite. Both actinolite and magnesian hastingsite may subsequently undergo patchy alteration to weakly pleochroic pale green to light brown chlorite.

Strongly pleochroic, bright blue to greenish-yellow magnesio-riebeckite is present in sheared syenitic rocks associated with late emplacement of the pegmatitic alkali-feldspar syenite dykes. The shearing produced a cataclastic texture, where fibrous magnesio-riebeckite weaves around fragmented and intensely reddened (hematized) perthite grains (fig. 3e). Where cataclasis is less severe, magnesio-riebeckite may completely pseudomorph euhedral diopside crystals.

The only primary amphibole encountered in this study occurs in the hornblendite unit. Equant, euhedral, twinned, moderately pleochroic crystals of yellowish-green to green-brown hornblende (3 to 15 mm across) produce a cumulate texture, though once

again, gravitational crystal settling is not necessarily implied (fig. 3f). Common inclusions within hornblende include the previously mentioned pale green diopside and greenish-brown biotite, as well as euhedral apatite and subhedral magnetite. Faint optical zonation is present in some hornblende crystals, where pale green actinolitic hornblende is preferentially developed along grain margins.

Magnetite.-Primary magnetite is an abundant accessory phase in all units of the intrusion, particularly the early mafic differentiates. Other primary Fe-Ti oxides which frequently occur with magnetite in felsic plutonic rocks were not identified. The crystal habit of primary magnetite is highly variable, ranging from discrete euhedral cubes (0.05 to 2 mm across) or needles (e.g., fig. 3b) to large, anhedral polycrystalline aggregates (long dimension up to 6 mm), commonly associated with euhedral apatite. Under reflected light, the grain surface may be either smooth or pitted. Weakly pleochroic, pale brownish-grey magnetite grains may display variable degrees of alteration to bluish-white hematite. Most frequently this hematization has taken place preferentially along the margins and fractures in the magnetite grains. Less commonly, hematization is along (111) spinel planes. Numerous magnetite grains possess substantial rims of titanite, the result of subsolidus oxidation referred to as sphenitization (Carmichael and Nicholls 1967; Dillet and Czamanske 1988). Primary magnetite in all rock types occurs as, (1) inclusions in diopside, biotite, plagioclase, and alkali-feldspar and (2) as

individual grains or polycrystalline aggregates (typically associated with mafic clots) interstitial to larger and more voluminous silicate phases.

The various generations of secondary magnetite can usually be identified on the basis of the following criteria: small grain size, anhedral habit, and the presence of well known replacement textures, one of the most common being the localization of fine-grained magnetite granules along the edges of partially decomposed biotite, clinopyroxene, and secondary amphibole (Ramdohr 1969; Haggerty 1976).

MINERAL CHEMISTRY

Analytical Techniques.-Most mineral analyses were by wavelength-dispersive X-ray spectrometry on a Camebax electron microprobe at McGill University (Montreal) using the Cameca ONQUANT software package and a series of natural and synthetic standards. Analyses were also carried out at the Geological Survey of Canada, on a similar Camebax instrument using "PAP" software developed by Pouchou and Pichoir (1984). For both instruments accelerating potential was 15 kV, with a beam current of 7 nA and 30 s counting times. Data reported are in most cases averages of several analyses performed on single grains. Biotite and amphibole separates obtained using magnetic and heavy liquid techniques, followed by purification by hand under a binocular microscope, were analysed for Fe^{2+} and Fe^{3+} by the Pratt method.

Nomenclature.-Pyroxene and amphibole terminology follows the

recommendations of the IMA (Morimoto 1988, and Leake 1978, respectively). Biotite nomenclature uses the biotite-annite-siderophyllite-eastonite rectangle of Deer et al. (1963). Fe-Ti oxides are named according to Haggerty (1976).

Clinopyroxene.-Primary pyroxene (table 1) is all high-Ca clinopyroxene and plots as a tight, overlapping group in the diopside field of the pyroxene quadrilateral (fig. 4). Microprobe traverses confirm that primary zonation is absent; crystals typically exhibit only minor, unsystematic, intra-grain variation. The proportions of Fe^{2+} and Fe^{3+} were calculated assuming stoichiometry and electrostatic neutrality. Sufficient FeO was converted to Fe_2O_3 to give a structural recalculation to 4 cations and 6 anions. Although the stoichiometry of low-pressure igneous pyroxenes has been demonstrated by Cawthorn and Collerson (1974), the calculated Fe^{3+}/Fe^{2+} ratio may not always be accurate and should be accepted with caution (McGuire et al. 1989). Aegirine-augite, which is typically confined to diopside crystal margins, fractures, and cleavages, is the product of subsolidus metasomatism involving the replacement of $Ca(Mg^{2+},Fe^{2+})$ by $NaFe^{3+}$ during interaction with a late, Na-rich vapour phase. Similar patchy zonation of aegirine-augite in diopside, also attributed to metasomatism, has been noted in other alkaline complexes (e.g., Tyler and King 1967; Parsons 1979). A deuteric origin for this late Na-rich vapour phase is supported by the frequent coexistence of aegirine-augite with blue magnesio-riebeckite (replacing primary clinopyroxene) and

TABLE 1

Compositions and Structural Formulae of Representative Clinopyroxene

ROCK UNIT[a]	AS	AS	AS	AS	AS	MS	MS	MM	MM	MD	CP	CP	CP	HB	HB
SAMPLE	10821	10495	118C3	10536[b]	10491[b]	13382	13387	29525	29526	132C2	130C6	115C1	13588	32928	32930
# OF ANALYSES[c]	2	2	3	2	2	3	2	2	1	2	2	2	3	3	4
SiO_2	53.38	52.02	53.03	51.40	50.87	50.79	52.03	52.69	52.50	52.97	53.69	53.80	52.38	53.87	54.18
TiO_2	.45	.50	.42	.52	.60	.41	.16	.12	.15	.14	.22	.21	.21	.05	.05
Al_2O_3	1.87	2.03	1.92	2.67	2.38	2.31	1.54	1.19	1.29	1.96	.95	1.23	1.91	.36	.40
Cr_2O_3	na	na	na	na	na	na	na	...	...	na	na	na	na	.05	...
Fe_2O_3	2.94	7.00	3.09	8.36	9.19	5.84	5.44	3.22	4.01	1.84	1.53	1.03	4.67	2.08	1.09
FeO	5.76	1.25	3.74	4.76	4.17	3.66	3.07	5.66	5.43	6.57	3.49	6.01	2.75	3.89	4.29
MnO	.38	.38	.27	.31	.39	.48	.38	.37	.39	.35	.23	.25	.27	.19	.21
MgO	12.36	13.49	13.75	9.78	10.34	12.88	14.64	13.42	13.41	13.51	16.39	14.18	14.31	14.75	15.18
CaO	21.05	21.52	21.88	18.83	19.54	22.28	21.70	22.72	22.57	22.22	23.36	23.10	22.64	24.57	24.62
Na_2O	1.96	2.02	1.56	3.30	2.88	1.17	1.08	.86	.90	.86	.33	.73	1.14	.53	.36
K_2O	...	.01	...	...	...	.01	...	.02	.03	...	...	...	...	.05	.02
Total	100.15	100.22	99.66	99.93	100.36	99.83	100.04	100.27	100.68	100.42	100.19	100.54	100.28	100.39	100.40
FeO[d]	8.41	7.55	6.52	12.28	12.44	8.91	7.96	8.56	9.04	8.23	4.87	6.94	6.95	5.76	5.27
Structural formulae based on 4 cations and 6 oxygens															
Si	1.976	1.917	1.959	1.928	1.906	1.898	1.925	1.957	1.945	1.959	1.964	1.979	1.929	1.981	1.988
Al^{iv}	.024	.083	.041	0.072	.094	.102	.067	.043	.055	.041	.036	.021	.007	.016	.012
Fe^{3+iv}	...	...	...	...	...	...	.008	...	...	...	...	...	...	.003	...
Al^{vi}	.058	.006	.043	.046	.011	...	...	.009	.001	.044	.005	.033	.012	...	.005
Ti	.013	.014	.012	.015	.017	.012	.005	.003	.004	.004	.006	.006	.006	.001	.001
Cr	na	na	na	na	na	na	na	...	...	na	na	na	na	.001	...
Fe^{3+}	.082	.194	.086	.236	.259	.164	.143	.090	.112	.051	.042	.029	.129	.055	.030
Fe^{2+}	.178	.039	.115	.149	.130	.114	.095	.176	.168	.203	.107	.185	.085	.120	.132
Mn	.012	.012	.008	.010	.013	.015	.012	.012	.012	.011	.007	.008	.008	.006	.007
Mg	.682	.741	.757	.547	.578	.718	.808	.743	.741	.745	.894	.777	.786	.809	.830
Ca	.835	.850	.866	.757	.785	.892	.860	.904	.896	.880	.916	.910	.893	.968	.968
Na	.141	.144	.112	.240	.209	.085	.077	.062	.065	.062	.023	.052	.081	.038	.026
K	...	...	...	...	...	...	...	.001	.001	...	...	...	...	.002	.001
Fe/(Fe+Mg)	.276	.239	.210	.413	.402	.280	.234	.264	.274	.255	.143	.215	.214	.180	.163
Fe^{3+}/(Fe^{3+}+Fe^{2+})	.315	.834	.428	.613	.666	.590	.615	.339	.399	.201	.283	.134	.604	.325	.187
Na/(Na+Ca)	.144	.145	.115	.241	.210	.087	.083	.064	.067	.065	.025	.054	.084	.038	.026
Rock P.I.[e]	73.00	63.93	69.96	69.90	63.93	52.71	52.71	34.35	34.35	35.37	11.52	29.97	16.28	22.62	22.62
Rock Agpaicity[f]	.96	.95	.88	.95	.95	.73	.73	.76	.76	.58	.51	.60	.65	.59	.59

NOTE.-na = not analysed.

[a] Rock units as follows: AS, alkali-feldspar syenite; MS, melasyenite; MM, melamonzodiorite; MD, meladiorite; CP, clinopyroxenite; HB, hornblendite.

[b] Secondary aegirine-augite (all other analyses are for primary diopside).

[c] Number of analyses averaged.

[d] Total Fe calculated as FeO.

[e] Rock P.I. = host-rock normative fractionation index (wt.% Qtz + Ab + Or + Ne + Lc + Ns).

[f] Host-rock agpaicity index = molecular ratio (Na+K)/Al.

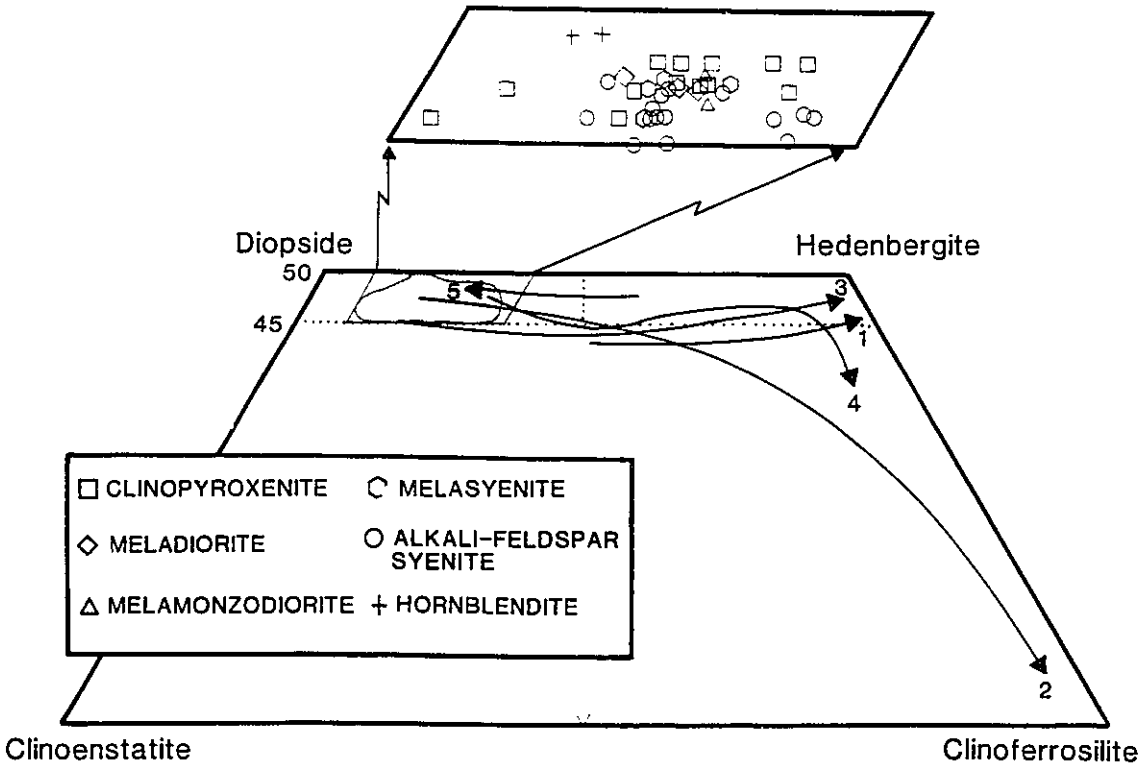

Fig. 4.-Composition of Murdock Creek clinopyroxene in terms of the pyroxene quadilateral (fig. 4 from Morimoto 1988). For comparative purposes, clinopyroxene crystallization trends from several other differentiated alkaline intrusions are shown. 1, Kûngnât syenites (Upton 1960); 2, Shonkin Sag laccolith, soda syenite (Nash and Wilkinson 1970); 3, Shiant Isles sill (Gibb 1973); 4, Klokken gabbro-syenite complex (Parsons 1979); 5, Baie-des-Moutons syenitic complex, early group syenites (Lalonde and Martin 1983). Shaded field represents the range of Murdock Creek clinopyroxene compositions. Symbols in expanded portion of the diopside field are averages for analyses of Murdock Creek clinopyroxene from the various plutonic units.

the observation that aegirine-augite rims are most prominently developed in pyroxene grains from rocks adjacent to the late-magmatic pegmatitic dykes of alkali-feldspar syenite.

The restricted range of primary clinopyroxene compositions is remarkable (fig. 4) given the fact that units of the Murdock Creek intrusion have SiO_2 contents ranging from 42 to 59 wt.%. As shown in figure 4, clinopyroxenes from differentiated alkaline intrusive suites normally evolve towards more Fe-rich compositions with magmatic differentiation (hedenbergite enrichment trend). Clinopyroxene crystallization trends from the Kûngnât (Upton 1960), Shiant Isles (Gibb, 1973) and Klokken (Parsons 1979) alkaline intrusive complexes lie approximately parallel to the diopside-hedenbergite join, indicating extensive substitution of Fe^{2+} for Mg, with very little involvement of Ca. The downward curved trend towards the clinoferrosilite corner displayed by clinopyroxenes from the Shonkin Sag soda syenite and, to a much lesser extent, the Klokken syenites, is the result of $NaFe^{3+}$ replacing $CaFe^{2+}$ (trend away from the Wo-En-Fs plane towards acmite, $NaFe^{3+}Si_2O_6$). In the Murdock Creek intrusion however, Fe/(Fe+Mg) ratios in clinopyroxene remain consistently low (0.10 to 0.33) throughout all stages of crystallization (fig. 5). In fact, a slight reversal of the normal Fe enrichment trend may be observed, whereby some pyroxenes from the more highly evolved alkali-feldspar syenite core display Mg enrichment relative to pyroxenes found in the mafic marginal rocks. This departure from the expected Fe enrichment trend has also been

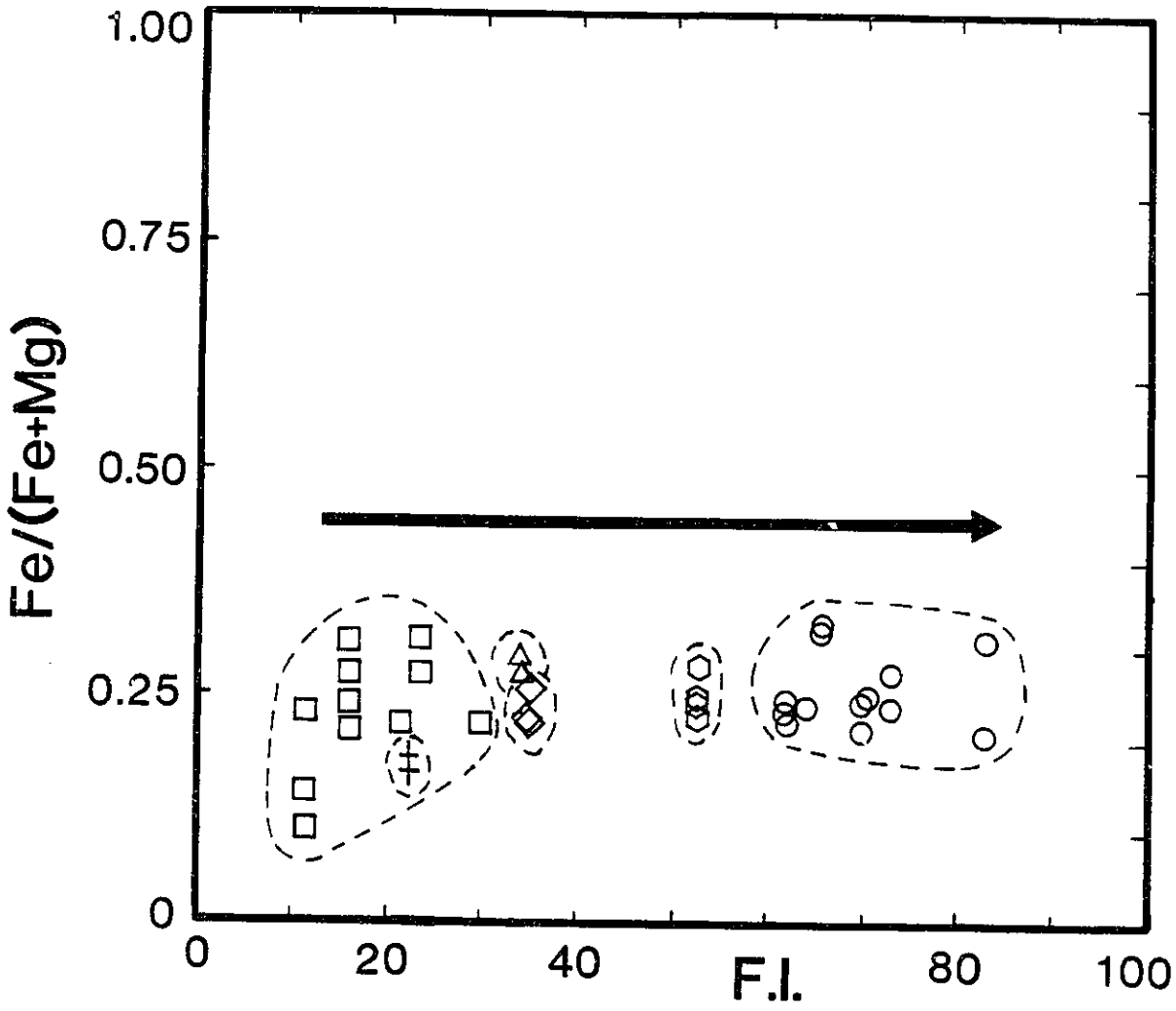

Fig. 5.-Fe/(Fe+Mg) content of Murdock Creek clinopyroxene vs. the host-rock normative fractionation index (F.I. = wt.% Qtz+Ab+Or+Ne+Lc+Ns). Symbols as in fig. 4.

reported in clinopyroxenes from the Finnmarka (Czamanske and Wones 1973), Ben Nevis (Haslam 1968), and Baie-des-Moutons (Lalonde and Martin 1983) igneous complexes (refer to trend #5 in fig. 4). Note however, that none of these intrusions display the wide range of mafic to felsic rock types present in the Murdock Creek pluton, nor are the clinopyroxene compositions usually as magnesian. This reversal or lack of a normal Fe enrichment trend is believed to have resulted from highly oxidizing conditions in the magma from which the pyroxenes nucleated and grew. Under such circumstances Fe^{2+} is oxidized to Fe^{3+} and preferentially partitions into magnetite leading to a deficiency of Fe^{2+} for the crystallizing ferromagnesian minerals. Consequently, Mg^{2+} substitutes for Fe^{2+} in pyroxene. Magmatic oxidation is also suggested by the high $Fe^{3+}/(Fe^{2+}+Fe^{3+})$ ratio inferred for the pyroxenes. Although the ratio exhibits wide variability both within and between units (0.13 to 0.83, average $\approx$ 0.49), its tendency towards consistently high values is strong evidence for magmatic oxidation.

As shown in figure 4, high Wo-content in clinopyroxene from alkaline rocks is not unusual (also see Lebas 1962; Gibb 1973; Fodor et al. 1975) and, in the case of the Murdock Creek intrusion, Wo-content generally decreases slightly with differentiation. A sympathetic relationship also exists between the alkalinity of constituent pyroxene (Na/(Na+Ca)) and the agpaicity (molecular (Na+K)/Al) of its host-rock (refer to table 1). Both trends of decreasing Wo-content and increasing

alkalinity are consistent with crystal fractionation, especially of early-formed diopside (and plagioclase, An_{30-34}), which results in Ca depletion and the buildup of alkalis in the evolving melt. The acmite component ($NaFe^{3+}Si_2O_6$) is significant in some of the more sodic clinopyroxenes (max 16 mol% Ac), however pyroxenes of the intrusion do not display an acmite enrichment trend as seen in the Shonkin Sag and Klokken intrusions (fig. 4), and noted in other similar alkaline plutons (e.g., Yagi 1966; Tyler and King 1967; Larsen 1976; Mitchell and Platt 1978). Even after removal of this acmite molecule from the analysed diopsides, many grains still possess excess Fe^{3+}, suggesting the presence of a ferri-Tschermak's component ($CaFe_y^{3+}Fe_m^{3+}SiO_6$), consistent with crystallization under oxidizing conditions.

Although systematic variations in the Al and Ti contents of pyroxene with fractionation have been described by several authors (Evans and Moore 1968; Smith and Lindsley 1971; Gibb 1973; Fodor et al. 1975; Bédard et al. 1988), the relationship between the Ti and Al contents found in pyroxenes and those in their fractionating host magmas is complex and controlled by a variety of factors. These include the silica activity in the magma (Kushiro 1960; Verhoogen 1962; Brown 1967; Carmichael et al. 1970; Gupta et al. 1973), cooling rates (Grove and Bence 1979; Gamble and Taylor 1980), and changes in the temperature (Akella and Boyd 1973; Thompson 1974) and pressure of crystallization (Yagi and Onuma 1967; Edgar et al. 1980).

Additional complications in interpreting fractionation trends arise from contradictory experimental data (Bédard et al. 1988). In light of this, it is not unexpected that the Al contents in Murdock Creek clinopyroxenes fail to define any systematic variation with progressive crystallization, or that Al^{IV} and Ti, which are commonly related by a coupled substitution, are not correlative. Aluminum contents tend to be slightly lower than in typical diopside (c.f., Deer et al. 1978; Haslam 1968; Parsons 1979), with Al_2O_3 ranging between 0.36 and 2.90 wt.%. For pyroxenes, a strong positive correlation between Al in the octahedral position and pressure of crystallization has been found (Lebas 1962; Aoki and Kushiro 1968; Kushiro 1969; Wass 1979). The modest but appreciable amounts of Al in octahedral coordination in many of the analysed pyroxenes (up to 0.060 atoms per formula unit (a./f.u.)) suggests that these minerals crystallized under significant pressure, although compositional effects make it impossible to constrain the precise pressure (Thompson 1974).

A low Ti content (between 0.002 to 0.017 a./f.u.) is also characteristic of Murdock Creek clinopyroxene and like Al, Ti fails to define a consistent trend with fractionation. Gibb (1973) and Tracy and Robinson (1977) suggest that low-Ti clinopyroxene is caused by extensive fractionation of coexisting Ti-rich phases which deplete the melt in Ti. This explanation may apply equally well to the clinopyroxenes in the Murdock Creek intrusion where abundant magnetite, biotite, and titanite all

coexisted with clinopyroxene throughout primary crystallization.

Manganese contents are low in all analysed pyroxenes (0.001 to 0.016 a./f.u.) but tend to be higher in clinopyroxene from the more evolved felsic units. Inverse correlation between Mn and Ca contents suggest that some Mn substitution for Ca in the M_2 site may have occurred.

Biotite.-Biotite structural formulae (table 2) have been calculated on the basis of 22 oxygen atoms and assuming OH+F+Cl = 4.00 atoms. FeO and Fe_2O_3 were measured by wet chemical means for seven biotite separates from unaltered rock specimens considered representative of the different units comprising the intrusion. The appropriate $Fe^{3+}/(Fe^{2+}+Fe^{3+})$ ratios were then used to adjust the structural formulae for other analysed biotites where their total Fe content is reported as FeO (from microprobe analyses).

Systematic chemical zonation within individual grains was not observed. Octahedral site occupancy ranges between 5.421 to 5.822 a./f.u., indicative of trioctahedral micas. In terms of the phlogopite-annite-eastonite-siderophyllite diagram (fig. 6), igneous biotites from the Murdock Creek pluton display a remarkably low and uniform Fe/(Fe+Mg) ratio of $\approx$ 0.40, with a maximum deviation of $\leq$ 0.05 (excluding phlogopites from the intrusive hornblendite unit). The crystallization paths of biotite from the Finnmarka (Czamanske and Wones 1973), Ben Nevis (Haslam 1968), and Baie-des-Moutons (Lalonde and Martin 1983) igneous complexes show variable degrees of decreasing Fe/(Fe+Mg) with differentiation, believed to result from increasing or

TABLE 2

Compositions and Structural Formulae of Representative Biotite

ROCK UNIT[a]	AS	AS	AS	AS	AS	AS	MS	MM	MM	MD	MD	CP	CP	GR	HB
SAMPLE	105U1	108U2	669U5	11110[b]	13477[b]	638U2	13378[b]	29553[b]	29655[b]	13266[b]	129U1	11506	130U3[b]	32[illegible][b,c]	32945[c]
# OF ANALYSES[d]	2	3	2	2	3	3	3	3	3	2	3	2	2	3	3
SiO_2	37.34	38.29	38.12	37.74	36.27	38.39	36.58	36.92	37.04	36.79	36.55	38.33	36.30	38.00	38.24
TiO_2	2.03	2.61	2.95	3.07	3.50	2.65	3.87	3.57	2.78	3.12	3.95	2.38	4.14	1.85	2.12
Al_2O_3	14.16	12.92	13.25	13.06	14.27	13.20	14.26	13.54	13.42	14.53	15.35	14.60	15.04	14.34	14.52
Cr_2O_3	...	...	...	...	...	...	...	.07	.03	...	...	...	...	.26	.29
Fe_2O_3	6.20	5.10	4.60	4.86	5.23	4.84	6.20	6.42	6.32	5.68	4.10	6.00	5.60	4.85	4.80
FeO	11.60	12.10	11.00	11.47	12.36	11.83	11.73	12.16	11.97	10.76	11.10	11.60	10.60	9.36	9.27
MnO	.44	.64	.47	.34	.40	.51	.32	.27	.29	.22	.30	.14	.06	.12	.09
MgO	14.39	14.78	13.73	15.55	14.18	12.77	13.69	13.62	14.23	13.90	13.81	15.66	16.81	16.56	16.21
CaO	...	.04	.02	...	.07	...	...	...	.03	...	...	...	...	...	...
Na_2O	.09	.09	.05	.09	.06	.05	.05	.16	.15	.12	.29	.12	.40	.09	.17
K_2O	10.48	9.27	10.01	9.65	9.75	10.23	9.69	9.65	9.59	9.90	9.59	9.06	8.93	10.02	10.21
H_2O[e]	3.74	3.41	3.92	3.63	3.78	3.80	3.75	4.00	4.00	3.85	3.90	3.87	3.91	4.08	4.08
F	.53	1.27	.25	.79	.41	.45	.51	na	na	.35	.30	.32	.31	na	na
Cl	.01	...	.02	.06	.07	.02	.04	na	na	.05	.01	.12	.01	na	na
O=F, Cl	.22	.53	.11	.34	.19	.19	.22	...	...	.16	.13	.16	.13	...	...
Total	100.79	99.98	98.28	99.97	100.12	98.55	100.47	100.38	99.85	99.11	99.12	101.88	101.97	99.53	100.00
Structural formulae based on 22 oxygens															
Si	5.548	5.698	5.751	5.611	5.426	5.805	5.441	5.507	5.546	5.517	5.458	5.552	5.270	5.610	5.617
Z=8 Al^{IV}	2.452	2.266	2.249	2.288	2.516	2.195	2.500	2.380	2.368	2.483	2.542	2.448	2.573	2.390	2.383
Fe^{3+IV}	...	.036	...	.101	.058	...	.059	.113	.086	...	...	...	.157	...	...
Al^{VI}	.028	...	.108	...	...	.157	...	...	...	.085	.159	.044	...	.106	.131
Ti	.227	.292	.335	.343	.394	.301	.433	.400	.313	.352	.444	.259	.452	.205	.234
Cr	...	...	...	...	...	...	...	.008	.004	...	...	...	...	.038	.034
Fe^{3+}	.693	.535	.522	.443	.530	.551	.635	.608	.626	.641	.461	.654	.455	.539	.531
Fe^{2+}	1.441	1.506	1.388	1.426	1.546	1.496	1.459	1.517	1.499	1.349	1.386	1.405	1.287	1.156	1.139
Mn	.055	.081	.060	.043	.051	.065	.040	.034	.037	.028	.038	.017	.007	.015	.011
Mg	3.187	3.279	3.088	3.446	3.163	2.878	3.036	3.029	3.177	3.107	3.074	3.382	3.638	3.645	3.550
ΣY	5.631	5.693	5.501	5.701	5.684	5.448	5.603	5.596	5.656	5.562	5.562	5.761	5.839	5.696	5.630
Ca	...	.006	.003	...	.003	...	...	...	.005	...	...	...	...	...	...
Na	.026	.026	.015	.026	.017	.015	.014	.046	.044	.035	.084	.034	.113	.026	.048
K	1.987	1.760	1.927	1.830	1.861	1.973	1.839	1.836	1.832	1.894	1.827	1.674	1.654	1.887	1.913
ΣX	2.013	1.792	1.945	1.856	1.881	1.988	1.853	1.882	1.881	1.929	1.911	1.708	1.767	1.913	1.961
F	.249	.598	.119	.371	.194	.215	.240	na	na	.166	.142	.147	.142	na	na
Cl	.003	...	.005	.014	.018	.003	.010	na	na	.011	.003	.029	.002	na	na
Fe/(Fe+Mg)	.401	.388	.382	.364	.403	.416	.415	.425	.410	.390	.375	.378	.346	.317	.320
Fe^{3+}/ (Fe^{2+}+Fe^{3+})	.325	.275	.273	.276	.276	.269	.322	.322	.322	.322	.249	.318	.322	.318	.318
Rock F.I.[f]	69.90	73.00	69.79	65.72	62.13	68.20	52.71	34.35	34.35	35.37	21.54	29.97	11.52	22.62	22.62

NOTE.-na = not analysed.

[a] Rock units as in table 1.

[b] FeO/Fe_2O_3 estimated from analyses of biotite in the same rock unit.

[c] Phlogopite according to the biotite-annite-siderophyllite-eastonite classification scheme, Deer et al. (1963).

[d] Number of analyses averaged.

[e] H_2O calculated by assuming (OH,F,Cl) = 4.

[f] Rock F.I. = host-rock normative fractionation index.

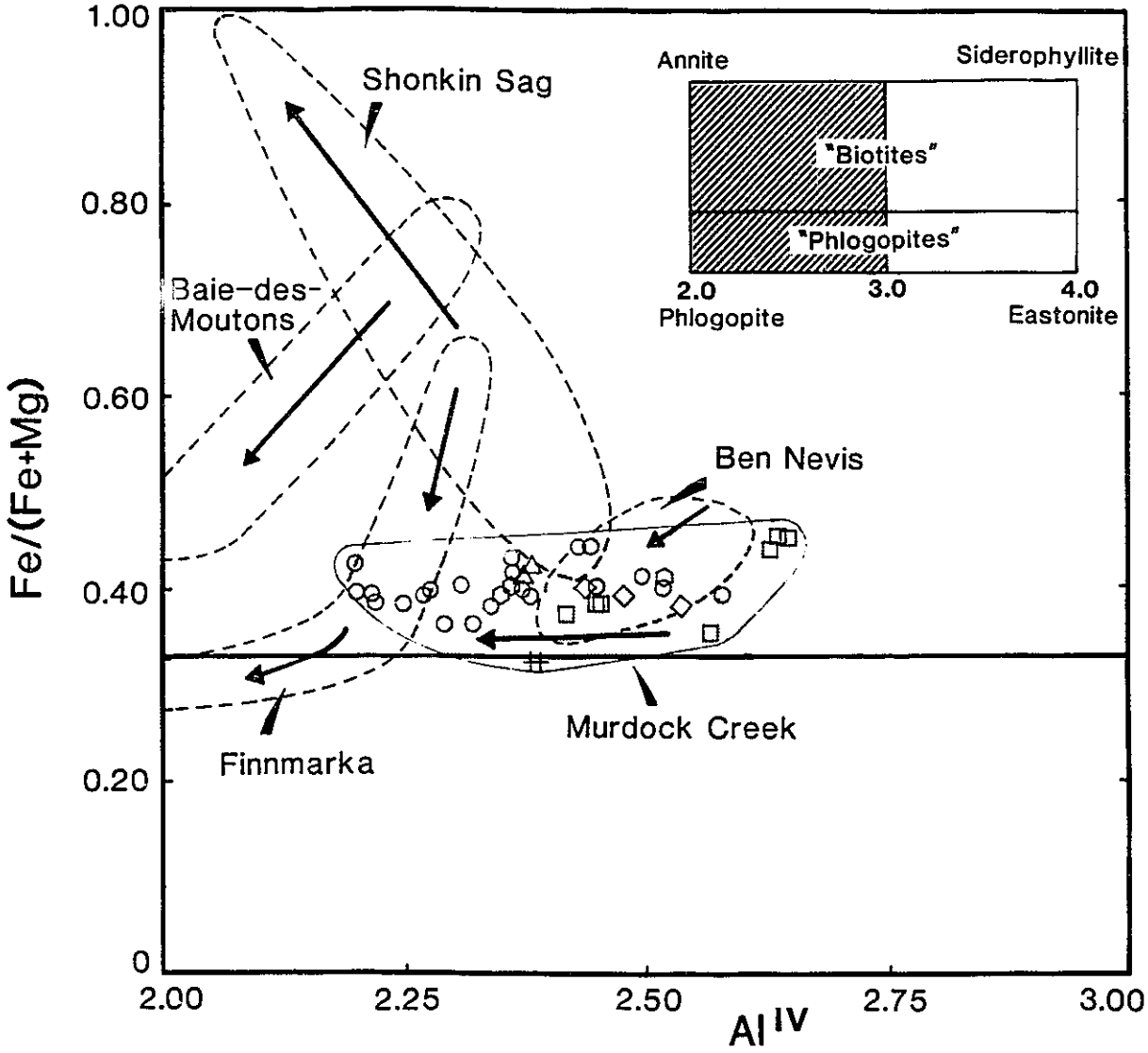

Fig. 6.-Biotite compositions from the Murdock Creek intrusion (shaded field) plotted on part of the phlogopite-annite-eastonite -siderophyllite quadrilateral showing decreasing Al^{IV}, but constant Fe/(Fe+Mg) contents during magmatic evolution. The crystallization paths (arrows) of biotite from the Finnmarka (Czamanske and Wones 1973), Ben Nevis (Haslam 1968), and Baie-des-Moutons (Lalonde and Martin 1983) igneous complexes show variable degrees of decreasing Fe/(Fe+Mg) with differentiation, believed to result from increasing or nearly constant (Ben Nevis) f_{O_2} duirng crystallization. Biotite from the Shonkin Sag laccolith (Nash and Wilkinson 1970) displays the opposite trend of increasing Fe/(Fe+Mg), compatible with falling f_{O_2} during its primary crystallization. Symbols as in fig. 4.

nearly constant (Ben Nevis) f_{O_2} during crystallization. Biotites from the Shonkin Sag laccolith (Nash and Wilkinson 1970) display the opposite trend, one of increasing Fe/(Fe+Mg), compatible with decreasing f_{O_2} reported during its primary crystallization. Figure 6 also shows that tetrahedral Al in Murdock Creek biotite generally decreases with magmatic evolution. Decreasing Al^{IV} (and total Al) in biotite from progressively more differentiated rock types has been observed in other felsic intrusions and has been attributed to increasing silica activity within the crystallizing magma (e.g., Czamanske and Wones 1973) or to the fact that six-fold coordination for Al is favored in silicate minerals formed at lower temperatures (Thompson 1947). As the Murdock Creek biotites show no corresponding increase in octahedral Al, the temperature argument is not convincing, nor would silica activity seem to be a factor because there is no evidence for increasing silica activity in the units of the Murdock Creek intrusion (all rocks are slightly Ne or very rarely Ol+Hy normative, with no modal quartz or feldspathoids). Changing pressure of crystallization is also unlikely to have affected the Al content, given the nature of pluton emplacement (single intrusive event) and the relatively uniform Al^{VI} content in diopside, which suggests that all rock units, and hence all biotite, crystallized under the same total pressure. Thus, it appears that some other factor(s), perhaps the composition of coexisting plagioclase (Anderson 1980), or the Al activity of coexisting mineral phases (Nockolds 1947), controlled Al

distribution in these biotites.

The atomic ratio [Fe/(Fe+Mg)]x100 in biotite has been related to the temperature and f_{O_2} which prevailed during its crystallization (Wones and Eugster 1965). Murdock Creek biotites which all have values near 40 and are in equilibrium with potassium feldspar and magnetite, crystallized at a nearly constant oxygen fugacity of approximately 10^{-12} bars, regardless of crystallization temperature (fig. 7). Primary biotite crystallization in the intrusion is inferred to have taken place for the most part between 1165 °C and 800 °C (for details refer to discussion on magma evolution). Wones and Eugster (1965) also stressed that total pressure will have little effect on the spatial relations of the equilibria shown in figure 7; increasing or decreasing the pressure will simply shift the biotite isopleths to higher or lower temperatures respectively. Thus all biotite in rocks of the Murdock Creek intrusion appears to have been in equilibrium with a magma possessing a constant oxygen fugacity of approximately 10^{-12} bars. It should be emphasized that these uniform Fe/(Fe+Mg) ratios in biotite (also reflected in coexisting clinopyroxenes to a slightly lesser degree) are believed to represent oxidizing magmatic conditions and are not the result of modification by an overprinting late-stage fluid as was interpreted to have caused similarly uniform Fe/(Fe+Mg) ratios in biotite in several other felsic plutons (e.g., Dodge and Moore 1968; Mahmood 1983). The lack of abundant pegmatites and miarolitic cavities together with the minor development of

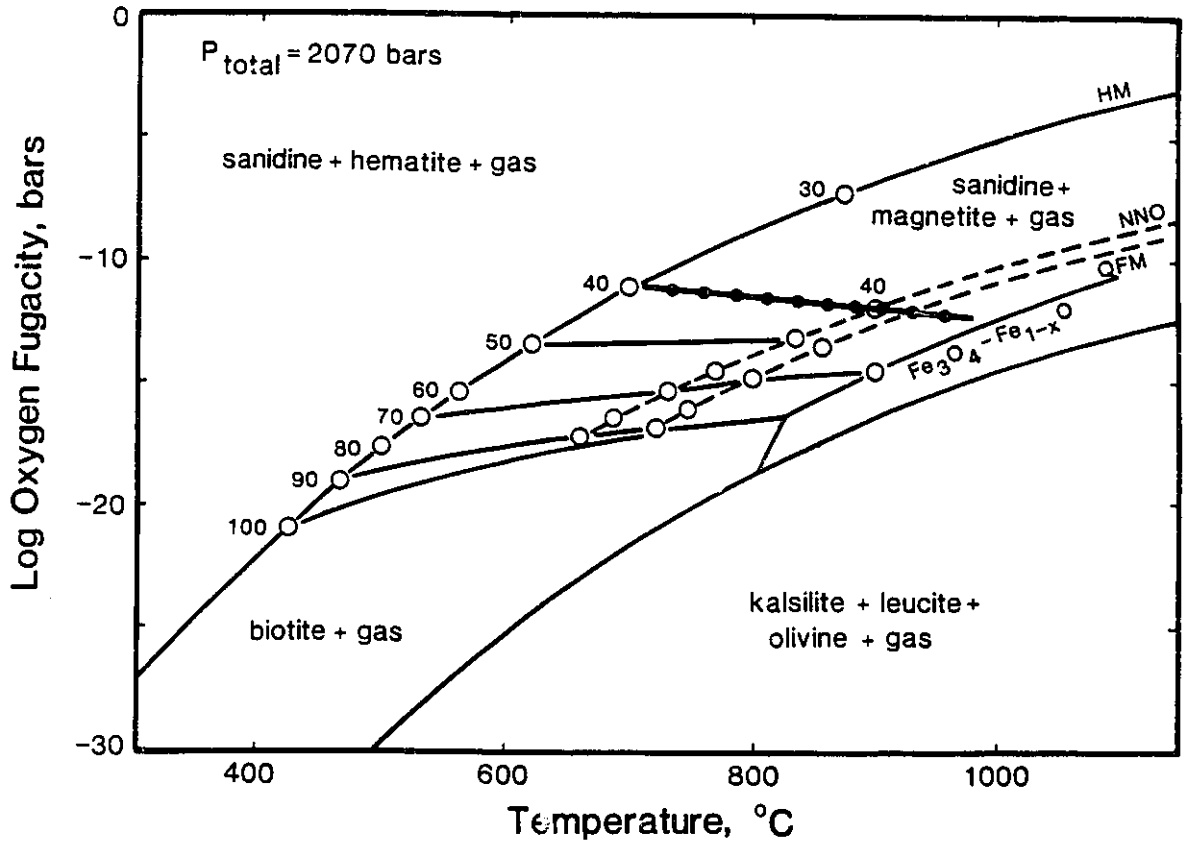

Fig. 7.-Stabilities of biotite with differing Fe/(Fe+Mg) ratios as a function of oxygen fugacity and temperature at 2070 bars total pressure (after Wones and Eugster 1965, fig. 4). Numbers 30 to 100 represent [Fe/(Fe+Mg)]x100 ratios for biotite in the assemblage biotite + K-feldspar + magnetite. Heavy dotted line represents compositions of biotite from the Murdock Creek intrusion (constant Fe/(Fe+Mg) ≈ 0.40). Primary biotite crystallization is inferred to have taken place for the most part above ≈ 800 °C.

hydrous replacement minerals indicate the limited extent of late- to post-magmatic fluid alteration.

Evidence for magmatic oxidation can also be shown by the atomic proportions of Fe^{2+}, Fe^{3+}, and Mg^{2+} in biotite. Wones and Eugster (1965) provided estimates of the composition of biotites coexisting with potassium feldspar and magnetite under various oxygen-buffered conditions. Atomic proportions of Fe^{2+}: Fe^{3+}: Mg^{2+} for analysed biotite separates are shown in the ternary diagram of figure 8. They plot as a tight group not far below the hematite-magnetite (HM) buffer, indicating a high and uniform oxygen fugacity throughout crystallization. Compared with well-documented biotite crystallization trends from other felsic plutonic rocks (also see figure 1 in Speer 1984), it is apparent that few reported igneous biotites have equilibrated with magmas as oxidized as that which crystallized as the Murdock Creek pluton. The trends in figure 8 are largely self explanatory; however, note that for Japanese granitoids the nickel-nickel oxide (NNO) buffer is the approximate boundary between biotites from "oxidized" magnetite-series and "reduced" ilmenite-series rocks (Ishihara 1977, 1981). The above results are in good agreement with the constant oxygen fugacity deduced from the Fe/(Fe+Mg) ratios of biotite.

Mn content in biotite shows an increase with late fractionation, ranging from a low of 0.007 a./f.u. in clinopyroxenite to a high of 0.081 a./f.u. in alkali-feldspar syenite (fig. 9). Similar trends of Mn enrichment have been

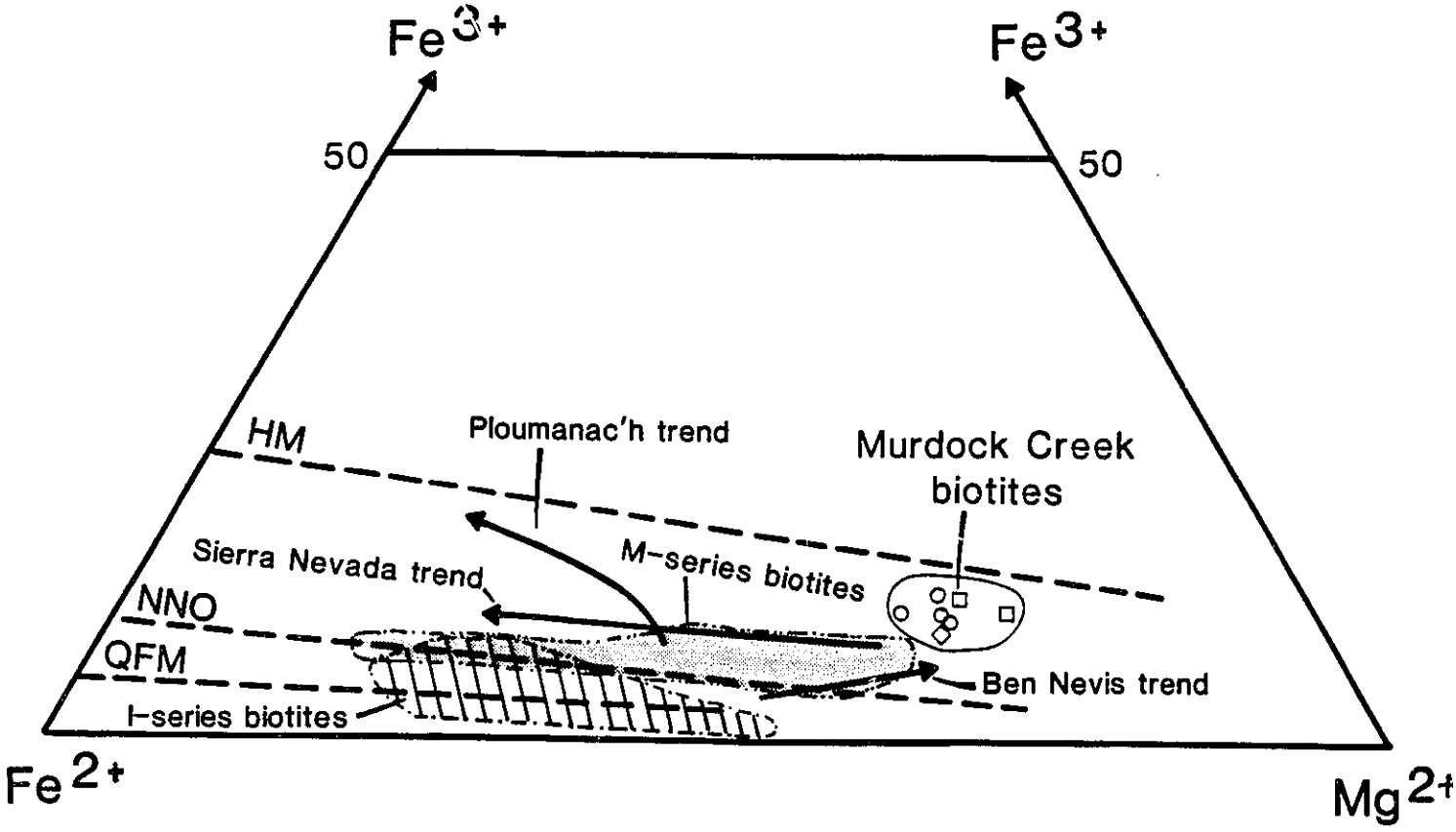

Fig. 8.-Fe^{3+}-Fe^{2+}-Mg^{2+} contents of Murdock Creek biotite. Dashed lines represent compositions of "buffered" biotite in the ternary system annite-phlogopite-$KFe_3^{+3}AlSi_3O_{12}(H_{-1})$ depicted in Wones and Eugster (1965). For comparative purposes, paths of crystallization (arrows) of biotite from other felsic plutons have been included. Data from Dodge et al. (1969) for the Sierra Nevada trend; Haslam (1968) for the Ben Nevis trend; Ishihara (1977) for the M-series and I-series fields; Barrière and Cotton (1979) for the Ploumanac'h trend. Symbols as in fig. 4.

observed in biotite from the Finnmarka (Czamanske and Wones 1973), Klokken (Parsons 1979, 1981), and Zaër (Mahmood 1983) igneous complexes and the Sierra Nevada batholith (Ague and Brimhall 1988). Although whole-rock chemistry shows MnO to decrease with increasing SiO_2 content, the molar ratio $MnO/(MnO+TiO_2+FeO+MgO)$ is observed to increase slightly with late SiO_2 enrichment. As discussed in Ague and Brimhall (1988), higher Mn content in biotite from more silicic units may therefore be explained in terms of higher $MnO/(MnO+TiO_2+FeO+MgO)$ in the bulk rock.

Titanium contents appear normal for igneous biotite (Deer et al. 1963, 1978), reaching 0.452 a./f.u. in clinopyroxenite; in more fractionated rocks, values range between 0.230 to 0.400 a./f.u. (table 2). In general, Ti content decreases with fractionation in accord with experimental studies of simple and natural systems, which show decreasing Ti solubility in phlogopite with lower temperatures of crystallization (Forbes and Flower 1974; Edgar et al. 1976; Robert 1976). Although these studies pertain to Fe-poor or Fe-free phlogopites the results can be applied to natural ferromagnesian micas, especially in the case of Murdock Creek where biotite is very Mg-rich. Indeed, studies by Carmichael (1967) on volcanic rocks, Guidotti et al. (1977) on metamorphic rocks, and Czamanske and Wones (1973) on granitic rocks have shown that the Ti content of biotite that coexists with titanite or ilmenite is higher in biotite that crystallized at higher temperatures. Other investigators have

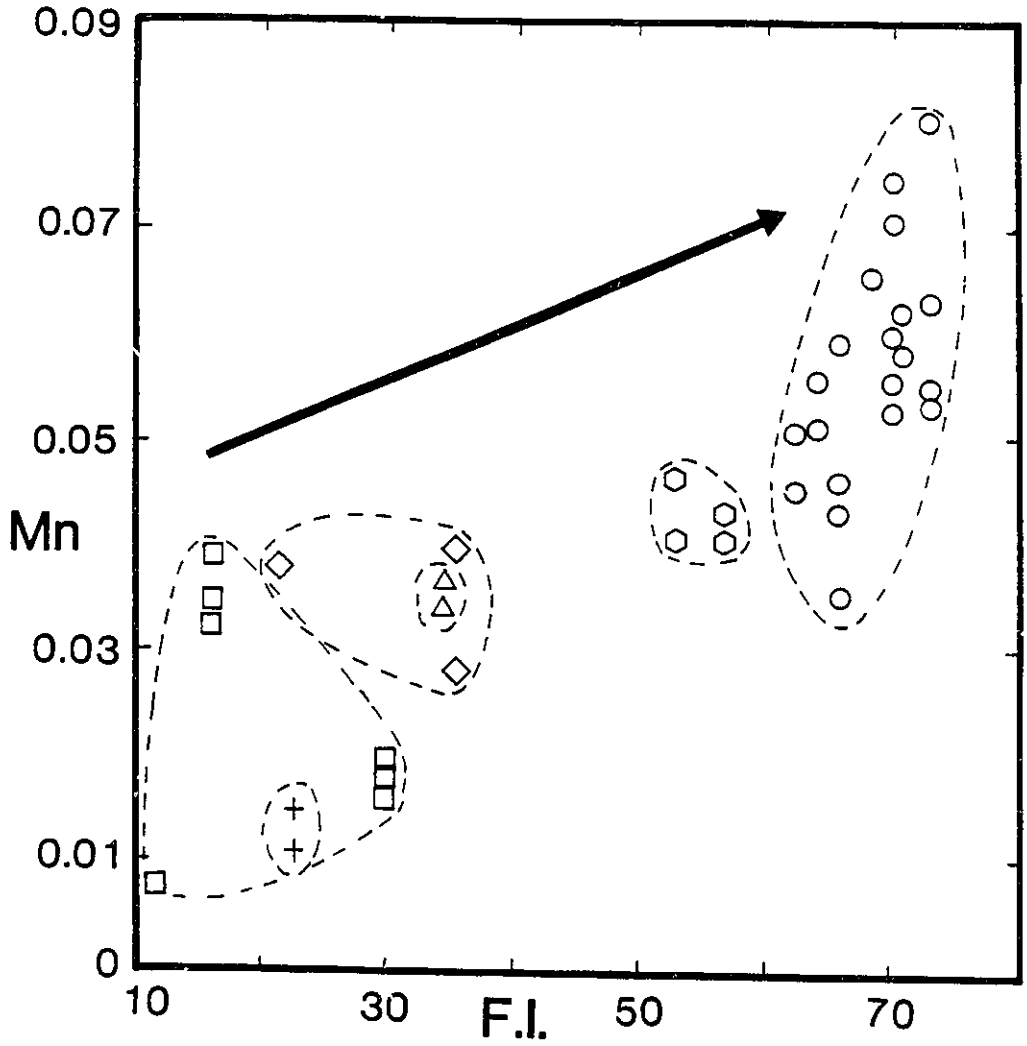

Fig. 9.-Mn content (a./f.u.) of Murdock Creek biotite vs. the host-rock normative fractionation index (F.I. defined in the caption to fig. 5). Symbols as in fig. 4.

ascribed Ti-poor rims in biotite to the decreasing solubility of Ti in biotite with decrease in temperature (e.g., Anderson 1980; Ague and Brimhall 1988). Another possible control on Ti distribution is the Fe content of the biotite, because increasing Fe in the phlogopite structure is known to enhance Ti solubility (Edgar et al. 1976; Robert 1976); however, biotites from Murdock Creek have uniform Fe contents. It has also been experimentally demonstrated that Ti solubility in phlogopite decreases with increasing pressure (Edgar et al. 1976; Robert 1976) but, as already noted, we consider the intrusion to be a single intrusive body.

Fluorine and Cl contents in biotite range from 0.051 to 0.598 a./f.u. and from nil to 0.082 a./f.u., respectively. Fluorine is observed to increase with differentiation of the magma (fig. 10), whereas Cl contents remain consistently low, showing no correlatable change with fractionation. In general, owing to the well-established Fe-F and Mg-Cl avoidance effects (Munoz 1984), the highest F contents should be found in more magnesian biotites, whereas Fe-rich biotites will contain the most Cl. However, because Murdock Creek biotites are all highly magnesian and do not show progressive Fe enrichment, increasing F content is likely due to an increase in the F content of the evolving melt (Fuge 1977; Czamanske et al. 1981). Fluorine buildup in the residual melt will be reflected in biotite, because it contains 70 to 90% of the F in muscovite- and fluorite-free granitoid rocks, the remainder being in apatite and titanite (Speer 1984).

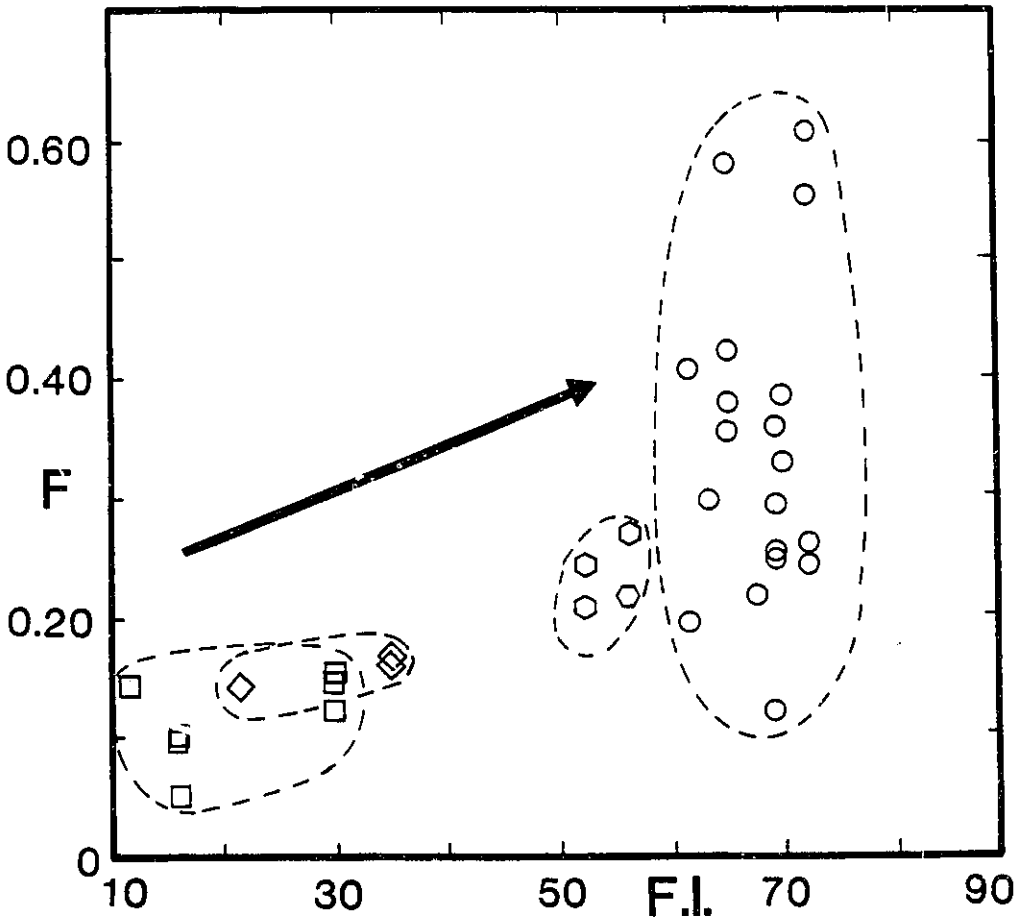

Fig. 10.-F content (a./f.u.) of Murdock Creek biotite vs. the host-rock normative fractionation index. Symbols as in fig. 4.

Because apatite is an abundant accessory in all rock types (up to 3 vol.%), it will have some minor influence on F distribution in the melt, but will not affect the observed F enrichment in biotite. Similar trends of F enrichment in biotite with increasing degree of magmatic fractionation have been observed in biotite from the Koloula igneous complex of the Solomon Islands (Chivas 1981) and the Inner Zone batholith of Japan (Czamanske et al. 1981).

Amphibole.-As previously noted, primary amphibole is absent in the differentiated suite of syenitic rocks comprising the Murdock Creek intrusion. However, magmatic amphibole ranging from edenitic hornblende to magnesio-hastingsitic hornblende occurs in the minor intrusive hornblendite unit. Because this unit is not part of the Murdock Creek intrusion proper, these amphibole compositions, though interesting, have limited bearing on the present study.

There is a wide compositional range of secondary amphiboles. Since these were formed almost entirely by the replacement of primary clinopyroxene, their abundance is dependent upon the extent of this replacement. In the western part of the intrusion, away from pluton margins, secondary amphibole is rare. Despite the paucity of secondary amphibole, their study is important in determining the composition and redox state of the deuteric fluids involved in their formation.

Mineral recalculation procedures for amphibole compositions listed in table 3 follow Leake (1978), with mineral formula based

TABLE 3

Compositions and Structural Formulae of Representative Amphibole

ROCK UNIT[a]	AS	AS	AS	AS	AS	AS	AS	MM	MD	CP	CP	CP	CP	CP	MB
SAMPLE	63028[b]	64037[b]	66001	10529[b]	11443	11747	10600[c]	29533[b]	12952	11598	11509[c]	13582[b]	65848	13037	32940[c]
AMPH. TYPE[d]	MG-HAS	MG-HAS	MG-HAS	ACTI	ACTI	ACTI	MGRIEB	MG-HAS	ACTI	MG-HHBL	TREM	MG-HAS	ACTI	PARGHB	MO-HHBL
# OF ANALYSES[e]	2	2	1	1	2	2	2	3	1	2	1	2	3	1	2
SiO_2	39.26	38.96	40.13	55.93	52.79	56.23	55.46	41.85	56.82	42.98	57.92	39.78	56.40	43.89	45.13
TiO_2	1.67	1.66	2.63	.08	.49	.09	.10	1.57	.04	1.53	.09	2.29	...	2.02	.89
Al_2O_3	10.75	10.51	11.07	.55	2.56	.56	.63	10.64	.99	10.83	.80	12.01	.36	10.94	9.34
Cr_2O_3	.05	.02	.02	...	...	...	...	.02	...	...	...	...	...	...	.19
Fe_2O_3	6.72	6.56	5.27	5.17	6.20	4.70	13.96	5.20	3.10	4.69	3.91	5.31	2.78	3.10	7.22
FeO	13.92	13.58	10.92	6.48	7.90	5.90	10.12	12.33	7.40	10.22	1.85	12.47	7.76	7.30	5.07
MnO	.41	.49	.42	.50	.48	.53	.24	.34	.25	.20	.23	.33	.50	.20	.26
MgO	9.13	9.18	11.05	17.26	15.69	16.99	9.85	11.61	18.06	12.49	21.32	10.62	17.41	13.47	15.76
CaO	10.19	10.13	10.99	10.41	9.31	11.35	1.90	11.76	12.59	11.52	11.85	11.29	11.28	11.64	11.56
Na_2O	3.58	3.86	3.49	1.41	2.62	.91	6.24	2.49	.31	2.51	.70	2.76	.75	2.08	2.56
K_2O	1.76	1.73	1.65	.18	.70	.14	.14	1.26	.06	1.15	.12	1.70	.08	1.21	.85
H_2O[f]	1.74	1.71	1.64	2.05	1.63	1.92	2.05	1.89	2.07	1.94	2.12	1.81	2.10	1.86	1.94
P	.41	.44	.71	.16	.99	.42	.06	.22	.19	.14	.17	.34	...	.33	.30
Cl	.03	.02	.02	...	.02	.02	...	.07	.03	.09	...	.09	.07	.02	.01
O≡F, Cl	.18	.19	.30	.07	.42	.18	.03	.11	.09	.08	.07	.16	.02	.14	.13
Total	99.44	98.66	99.77	100.11	100.96	99.58	100.72	101.14	101.82	100.21	101.01	100.63	99.47	97.92	100.95
Structural formulae based on 23 oxygens															
Si^{IV}	6.069	6.072	6.075	7.892	7.532	7.947	7.999	6.231	7.868	6.355	7.893	5.995	7.992	6.501	6.494
T=8 Al^{IV}	1.931	1.928	1.925	.091	.430	.053	.001	1.769	.132	1.645	.107	2.005	.008	1.499	1.506
Fe^{3+IV}	...	...	...	.017	.038	...	...	...	...	...	...	...	...	...	...
Al^{VI}	.027	.002	.050	...	...	.041	.106	.097	.029	.243	.021	.128	.052	.411	.077
Fe^{3+}	.782	.759	.600	.532	.628	.500	1.515	.583	.323	.522	.401	.602	.296	.346	.782
Ti	.194	.195	.299	.008	.053	.010	.011	.176	.004	.170	.009	.260	...	.225	.096
Cr	.006	.002	.002	...	...	...	...	.002	...	...	...	...	...	...	.022
Mg	2.104	2.133	2.494	3.631	3.337	3.580	2.118	2.577	3.728	2.753	4.331	2.386	3.678	2.974	3.381
Fe^{2+}	1.799	1.770	1.382	.765	.943	.697	1.221	1.535	.857	1.264	.211	1.572	.920	.904	.610
Mn	.054	.065	.054	.060	.039	.063	.029	.030	.029	.025	.026	.042	.054	.025	.032
EC	4.966	4.936	4.881	4.996	5.000	4.891	5.000	5.000	4.970	4.976	4.999	4.990	5.000	4.885	5.000
Mn	...	...	...	...	.019	...	...	.013	...	...	...	...	.006	...	...
Ca	1.688	1.691	1.783	1.574	1.423	1.719	.294	1.876	1.868	1.825	1.730	1.823	1.713	1.847	1.782
Na	.312	.309	.217	.386	.558	.249	1.706	.111	.083	.175	.185	.177	.206	.153	.218
EB	2.000	2.000	2.000	1.960	2.000	1.968	2.000	2.000	1.951	2.000	1.915	2.000	1.925	2.000	2.000
Na	.761	.858	.807	...	.167	...	.039	.607	...	.545	...	.629	...	.445	.496
K	.347	.344	.319	.032	.127	.025	.026	.239	.011	.217	.021	.327	.014	.229	.156
EA	1.108	1.202	1.126	.032	.294	.025	.065	.846	.011	.762	.021	.956	.014	.674	.652
F	.200	.217	.340	.071	.447	.188	.027	.104	.083	.065	.073	.162	...	.155	.137
Cl	.008	.005	.005	...	.005	.005	...	.018	.007	.023	...	.023	.017	.005	.002
Fe/(Fe+Mg)	.551	.543	.443	.266	.325	.251	.564	.451	.240	.393	.124	.477	.248	.296	.292
Fe^{3+}/ (Fe^{2+}+Fe^{3+})	.303	.303	.303	.418	.414	.418	.554	.275	.274	.292	.655	.277	.244	.276	.562
Rock F.I.[g]	68.20	70.13	69.79	69.90	65.72	70.69	na	34.35	21.54	29.97	29.97	16.28	23.50	11.52	22.62

NOTE.-na = not analysed.

[a] Rock units as in table 1.

[b] FeO/Fe_2O_3 estimated from analyses of amphiboles in the same rock unit.

[c] Fe^{3+} contents were calculated on the basis of 23 oxygens and then adjustment of the total cations, excluding (Ca+Na+K), to 13 by varying $Fe^{3+}/(Fe^{2+}+Fe^{3+})$.

[d] Amphibole classification according to the criteria of Leake (1978): MG-HAS, magnesian hastingsite; ACTI, actinolite; PARGHB, parqasitic hornblende; MG-HHBL magnesian hastingsitic hornblende; MGRIEB, magnesio-riebeckite; TREM, tremolite; MO-HHBL, magnesio-hastingsitic hornblende.

[e] Number of analyses averaged.

[f] H_2O calculated by assuming (OH,F,Cl) = 2.

[g] Rock F.I. = host-rock normative fractionation index.

on 23 oxygens and assuming OH+F+Cl = 2.00. In cases where Si and Al did not suffice to fill the tetrahedral site, Fe^{3+} was used before Cr^{3+} to complete site occupancy to 8.00, as suggested by Hawthorne (1983). Seven amphibole separates were obtained for wet chemical determination of Fe^{3+} and Fe^{2+}. As with biotite, the appropriate $Fe^{3+}/(Fe^{2+}+Fe^{3+})$ ratios were then used to adjust structural formulae for other amphibole analyses. For several types of amphibole where wet chemical determinations of $Fe^{3+}/(Fe^{2+}+Fe^{3+})$ were unavailable, Fe^{3+} contents were calculated on the basis of 23 oxygens and adjustment of the total cations, excluding (Ca+Na+K), to 13 by varying $Fe^{3+}/(Fe^{2+}+Fe^{3+})$, following procedures discussed by Robinson et al. (1982). However, because of the uncertainty introduced by stoichiometric calculation of Fe^{3+} (Hawthorne 1983), these particular ratios are used only for purposes of amphibole classification.

Except for secondary magnesio-riebeckite, which is classified as an alkali amphibole, all amphiboles including primary hornblende are calcic amphiboles. On the basis of textural and chemical characteristics three main varieties of secondary amphibole are defined: (1) actinolite (very minor tremolite could also be included in this group) (2) magnesian hastingsite, which also includes magnesio-hastingsitic hornblende and magnesian hastingsitic hornblende (plus one analysis of pargasitic hornblende (sample 13037 in table 3)) and (3) magnesio-riebeckite. All secondary amphiboles are rich in Mg, reflecting the low Fe/(Fe+Mg) ratios of the primary

clinopyroxenes which they have replaced. Fe/(Fe+Mg) ratios range from 0.20 to 0.33 in actinolite (0.12 for rare tremolite), 0.29 to 0.55 in hastingsite, and 0.55 to 0.60 in magnesio-riebeckite. $Fe^{3+}/(Fe^{2+}+Fe^{3+})$ ratios determined by wet chemical methods tend to be highest in actinolite (0.41-0.42) and lowest in magnesian hastingsite (0.25-0.30); both ranges are consistent with the high overall abundance of Fe^{3+} in precursor clinopyroxene. Although high Fe^{3+} was inherited from diopside, the retention of high $Fe^{3+}/(Fe^{2+}+Fe^{3+})$ ratios, especially in actinolites, suggests that the deuteric fluids were also relatively oxidized. Association of magnesio-riebeckite with alkali-feldspar syenite pegmatite is also compatible with the existance of highly oxidized late- to post-magmatic fluids. Ernst (1960) has shown that magnesio-riebeckite is stable over a wide range of temperatures and pressures (max 935 ^{o}C under P_{H_2O} = 2 kb) at high f_{O_2} along the HM buffer.

In addition to low Fe/(Fe+Mg) and high $Fe^{3+}/(Fe^{2+}+Fe^{3+})$ ratios, the major element chemistry of the secondary amphiboles, in particular magnesian hastingsite, is clearly reflective of the magmatic conditions under which the replaced clinopyroxenes crystallized. Both Al and Ti contents in magnesian hastingsite are noncorrelative with respect to each other and to changes in host-rock composition, mimicking the relationship which exists between these two cations in diopside. Ca, Na, and Mn contents also duplicate the magmatic fractionation trends recorded by these elements in diopside; Ca decreases slightly while both Na

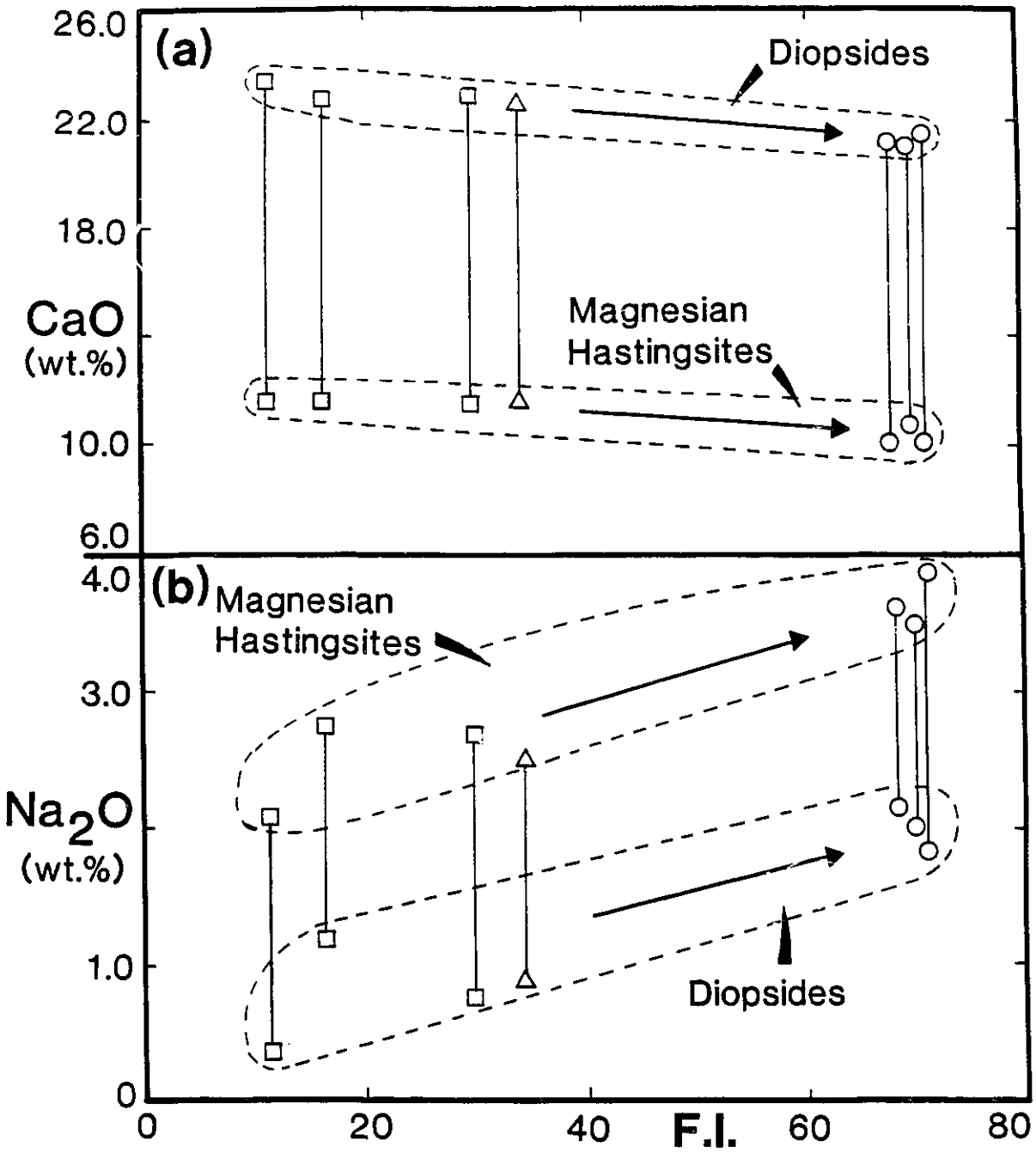

Fig. 11.-Covariation of (a) CaO and (b) Na_2O contents (wt.%) in primary diopside and secondary magnesian hastingsite with host-rock normative fractionation index. Tie-lines join individual grains of diopside with their replacement rims of magnesian hastingsite. Arrows indicate compositional trends with increasing degree of fractionation. Symbols as in fig. 4.

and Mn increase appreciably in magnesian hastingsites from progressively more differentiated units (fig. 11). Unlike the nearly isochemical replacement of clinopyroxene by actinolite (plus a minor calcic phase), the formation of magnesian hastingsite requires additional Al and Na not found in diopside. Mineral textures indicate that the required Al and Na is liberated from adjacent alkali-feldspar, or more rarely from plagioclase which has been replaced along with clinopyroxene (fig. 3d). Potassium derived from the breakdown of perthite is accomodated by the formation of small quantities of secondary biotite. Excess Ca left over from plagioclase and diopside yields epidote and calcite. Similar replacement reactions are associated with secondary amphibole formation in the East Bull Lake anorthosite-gabbro complex, Ontario (Kamineni 1986).

Magnetite.-Magnetite (table 4) is almost pure Fe_3O_4 due to recrystallization and now contains little Ti, Cr, Mn, Mg, or Ni (total, 0.41-0.60 wt.%). Energy dispersive X-ray spectra showed negligible amounts of Si, Al, V, and Zn, which are not reported. Fe^{3+} was calculated on a stoichiometric basis assuming 3 cations and 4 oxygens. The methods of Buddington and Lindsley (1964) and Spencer and Lindsley (1981) permit estimation of the f_{O_2} and temperature of a magma from the compositions of coexisting magnetite and ilmenite. However, coexisting ilmenite is not present and this method cannot be used. It would still be possible to obtain a rough approximation of f_{O_2} using the Ti content of magnetite (usually in the percent range) were its

TABLE 4

Compositions and Structural Formulae of Representative Magnetite

ROCK UNIT[a]	AS	AS	AS	MD	CP	CP
SAMPLE	11869	11870	11872	13273	13574	13575
TiO_2	.03	.04	.03	.22	.02	.07
Cr_2O_3	.26	.36	.25	.28	.31	.29
Fe_2O_3	68.85	68.71	68.94	68.62	68.91	68.90
FeO	30.98	31.00	30.96	31.30	31.11	31.06
MnO	.12	.12	.12	.04	.04	.09
MgO	.02	.01	.03	...	...	.02
NiO	.01	.01	.05	.06	.04	.07
Total	100.27	100.25	100.37	100.53	100.43	100.50
FeO[b]	92.94	92.84	93.00	93.06	93.13	93.07
Structural formulae based on 3 cations and 4 oxygens						
Ti	.001	.001	.001	.006	.001	.002
Cr	.008	.011	.007	.008	.009	.009
Fe^{3+}	1.990	1.987	1.991	1.979	1.989	1.988
Fe^{2+}	.995	.996	.994	1.003	.998	.996
Mn	.004	.004	.004	.001	.001	.003
Mg	.001	.001	.002	...	...	.001
Ni	...	...	.002	.002	.001	.002

[a] Rock units as in table 1.
[b] Total Fe calculated as FeO.

primary magmatic value undisturbed (Buddington and Lindsley 1964). Unfortunately, low minor-element contents and the widespread sphenitization of magnetite indicate a loss of Ti from the magnetite structure and preclude any precise estimation of magmatic f_{O_2}. Thus only a qualitative statement can be made about magmatic f_{O_2} using magnetite found in these rocks.

The fact that all units are devoid of ilmenite but contain abundant magnetite (typically 1-3 vol.%, but may be up to 5 vol.% in mafic rocks) is further evidence of high f_{O_2} in the magma throughout crystallization. A comparison may be drawn with the more "oxidized" magnetite-series granitoids of Ishihara (1977, 1981) which typically contain 1 to 2 vol.% magnetite and little or no ilmenite. Note that the greater abundance of primary magnetite in the mafic units does not imply higher magmatic f_{O_2}. The amount of magnetite precipitated from a magma is not only dependent on f_{O_2}, but also on the Fe content in the magma, which is higher for mafic magmas.

DISCUSSION

Magma Evolution.-Octahedral-Al contents of diopside from all rock types support field evidence (e.g., absence of a thermal contact aureole or fine-grained chilled-margin) for emplacement of the Murdock Creek pluton at mid-crustal depths. The Al^{VI} contents are higher than those found in many well-documented shallow-level intrusions such as Ben Nevis (Haslam 1968), Finnmarka (Czamanske and Wones 1973), and Baie-des-Moutons

(Lalonde and Martin 1983). Constancy of Al^{VI} content from one unit to another supports the interpretation that the pluton is a single differentiated body which crystallized under a constant total pressure.

Evidence that the intrusion has evolved under low water pressure throughout its crystallization history includes: (1) the minor abundance of primary hydrous phases, (2) hypersolvus feldspar mineralogy (Martin and Bonin, 1976), (3) the absence of vesiculation features (e.g., miarolitic cavities), (4) the scarcity of alkali-feldspar syenite pegmatites, and (5) the general lack of deuteric alteration in the western rock units studied. A low content of dissolved water in the melt favoured the early formation of anhydrous mineral phases. Thus, diopside and calcic plagioclase (An_{30-34}) crystallized first, causing a gradual depletion of Ca and a buildup of alkalis in the evolving melt. This is reflected in decreasing Ca and increasing Na contents of diopside from later differentiates. Similarly, the regular trends of increasing F and decreasing Ti contents in biotite from progressively more evolved rock types are consistent with a slowly cooled magma undergoing minor volatile buildup. Increasing Mn content in biotite from more felsic units reflects the control of host-rock composition over mineral/melt partitioning.

Lack of primary compositional zoning in the ferromagnesian phases can be interpreted to indicate that the minerals crystallized under nearly constant conditions, especially f_{O_2}.

Less likely, in our opinion, is the possibility they had time to continually re-equilibrate with the magma during their growth (e.g., Neumann 1976). These two interpretations however are not mutually exclusive, and it is possible that both re-equilibration during slow cooling and uniform crystallization conditions combined to yield homogeneous crystals. Unfortunately the absence of orthopyroxene, olivine, and fresh Fe-Ti oxides precludes the application of a number of potentially useful geothermometers for directly estimating the temperature drop between units, or the likely crystallization interval. However, melting experiments on chemically and mineralogically similar syenites can provide reasonable estimates of liquidus and solidus temperatures. A nepheline syenite from Tugtutôq, South Greenland (Piotrowski and Edgar 1970, specimen 50241) possessing an agpaitic index of 0.91, hypersolvus feldspar, and only minor amounts of primary hydrous ferromagnesian minerals (5.0 modal%) had a melting interval of ≈ 233 °C with a liquidus temperature of 1165 °C and a solidus temperature of 932 °C at 1 atm in air (dry). Similar melting experiments by McDowell and Wyllie (1971) on a ferroaugite syenite (26135) and a syenite (26005) from the Kûngnât syenite complex of southwest Greenland also warrant comparison; both specimens are hypersolvus syenites with agpaicities of 0.82 and 0.95 respectively, contain relatively Mg-rich pyroxene (ferroaugite) and minor biotite, and are just-undersaturated with 0.9 wt.% nepheline in the CIPW norm. At a relatively "dry" low pressure (P_{H_2O} = 1 kb) they measured a liquidus temperature of ≈

900 °C, but noted that the hypersolvus feldspar mineralogy suggests a liquidus temperature on the order of 1000 °C (i.e., less than 1 kb P_{H_2O} is required for the precipitation of one feldspar in the Kûngnât syenites). The solidus temperature at P_{H_2O} = 1 kb was about 800 °C, but in fact is probably somewhat higher, once again due to the hypersolvus nature of the rocks.

It is thus a reasonable assumption that the melasyenite and alkali-feldspar syenite forming the main mass of the Murdock Creek intrusion had a crystallization interval ranging below a liquidus temperature of 1165 °C and above a solidus temperature of approximately 800 °C. The liquidus temperatures of the earlier crystallizing mafic and ultramafic differentiates may have been higher.

Late-stage volatile saturation was apparently achieved for only a small quantity of residual syenitic melt, hence the restricted occurrence of pegmatitic alkali-feldspar syenite, in contrast to the widespread development of pegmatite common in water-rich, near-surface plutons.

Magmatic oxidation in the Murdock Creek intrusion.-Our most significant finding is the unusually high intrinsic oxygen fugacity ($\approx 10^{-12}$ bars) that prevailed throughout crystallization. This is evidenced by (1) the presence of early-formed magnetite and titanite inclusions in diopside and calcic plagioclase from the early-crystallized mafic marginal units; (2) the absence of ilmenite in the intrusion; and (3) the exceptionally low Fe/(Fe+Mg) and high $Fe^{3+}/(Fe^{2+}+Fe^{3+})$ ratios in

clinopyroxene and biotite from all rock units. Titanite formation was first shown by Verhoogen (1962) to require relatively oxidizing conditions, confirmed by the subsequent studies of Wones (1966, 1989), Carmichael and Nicholls (1967), Lipman (1971), and Czamanske and Wones (1973). Note that the ferric-ferrous ratio in the primary ferromagnesian minerals may have been enhanced to some extent by the alkalinity of the already evolved pulse of syenitic magma forming the intrusion (e.g., Paul and Douglas 1965; Carmichael and Nicholls 1967), although the Fe_2O_3/FeO ratio in natural silicate liquids (and hence crystallizing solid phases) is dominantly a function of oxygen fugacity and temperature (Kilinc et al. 1983; Cristie et al. 1986).

There have been numerous explanations for high magmatic f_{O_2}; most involve processes that cause f_{O_2} to <u>increase</u> during crystallization. For water to facilitate oxidation, it must first be exsolved, then dissociate into H_2 and O_2, followed by the preferential escape of H_2 gas (Osborn 1959; Sato and Wright 1966). This process was invoked by Czamanske and Wones (1973) to account for ferromagnesian silicate and opaque oxide evidence of increasing f_{O_2} during evolution of the Finnmarka complex, Norway. With this process, oxidation of magma should balance with reduction above the crystallizing pluton. Evidence of such reactions has been reported for the high-level magmatic system at Questa, New Mexico (Czamanske 1989). This process of progressive magmatic oxidation by dissociation of H_2O and loss of H_2 has been

evaluated by Candela (1986) who showed that it would only be effective for magmas with high water contents relative to Fe ($H_2O/FeO \geq 10$, wt.% ratio). The relatively high Fe and low water content of the Murdock Creek magma, together with a lack of evidence for reduction during alteration near the intrusion, suggests that H_2O evolution did not significantly contribute to oxidation at Murdock Creek.

An example of a magma that started crystallizing at relatively high f_{O_2}, which was maintained throughout crystallization, is the Ben Nevis intrusion, Scotland. Haslam (1968) suggested that the maintenance of high f_{O_2} through the last stages of crystallization was caused by the addition of O_2 from an external source. Ring fractures associated with the high-level intrusion were suggested to have provided a means through which the magmas cooling below could have become directly contaminated with atmospheric oxygen. Wones (1981) and Candela (1986) postulated that oxygenated meteoric water may have been indirectly involved in the oxidation of some intrusions. For the Murdock Creek pluton, externally imposed (open-system) oxidation is neither feasible nor necessary, as both the hydrosphere and atmosphere were reduced during the Archean (Cameron 1982). We suggest that the magma was able to maintain the high initial f_{O_2} throughout its evolution, without requiring the gain/loss of oxidized/reduced species. In other words, magmatic evolution took place in a closed system with respect to oxygen and the magma was intrinsically oxidized. This conclusion is entirely congruent

with our interpretation that the intrusion was emplaced at mid-crustal depths; progressive oxidation by H_2 loss is more to be expected in high level magma chambers.

Implications for gold mineralization.-The relevance of this study to concepts for the origin of Archean quartz-carbonate gold deposits derives from the observation that the mafic magma from which the pluton was derived, was intrinsically oxidized, rather than being oxidized in situ during crystallization. This implies an oxidized source region where partial melting occurred. Whether an oxidized fluid evolved from the source region, or from the melt, extraction of gold would be facilitated, analogous to heap leaching where oxygenated fluids percolate the ore.

Detailed consideration of the source of the mafic magma is beyond the scope of this paper. However, it is widely believed that large-ion-lithophile element (LILE) enriched alkaline magmas, such as that which crystallized to form the Murdock Creek intrusion (Rowins et al. in prep.), were derived from metasomatized mantle (e.g., Boettcher et al. 1979; Harte 1987). Mantle metasomatism is frequently accompanied by the evolution of CO_2-rich fluids, which may extract gold as they rise through pervasively permeable, ductile shear zones in the upper mantle and lower crust (Cameron 1989b, 1989c). Further, silicate melts formed in such an environment are initially saturated in CO_2, which causes a CO_2-H_2O fluid to be released in response to declining pressure as the melt rises (Holloway 1976). Such fluids also may extract gold (Cameron and Hattori 1987). One possible

explanation for the low H_2O content of the magma is dehydration imposed by early evolution of CO_2 from the melt, a process which extracts H_2O even if the melt was not saturated in H_2O.

CONCLUSIONS

The Murdock Creek intrusion crystallized from intrinsically oxidized magma under conditions of low P_{H_2O} and unusually high and constant $f_{O_2} \approx 10^{-12}$ bars. The compositions of secondary amphibole, formed by post-magmatic alteration of diopside and biotite, and the oxidation of magnetite, show that deuteric fluids were likewise strongly oxidized. Textural and chemical changes recorded in the ferromagnesian minerals support field relations and confirm the earlier interpretation by Rowins et al. (1989a) that the pluton represents a single pulse of already evolved syenitic magma which crystallized and differentiated *in situ* at mid-crustal levels. The rock units produced are essentially simple modal variants related mainly through the fractionation of early-formed diopside and plagioclase (An_{30-34}), with alkali-feldspar becoming increasingly important as crystallization proceeds.

Compositional trends in diopside and biotite accord with magmatic fractionation of early-formed diopside and calcic plagioclase and reflect the increasing buildup of alkalis and minor volatiles in the residual melt. Volatile saturation achieved during the terminal stages of magma consolidation resulted in hydrofracturing of enclosing syenitic rocks and

intrusion of minimal amounts of residual H_2O-rich melt along such fractures, giving rise to a minor series of pegmatitic alkali-feldspar syenite dykes. Volatiles were also involved in relatively minor secondary alteration phenomena: patchy metasomatic replacement of diopside by aegirine-augite; incipient chloritization of biotite; the growth of various secondary amphiboles; subsolidus oxidation of primary magnetite; and formation of secondary magnetite and hematite by oxidation of diopside and biotite. High, constant f_{O_2}, maintained to the last stages of crystallization, is believed to have been caused by slow cooling in a closed system with respect to oxygen over a wide temperature interval.

Intrinsic oxidation of the original mafic alkaline melt, from which the other rock units of the pluton were ultimately derived, implies an oxidized source region, presumably metasomatized mantle. Low water content in the magma is consistent with formation of the partial melt in the presence of CO_2-rich fluid. The resulting saturation of the melt in CO_2 would cause the extraction of a CO_2-H_2O fluid as the melt rose, effectively dehydrating the melt. The presence of oxidized source rocks and melts and of a CO_2-H_2O fluid creates the appropriate conditions for the extraction of gold from the source region, from the melt, or from the lower crust through which the fluids rose. This accords with previous studies that have shown the gold mineralization within this important camp to have been formed from oxidized, CO_2-bearing fluids. It is unlikely that the

specific pulse of magma responsible for the Murdock Creek intrusion was, itself, directly involved in the formation of these ores, since portions of the pluton have been affected by gold-related alteration and thus pre-date the mineralization.

Acknowledgments.-We thank Dr. Moyra MacKinnon for instruction on the use of the McGill probe, and Mr. Maurizio Bonardi for assistance with probe work carried out at the Geological Survey of Canada. A careful review of the manuscript by G.K. Czamanske is gratefully acknowledged. This research was funded by an NSERC grant to E.M.C.

REFERENCES CITED

Ague, J.J., and Brimhall, G.H., 1988, Regional variations in bulk chemistry, mineralogy, and the compositions of mafic and accessory minerals in the batholiths of California: Geol. Soc. Amer. Bull., v. 100, p. 891-911.

Akella, J., and Boyd, F.R., 1973, Partitioning of Ti and Al between coexisting silicates, oxides, and liquids: Proceedings of the 4th lunar science conference, v. 4, p. 1049-1059.

Anderson, J.L., 1980, Mineral equilibria and crystallization conditions in the late Precambrian Wolf River rapakivi massif, Wisconsin: Amer. Jour. Sci., v. 280, p. 289-332.

Aoki, K., and Kushiro, I., 1968, Some clinopyroxenes from ultramafic inclusions in Dreiser Weiher, Eifel: Contrib. Mineral. Petrol., v. 18, p. 326-337.

Bédard, J.H.J.; Francis, D.M.; and Ludden, J.N., 1988, Petrology and pyroxene chemistry of Monteregian dykes: The origin of concentric zoning and green cores in clinopyroxenes from alkali basalts and lamprophyres; Can. Jour. Earth Sci., v. 25, p. 2041-2058.

Boettcher, A.E.; O'Neil, J.R.; Windom, K.E.; Stewart, D.C.; and Wilshire, H.G., 1979, Metasomatism of the mantle and the genesis of kimberlites and alkali basalts, in Boyd, F.R., and Meyer, H.O.A., eds., The mantle sample: inclusions in kimberlites and other volcanics: Amer. Geophys. Un. Spec. Publ., p. 173-182.

Brown, G.M., 1967, Mineralogy of basaltic rocks, in Hess, H.H., and Poldervaart, A., eds., Basalts 1: New York, Interscience, p. 103-162.

Buddington, A.F., and Lindsley, D.H., 1964, Iron-titanium oxide minerals and synthetic equivalents: Jour. Petrol., v. 5, p. 310-357.

Burrows, A.G., and Hopkins, P.E., 1923, Kirkland Lake gold area: Ont. Dept. Mines Ann. Rep. 1923, v. 32, pt. 4, 96 p.

Cameron, E.M., 1982, Sulphate and sulphide reduction in early Precambrian oceans: Nature, v. 296, p. 145-148.

_____ 1988, Archean gold: Relation to granulite formation and redox zoning in the crust: Geology, v. 16, p. 109-112.

_____ 1989a, Scouring of gold from the lower crust: Geology, v. 17, p. 26-29.

_____ 1989b, Derivation of gold by oxidative metamorphism of a deep ductile shear zone: Part 1. Conceptual model: Jour. Geochem. Explor., v. 31, p. 135-147.

_____ 1989c, Derivation of gold by oxidative metamorphism of a deep ductile shear zone: Part 2. Evidence from the Bamble belt, south Norway: Jour. Geochem. Explor., v. 31, p. 149-169.

_____, and Carrigan, W.J., 1987, Oxygen fugacity of Archean felsic magmas: Relationship to gold mineralization, in Current research. Part A: Geol. Surv. Can. Pap. 87-1A, p. 281-298.

_____, and Hattori, K., 1987, Archean gold mineralization and

oxidized hydrothermal fluids: Econ. Geol., v. 82, p. 1177-1191.

Candela, P.A., 1986, The evolution of aqueous vapour from silicate melts: Effect on oxygen fugacity: Geochim. Cosmochim. Acta, v. 50, p. 1205-1211.

Carmichael, I.S.E., 1967, The iron-titanium oxides of salic volcanic rocks and their associated ferromagnesian silicates: Contrib, Mineral. Petrol., v. 14, p. 36-64.

_____, and Nicholls, J., 1967, Iron-titanium oxides and oxygen fugacities in volcanic rocks: Jour. Geophys. Res., v. 72, p. 4665-4687.

_____; _____; and Smith, A.L., 1970, Silica activity in igneous rocks: Amer. Mineral., v. 55, p. 246-263.

Cawthorn, R.G., and Collerson, K.D., 1974, The recalculation of pyroxene end-member parameters and the estimation of ferrous and ferric iron content from electron microprobe analyses: Amer. Mineral., v. 59, p. 1203-1208.

Chivas, A.R., 1981, Geochemical evidence for magmatic fluids in porphyry copper mineralization. Part 1. Mafic silicates from the Koloula igneous complex: Contrib. Mineral. Petrol., v. 78, p. 389-403.

Czamanske, G.K., 1989, Evidence of reduction and the evolution of metaluminous to peralkaline magma, Questa, New Mexico, U.S.A.: New Mex. Bur. Mines and Min. Res. Bull., no. 131, p. 65.

_____; Ishihara, S.; and Aitkin, S.A., 1981, Chemistry of

rock-forming minerals of the Cretaceous-Paleocene batholith in southwestern Japan and implications for magma genesis: Jour. Geophys. Res., v. 86, no. B11, p. 10431-10469.

_____, and Wones, D.R., 1973, Oxidation during magmatic differentiation, Finnmarka complex, Oslo area, Norway. Part II: The mafic silicates: Jour. Petrol., v. 14, p. 349-380.

Cristie, D.M.; Carmichael, I.S.E.; and Langmuir, C.H., 1986, Oxidation states of mid-ocean ridge basalt glasses: Earth Planet. Sci. Lett., v. 79, p. 397-411.

Deer, W.A.; Howie, R.A.; and Zussman, J., 1963, Rock-forming minerals. Volume 3, sheet silicates: London, Longmans, Green and Co., Ltd., 270 p.

_____; _____; and _____ 1978a, Rock-forming minerals. Volume 3, sheet silicates: London, Longmans Group Ltd., p. 114-123.

_____; _____; and _____ 1978b, Rock-forming minerals. Volume 2A, single-chain silicates: London, Longmans Group Ltd., p. 202-220.

Dillet, B., and Czamanske, G.K., 1987, Aspects of the petrology, mineralogy, and geochemistry of the granitic rocks associated with Questa caldera, New Mexico: U.S. Geol. Surv. Open-File Rep., v. 258, 238 p.

Dodge, F.C.W., and Moore, J.G., 1968, Occurrence and composition of biotites from the Cartridge Pass pluton of the Sierra Nevada batholith, California: U.S. Geol. Surv. Prof. Pap. 600-B, p. B6-B10.

Edgar, A.D.; Condliffe, E.; Barnett, R.L.; and Shirran, R.J., 1980, An experimental study of an olivine ugandite magma and mechanisms for the formation of its K-enriched derivatives: Jour. Petrol., v. 21, p. 475-497.

_____; Green, D.H.; and Hibberson, W.O., 1976, Experimental petrology of a highly potassic magma: Jour. Petrol., v. 17. p. 339-356.

Evans, B.W., and Moore, J.G., 1968, Mineralogy as a function of depth in the prehistoric Makaopuhi tholeiitic lava lake, Hawaii: Contrib. Mineral. Petrol., v. 17, p. 85-115.

Ernst, W.G., 1960, The stability relations of magnesioriebeckite: Geochim. Cosmochim. Acta, v. 19, p. 10-40.

Fodor, R.V.; Keil, K.; and Bunch, T.E., 1975, Contributions to the mineral chemistry of Hawaiian rocks. Part IV. Pyroxenes in rocks from Haleakala and West Maui volcanoes, Maui, Hawaii: Contrib. Mineral. Petrol., v. 50, p. 173-195.

Forbes, W.C., and Flower, M.F.J., 1974, Phase relations of titano-phlogopite, $K_2Mg_4TiAl_2Si_6O_{20}(OH)_4$: A refractory phase in the upper mantle?: Earth Planet. Sci. Lett., v. 22, p. 60-66.

Fudali, R.F., 1965, Oxygen fugacities of basaltic and andesitic magmas: Geochim. Cosmochim. Acta, v. 29, p. 1063-1075.

Fuge, R., 1977, On the behaviour of fluorine and chlorine during magmatic differentiation: Contrib. Mineral. Petrol., v. 61, p. 245-249.

Gamble, R.P., and Taylor, L.A., 1980, Crystal/liquid partioning

in augite: Effects of cooling rate: Earth Planet. Sci. Lett., v. 47, p. 21-33.

Gibb, F.G.F., 1973, The zoned clinopyroxenes of the Shant Isles sill, Scotland: Jour. Petrol., v. 4, p. 203-230.

Gupta, A.K.; Onuma, K.; Yagi, K.; and Lidiak, E.G., 1973, Effect of silica concentration on the diopsidic pyroxenes in the system diopside-$CaTiAl_2O_6$-SiO_2: Contrib. Mineral. Petrol., v. 41, p. 333-344.

Grove, T.L., and Bence, A.E., 1979, Crystallization kinetics in a multiply saturated basalt magma: An experimental study of Luna 24 ferrobasalt: Proceedings of the 10th lunar and planetary sciences conference, p. 439-478.

Groves, D.I., and Phillips, G.N., 1987, The genesis and tectonic control on Archaean gold deposits of the Western Australian Shield - a metamorphic replacement model: Ore Geol. Rev., v. 2, p. 287-322.

Haggerty, S.E., 1976, Opaque mineral oxides in terrestrial igneous rocks, in Rumble, D., ed., Reviews in mineralogy. Oxide minerals: Mineral. Soc. Amer., v. 3, p. 101-169.

Harte, B., 1987, Metasomatic events recorded in mantle xenoliths: An overview, in Nixon, P.H., ed., Mantle xenoliths: Chichester, John Wiley and Sons, p. 625-640.

Haslam, H.W., 1968, The crystallization of intermediate and acid magmas at Ben Nevis, Scotland: Jour. Petrol., v. 9, p. 84-104.

Hawthorne, F.C., 1981, The crystal chemistry of amphiboles: Can.

Mineral., v. 21, p. 173-480.

Hodgson, C.J., and MacGeehan, P.J., 1982, A review of the geological characteristics of " gold-only " deposits in the Superior Province of the Canadian Shield, in Geology of Canadian gold deposits: Can. Inst. Min. Metal. Spec. Vol. 24, p. 211-229.

Holloway, J.R., 1976, Fluids in the evolution of granitic magmas: Consequences of finite CO_2 solubility: Geol. Soc. Amer. Bull., v. 87, p. 1513-1518.

Hubert, C.; Trudel, P.; and Gelinas, L., 1984, Archean wrench fault tectonics and structural evolution of the Blake River Group, Abitibi belt, Quebec: Can. Jour. Earth Sci., v. 21, p. 1024-1032.

Hyde, R.S., 1980, Sedimentary facies in the Archean Timiskaming Group and their tectonic implications, Abitibi greenstone belt, northeastern Ontario, Canada: Precambrian Res., v. 12, p. 161-195.

Irvine, T.N., Terminology for layered intrusions: Jour. Petrol., v. 23, p. 127-162.

Ishihara, S., 1977, The magnetite-series and ilmenite-series granitic rocks: Mining Geol., v. 27, p. 293-305.

_____ 1981, The granitoid series and mineralization: Econ Geol. 75th Anniversary Vol., p. 458-484.

Jensen, L.S., 1978, Archean komatiitic, tholeiitic, calc-alkaline and alkalic volcanic sequences in the Kirkland Lake area, in Currie, A.L., and Mackasey, W.O., eds., Toronto '78 field

trips guidebook: Geol. Assoc. Can., p. 327-359.

_____, and Langford, F.F., 1985, Geology and petrogenesis of the Archean Abitibi belt in the Kirkland Lake area, Ontario: Ont. Geol. Surv. Misc. Pap. 123, 130 p.

Jolly, W.T., 1974, Regional metamorphic zonation as an aid in the study of Archean terrains: Abitibi regions, Ontario: Can. Mineral., v. 12, p. 499-508.

Kamineni, D.C., 1986, A petrochemical study of calcic amphiboles from the East Bull Lake anorthosite-gabbro layered complex, District of Algoma, Ontario: Contrib. Mineral. Petrol., v. 93, p. 471-481.

Kerrich, R., 1987, The stable isotope geochemistry of Au-Ag vein deposits in metamorphic rocks, in Kyser, T.K., ed., Stable isotope geochemistry of low-temperature fluids: Mineral. Assoc. Can. Short Course, no. 13, p. 287-336.

_____, 1989, Source processes for Archean Au-Ag vein deposits: evidence from lithophile-element systematics of the Hollinger-McIntyre and Buffalo Ankerite deposits, Timmins: Can. Jour. Earth Sci., v. 26, p. 755-781.

Kilinc, A.: Carmichael, I.S.E.; Rivers, M.L.; and Sack, R.O., 1983, The ferric-ferrous ratio of natural silicate liquids equilibrated in air: Contrib. Mineral. Petrol., v. 83, p. 136-140.

Kushiro, I., 1960, Si-Al relation in clinopyroxenes from igneous rocks: Amer. Jour. Sci., v. 258, p. 548-554.

_____ 1969, Clinopyroxene solid solutions formed by reactions

between diopside and plagioclase at high pressures: Mineral. Soc. Amer. Spec. Pap. 2, p. 179-191.

Lalonde, A.E., and Martin, R.F., 1983, The Baie-des-Moutons syenitic complex, La Tabatière, Quebec. Part II. The ferromagnesian minerals: Can. Mineral., v. 21, p. 81-91.

Larsen, L.M., 1976, Clinopyroxenes and coexisting mafic minerals from the alkaline Ilimaussaq intrusion, South Greenland: Jour. Petrol., v. 17, p. 258-290.

Leake, B.E., 1978, Nomenclature of amphiboles: Can. Mineral., v. 16, p. 501-520.

Lebas, M.J., 1962, The role of aluminum in igneous clinopyroxenes with relation to their parentage: Amer. Jour. Sci., v. 260, p. 267-288.

Lipman, P.W., 1971, Iron-titanium oxide phenocrysts in compositionally zoned ash-flow sheets from southern Nevada: Jour. Geol., v. 79, p. 438-456.

Mahmood, A., 1983, Chemistry of biotites from a zoned granitic pluton in Morocco: Mineral. Mag., v. 47, p. 364-369.

Marmont, S., and Corfu, F., 1988, Timing of gold introduction in the late Archean tectonic framework of the Canadian Shield: Evidence from U-Pb zircon geochronology of the Abitibi Sub-Province, in Goode, A.D.T., and Bosma, L.I., eds., Bicentennial gold '88 extended abstracts and oral program: Geol. Soc. Australia Abs. Ser., no. 22, p. 45-50.

Martin, R.F., and Bonin, B., 1976, Water and magma genesis: The association hypersolvus granite-subsolvus granite: Can.

Mineral., v. 14, p. 228-237.

M^{c}Dowell, S.D., and Wyllie, P.J., 1971, Experimental studies of igneous rock series: The Kûngnât syenite complex of southwest Greenland: Jour. Geol., v. 79, p. 173-194.

McGuire, A.V.; Dyar, M.D.; and Ward, K.A., 1989, Neglected Fe^{3+}/Fe^{2+} ratios - A study of Fe^{3+} content of megacrysts from alkali basalts: Geology, v. 17, p. 687-690.

Mitchell, R.H., and Platt, R.G., 1978, Mafic mineralogy of ferroaugite syenite from the Coldwell alkalic complex, Ontario, Canada: Jour. Petrol., v. 19, p. 627-651.

Morimoto, N., 1988, Nomenclature of pyroxenes: Mineral. Petrol., v. 39, p. 55-76.

Munoz, J.L., 1984, F-OH and Cl-OH exchange in micas with applications to hydrothermal ore deposits, in Bailey, S.W., ed., Reviews in mineralogy. Micas: Mineral. Soc. Amer., v. 13, p. 469-491.

Nash, W.P., and Wilkinson, J.F.G., 1970, Shonkin Sag laccolith, Montana. Part 1. Mafic minerals and estimates of temperature, pressure, oxygen fugacity and silica activity: Contrib. Mineral. Petrol., v. 25, p. 241-269.

Neumann, E.-R., 1976, Compositional relations among pyroxenes, amphiboles and other mafic phases in the Oslo region plutonic rocks: Lithos, v. 9, p. 85-109.

Newton, R.C., 1986, Fluids of granulite facies metamorphism, in Walther, J.V., and Wood, B.J., eds., Fluid-rock interactions during metamorphism: Berlin, Springer-Verlag, p. 36-59.

Nockolds, S.R., 1947, The relation between chemical composition and paragenesis in the biotite micas of igneous rocks: Amer. Jour. Sci., v. 245, no. 7, p. 401-420.

Nunes, P.D., and Jensen, L.S., 1980, Geochronology of the Abitibi metavolcanic belt, Kirkland Lake area - progress report, in Pye, E.G., ed., Summary of geochronological studies 1977-1979: Ont. Geol. Surv. Misc. Pap. 92, p. 34-39.

Osborn, E.F., 1959, Role of oxygen pressure in the crystallization and differentiation of basaltic magma: Amer. Jour. Sci., v. 257, p. 609-647.

Parsons, I., 1979, The Klokken gabbro-syenite complex, South Greenland: Cryptic variation and origin of inversely graded layering: Jour. Petrol., v. 20, p. 653-694.

_____ 1981, The Klokken gabbro-syenite complex, South Greenland: Quantitative interpretation of mineral chemistry: Jour. Petrol., v. 22, p. 233-260.

Paul, A., and Douglas, R.W., 1965, Ferrous-ferric equilibrium in binary alkali silicate glasses: Phys. Chem. Glasses, v. 6, p. 212-215.

Piotrowski, J.M., and Edgar, A.D., 1970, Melting relations of undersaturated alkaline rocks from South Greenland: Meddr. Groenl., v. 181, no. 9, p. 1-62.

Pouchou, J.L., and Pichoir, F., 1984, A new model for quantitative X-ray microanalysis. Part 1: Application to the analysis of homogeneous samples: Rech. Aérosp., v. 3, p. 13-38.

Ramdohr, P., 1969, The ore minerals and their intergrowths: London, Pergamon, 1207 p.

Robert, J.-L., 1976, Titanium solubility in synthetic phlogopite solid solutions: Chem. Geol., v. 17, p. 213-227.

Robinson, P.; Spear, F.S.; Schumacher, J.C.; Laird, J.; Klein, C.; Evans, B.W.; and Doolan, B.L., 1982, Phase relations of metamorphic amphiboles: Natural occurrence and theory, in Veblen, D.R., and Ribbe, P.H., eds., Reviews in mineralogy. Amphiboles: Petrology and experimental phase relations: Mineral. Soc. Amer., v. 9B, p. 1-227.

Rowins, S.M.; Lalonde, A.E.; and Cameron, E.M., 1989a, Geology of the Archean Murdock Creek intrusion, Kirkland Lake, Ontario, in Current research. Part C: Geol. Surv. Can. Pap. 89-1C, p. 313-323.

_____; _____; and _____, 1989b, Petrogenesis of the Archean Murdock Creek intrusion, Kirkland Lake, Ontario: Evidence of magmatic oxidation: Geol. Assoc. Can. Ann. Meet. Prog. with Abs., v. 14, p. A34.

_____; Cameron, E.M.; and Lalonde, A.E., Geochemistry and petrogenesis of the syenitic Murdock Creek intrusion, Kirkland Lake, Ontario: in prep.

Sato, M., and Wright, T.C., 1966, Oxygen fugacities directly measured in magmatic gases: Science, v. 153, p. 1103-1105.

Smith, D., and Lindsley, D.H., 1971, Stable and metastable augite crystallization trends in a single basalt flow: Amer. Mineral., v. 56, p. 225-233.

Smith, A.R., and Sutcliffe, R.H., 1988, Plutonic rocks of the Abitibi Subprovince, in A.C. Colvine, ed., Summary of field work and other activities: Ont. Geol. Surv. Misc. Pap. 141, p. 188-196.

Speer, J.A., 1984, Micas in igneous rocks, in Bailey, S.W., ed., Reviews in mineralogy. Micas: Mineral. Soc. Amer., v. 13, p. 299-356.

Spencer, K.L., and Lindsley, D.H., A solution model for coexisting iron-titanium oxides: Amer. Mineral., v. 66, p. 1189-1201.

Streckeisen, A., 1976, To each plutonic rock its proper name: Earth Sci. Rev., v. 12, p. 1-33.

Thompson, J.B.Jr., 1947, Role of aluminum in the rock-forming silicates: Bull. Geol. Soc. Amer., v. 58, p. 1232.

Thompson, R.N., 1974, Some high-pressure pyroxenes: Mineral. Mag., v. 39, p. 768-787.

Thomson, J.E.; Charlewood, G.H.; Griffin, K.; Hawley, J.E.; Hopkins, H.; MacIntosh, C.G.; Ogrizlo, S.P.; Perry, O.S.; and Ward, W., 1950, Geology of the main ore zone at Kirkland Lake: Ont. Dept. Mines Ann. Rep. 1948, v. 57, pt. 5, p. 54-188.

Tracy, R.J., and Robinson, P., 1977, Zoned titanian augite in olivine basalt from Tahiti and the nature of titanium substitution in augite: Amer. Mineral., v. 62, p. 634-645.

Tyler, R.C., and King, B.C., 1967, The pyroxenes of the alkaline igneous complexes of eastern Uganda: Mineral. Mag., v. 36, p.

5-21.

Upton, B.G.J., 1960, The alkaline igneous complex of Kûngnât Fjeld South Greenland: Meddr. Groenl., v. 123, no. 4, p. 5-145.

Verhoogen, J., 1962, Distribution of titanium between silicates and oxides in igneous rocks: Amer. Jour. Sci., v. 260, p. 211-220.

Wass, S.Y., 1979, Multiple origins of clinopyroxenes in alkali basaltic rocks: Lithos, v. 12, p. 115-132.

Woermann, E., and Rosenhauer, M., 1985, Fluid phases and the redox state of the earth's mantle. Extrapolations based on experimental phase-theoretical and petrological data: Fortschr. Mineral., v. 63, p. 263-349.

Wones, D.R., 1966, Mineralogical indicators of relative oxidation states of magmatic systems: Amer. Geophys. Un. Trans., v. 47, p. 216.

_____ 1981, Mafic silicates as indicators of intensive variables in granitic magmas: Mining Geol. (Japan), v. 31, p. 191-212.

_____ 1989, The significance of the assemblage titanite-magnetite -quartz in granitic rocks: Amer. Mineral., v. 74, p. 1744-1749.

_____, and Eugster, H.P., 1965, Stability of biotite: Experiment, theory, and application: Amer. Mineral., v. 50, p. 1228-1271.

Yagi, K., 1966, The system acmite-diopside and its bearing on the

stability relations of natural pyroxenes of the acmite-hedenbergite-diopside series: Amer. Mineral., v. 51, p. 976-1000.

Yagi, K., and Onuma, K., 1967, The join $CaMgSi_2O_6$ - $CaTiAl_2SiO_6$ and its bearing on the titanaugites: Jour. Fac. Sci. Hokkaido Univ., Ser. 4, v. 13, p. 117-138.

GEOCHEMISTRY AND PETROGENESIS OF THE SYENITIC MURDOCK CREEK INTRUSION, KIRKLAND LAKE, ONTARIO

STEPHEN M. ROWINS, EION M. CAMERON[1], AND ANDRÉ E. LALONDE

Ottawa-Carleton Geoscience Centre, Department of Geology, University of Ottawa, Ottawa, Ontario, K1N 6N5, Canada.

[1]Geological Survey of Canada, Ottawa, Ontario, K1A 0E8, Canada, and Ottawa-Carleton Geoscience Centre, Department of Geology, University of Ottawa, Ottawa, Ontario, K1N 6N5, Canada.

ABSTRACT

The Murdock Creek intrusion, immediately southwest of Kirkland Lake, Ontario, in the Abitibi belt, belongs to a suite of late Archean syenitic intrusions located within and adjacent to the Kirkland Lake-Larder Lake fault zone (KLF), which host virtually all of the gold mineralization in the Kirkland Lake camp. The pluton is composed of six cogenetic units which define a continuous compositional spectrum (SiO_2 ≈ 42-59 wt.%). An early crystallizing mafic margin consisting of clinopyroxenite, meladiorite, melamonzodiorite, and melasyenite encloses an extensive felsic core of alkali-feldspar syenite. A coeval hornblendite unit with lamprophyric affinities, intrudes throughout the pluton and most closely approximates the mantle-derived liquids which differentiated to produce the suite of syenitic intrusions as well as the other expressions of Archean potassic alkaline magmatism in the Kirkland Lake area. The behavior of both major and trace elements during evolution of the Murdock Creek intrusion support a fractional crystallization model, with incompatible elements (e.g., light rare earth elements (LREE's) and large-ion-lithophile elements (LILE's)) and the ratios K/Rb, La/Yb increasing, compatible transition elements (Sc, V, Cr, Co, Ni) and Ca/Y decreasing, and coherent ratios such as Th/U, Zr/Hf, Cr/Ni, and the standard LILE ratios K/Sr, K/Ba, Rb/Sr, Rb/Ba showing relatively little change. Enhanced K_2O, LILE and LREE contents, and depletions in Ti-group elements (Nb, Ta, Ti) are notable geochemical characteristics of all units.

Petrogenesis of the Murdock Creek intrusion begins with partial melting of metasomatically LILE- and LREE-enriched upper mantle, the fusion initiated by mantle upwelling via lithosphere extension along the KLF leading to a pulse of potassic mafic alkaline magma which generated the evolved rock compositions primarily by in situ crystal fractionation, first of clinopyroxene (and lesser biotite), then plagioclase and later K-feldspar subsequent to final emplacement at mid-crustal levels. The many petrographic, mineralogical, and geochemical similarities between the Murdock Creek intrusion and the Kirkland Lake syenite complex (KLSC), and also with other proximal late Archean syenites, trachytic volcanic rocks, calc-alkaline lamprophyres, and hornblenite intrusions suggest derivation via a common tectono-magmatic event in the late Archean.

INTRODUCTION

Late Archean syenitic intrusions (≈ 2680 Ma) near Kirkland Lake, Ontario, in the southern part of the ≈ 2.7 Ga Abitibi belt, show a strong spatial association with gold mineralization, carbonatization, and the Kirkland Lake-Larder Lake fault zone (KLF) (fig. 1). This has led to the suggestion of a genetic link between syenitic magmas and ore-fluids (Colvine et al. 1984, 1988; Cameron amd Carrigan 1987; Cameron and Hattori 1987). Notwithstanding this spatial association, which is common in Archean greenstone terranes and figures in many exploration strategies, studies on the petrological and geochemical aspects of these syenitic intrusions are lacking, a problem due in part to their frequent alteration by shear zone fluids. This paper examines the Murdock Creek intrusion, a relatively unaltered (western part at least) syenitic pluton comprising six cogenetic units shown through systematic geochemical variation in conjunction with previously reported field relations, petrographic features (Rowins et al. 1989), and ferromagnesian mineral chemistry (Rowins et al., in prep), to be related by fractional crystallization from a single pulse of mantle-derived, potassic mafic alkaline (syenitic) magma. An intrusive hornblendite unit with lamprophyric affinities, is coeval with pluton evolution and its high Cr, Ni, and Mg contents make it a good candidate for being the parental magma from which the compositionally diverse suite of Archean alkaline igneous rocks in the Kirkland Lake district were ultimately derived. The

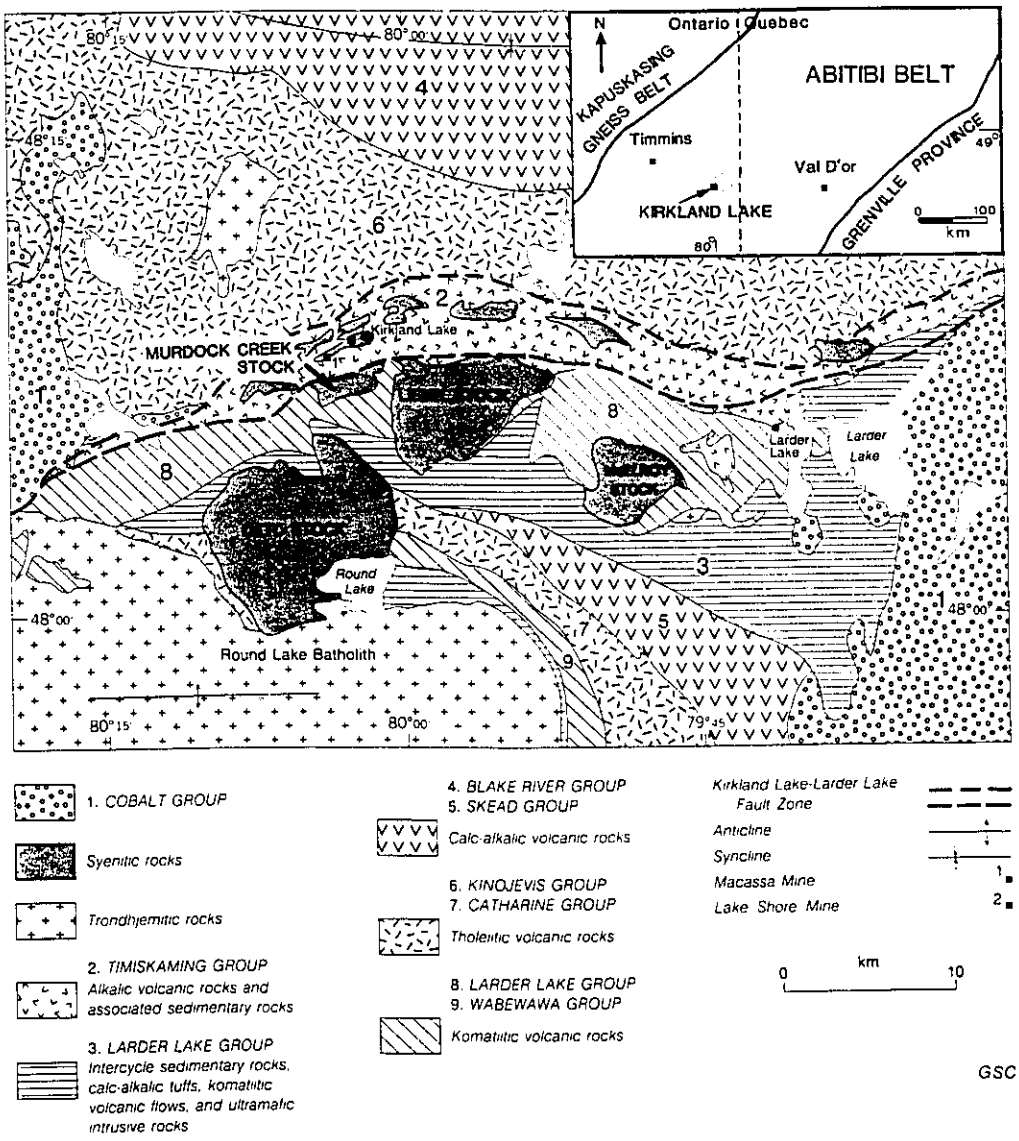

Fig. 1.-Geology of the Kirkland Lake area (modified from Jensen 1978).

Murdock Creek intrusion is interpreted as one manifestation of a larger tectono-magmatic event at the end of the Archean which produced the diverse suite of potassic alkaline igneous rocks in the Kirkland Lake area. This interpretation is compatible with current ideas on the origin of the Superior Province craton (e.g., Corfu 1987; Colvine et al. 1988 and references therein).

The trace element geochemistry of the Murdock Creek intrusion does not preclude a tectonic model which relates gold mineralization and alkaline magma genesis (Cameron, in press) to moderate degrees of lithosphere thinning and extension that resulted in mantle upwelling and low degrees of partial melting.

GEOLOGICAL SETTING

The Abitibi belt is the largest and most economically important Archean granite-greenstone terrane of the Canadian Shield, with gold production in excess of 137 million ounces (Hodgson and MacGeehan 1982). Of that, some 23 million ounces (Grabowski et al. 1987) have been recovered from seven mines in the Kirkland Lake camp, making it the second largest Archean gold camp in North America after Timmins, Ontario. Rocks in the Kirkland Lake region mainly comprise a thick upward succession of komatiitic, tholeiitic and calc-alkaline basalts, with lesser amounts of sedimentary rocks, belonging to the Larder Lake, Kinojévis, and Blake River groups (Jensen and Langford 1985). These form the southern limb of an elongate, east-plunging synclinorium (fig. 1) metamorphosed to sub-greenschist and

greenschist grade at low pressure (Jolly 1974). A felsic fragmental pyroclastic unit overlying thick komatiitic flows at the base of the Larder Lake Group (apparently the oldest of these groups) gave a precise U-Pb zircon age of 2705±2 Ma (Corfu et al. 1989). The Blake River Group has yielded younger U-Pb zircon ages of 2703±2 Ma and 2701±2 Ma (Nunes and Jensen 1980; Corfu et al. 1989). No age dating has yet been done on the Kinojévis Group.

The most prominent feature of the district is the east-trending Kirkland Lake-Larder Lake fault zone (KLF) which is the western termination of a regional strike-slip fault, the Larder Lake-Cadillac fault (Hubert et al. 1984). The KLF is chiefly occupied by the Timiskaming Group (Hewitt 1963; Cooke and Moorehouse 1969; Hyde 1980), a sequence of interbedded sedimentary and alkaline volcanic rocks unconformably overlying the older basaltic rocks cited above. The south margin of the KLF is a fault contact against uplifted Larder Lake Group basalts, while the north margin is, in part, an unconformity of Timiskaming rocks over Kinojévis basalts and everywhere else a fault. Timiskaming alkaline volcanic rocks have recently been dated by the U-Pb zircon method at ≈ 2677 Ma (D.W. Davis pers. comm.).

The district is also notable in containing numerous composite syenitic intrusions which are uncommon in Archean terranes. The large, sub-circular plutons south of the KLF (fig. 1) appear to have been forcefully emplaced as diapirs into the surrounding supracrustal rocks, whereas the smaller syenitic intrusions

within or truncated by the KLF, are elongated parallel to the strike of the fault zone, a form suggesting passive intrusion into extensional fractures (Cameron, in press). The Otto stock, one of the large, rounded plutons south of the KLF was dated by U-Pb zircon at 2680±1 Ma (Corfu et al. 1989) and a feldspar porphyry dike from the Macassa Mine (fig. 1) gave a poorly constrained U-Pb zircon age of 2680-2700 Ma (Marmont and Corfu 1988). Calc-alkaline lamprophyres (mainly minettes and vogesites) occur throughout the area and are frequently associated with syenitic intrusions which they both predate and postdate. A dike set which cross-cuts syenite has been dated by U-Pb titanite methods at 2674±2 Ma (Wyman and Kerrich 1988).

Carbonatization of rocks within, and proximal to, the KLF is extensive and structurally controlled (Thomson 1950). Syenitic intrusions are affected to varying degrees, but are also in some places observed to cut carbonatized zones. This feature together with the occurrence of pebbles of carbonatized rock in the upper beds of the Timiskaming Group (Hewitt 1963), suggests that alteration by CO_2-rich fluids occurred over a long period of time.

GENERAL GEOLOGY OF THE MURDOCK CREEK INTRUSION

The Murdock Creek intrusion is a crudely elliptical body, elongated in an east-west direction parallel to the strike of the KLF. It intrudes komatiitic basalts of the Larder Lake Group and at the intrusive contact, there is a heterogeneous zone

consisting of intermingled clinopyroxenite and altered basaltic country rock. Along the northern and southern perimeters of the intrusion, this contact zone is generally absent or obscured by post-emplacement faulting and alteration.

The intrusion may be subdivided into two separate domains on the basis of degree of alteration and deformation. West of the north-trending Lake Shore fault (fig. 2), rock units are fresh with only minor shearing and alteration in contrast to those in the east. It is primarily from this unaltered western portion of the intrusion that the samples used in this study were collected.

Six plutonic units are defined using the IUGS nomenclature (Streckeisen 1976). A thin, early-crystallizing mafic margin consists of (oldest to youngest) clinopyroxenite, meladiorite, melamonzodiorite, and melasyenite. This encloses an extensive felsic core of alkali-feldspar syenite (fig. 2). Note that melanocratic alkali-feldspar syenite is not distinguished from normal alkali-feldspar syenite in figure 2 because the two units are intergradational, although towards the core of the intrusion melanocratic alkali-feldspar syenite is far less abundant. An intrusive hornblendite unit outcrops sporadically throughout the intrusion except in the northeastern extremity of the pluton where it forms an extensive (700 x 500 m) peripheral body. Because the hornblendite intrusions are cut by late dykes of alkali-feldspar syenite, their emplacement is interpreted to be coeval with the intrusion and solidification of the Murdock Creek pluton. Except for this hornblendite, all rock types exhibit

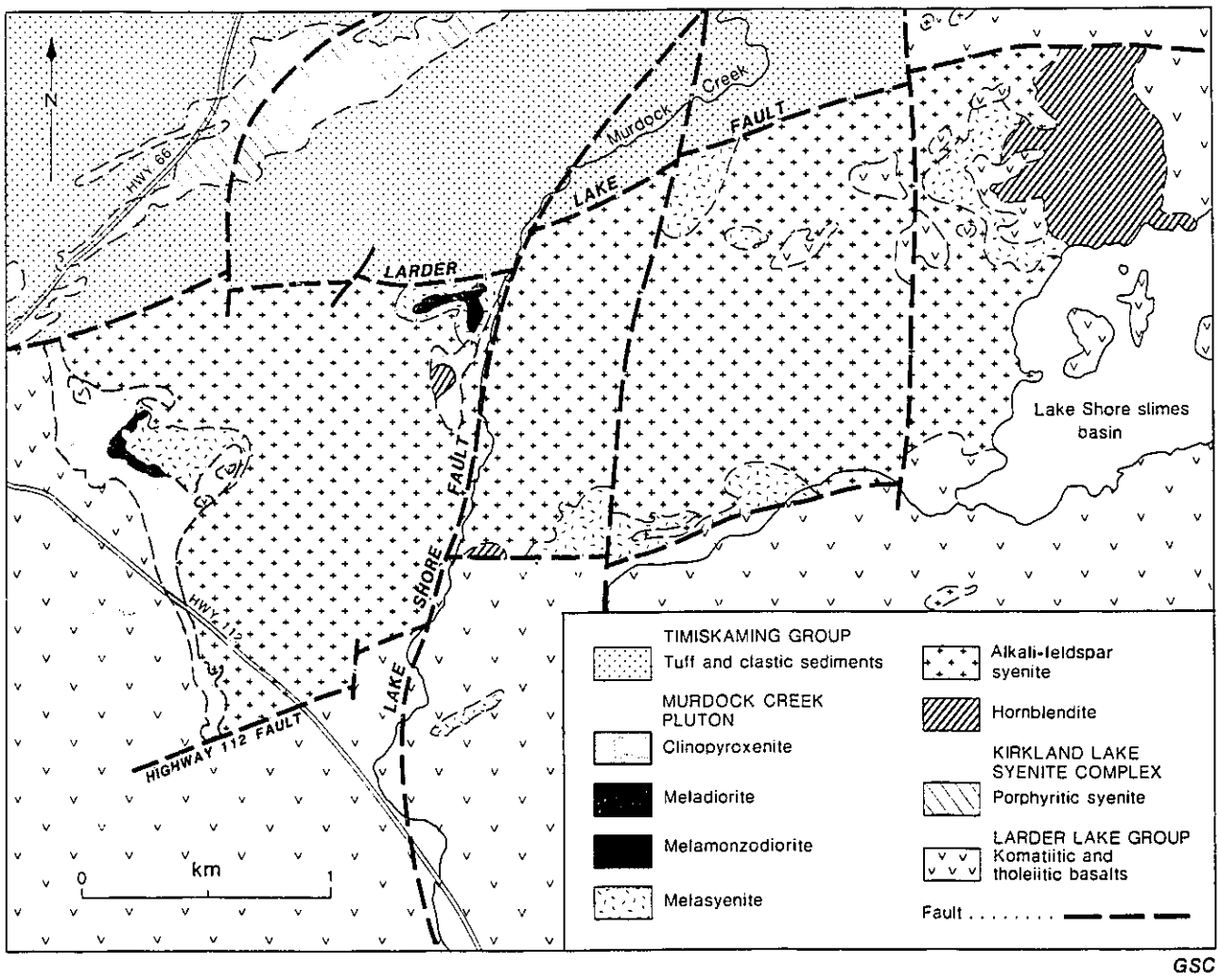

Fig. 2.-Geology of the Murdock Creek intrusion (Thomson 1950; Rowins et al. 1989; Rowins et al., in prep.).

gradational contacts in the field; abrupt contacts sometimes observed are produced by the movement of unconsolidated magma intruding into earlier solidified rock units. Detailed field relations and petrographic features of the various plutonic units can be found in Rowins et al. (1989) and typical mineral modes are summarized here in table 1.

WHOLE-ROCK GEOCHEMISTRY

Analytical Methods.-Major elements and Cr, Rb, Sr, Y, Zr, Nb, and Ba were analysed on fused glass disk by X-ray fluorescence spectroscopy (XRF) at the Geological Survey of Canada and at the University of Ottawa. Results were calibrated against standard rock samples and major elements are accurate to better than 1% of the reported concentration, with the exception of FeO and MnO (± 2% relative). Trace element analyses by XRF are accurate to ± 10% of the given value, except for Rb (± 2% relative). Fe^{3+}/Fe^{2+} were done by titration employing the Wilson (1960) method; H_2O and loss-on-ignition (LOI) were by the furnace method; CO_2 was by combustion followed by infrared detection; and S was by ion chromatography and is accurate to ± 5% of the reported concentration.

Scandium, V, Co, Ni, Cu, Zn, As, Mo, Sb, Hf, Ta, Au, Th, U, and the REE's were determined by instrumental neutron activation analysis (INAA) on 10-15 g of sample (Bondar-Clegg and Company), and concentrations are accurate to better than ± 20% of the stated value (except for Au, ± 50%).

TABLE 1

Modal Mineralogy (Vol.%) of Rocks of the Murdock Creek Intrusion

ROCK UNIT[a]	AS	MAS	MS	MM	MD	CP	HB
Pimary Minerals							
K-Peldspar	66-80	42-45	44-57	8-12	0-2	0-1	<3
Plagioclase	0-2	1-3	5-13	38-45	26-30	0-10	6-9
Clinopyroxene	11-27	28-30	15-24	15-22	31-35	53-62	10-12
Biotite	0-9	9-13	7-12	16-27	15-20	14-27	9-11
Amphibole	...	...	...	...	...	...	66-70
Magnetite	1-4	4-5	1-3	1-2	2-4	1-6	<1
Secondary Minerals							
Biotite	0-2	2-5	1-3	<2	3-4	1-5	0-2
Amphibole[b]	0-2	<1	1-6	1-10	4-10	1-13	0-1
Quartz	...	...	...	...	tr	...	tr
Chlorite	0-1	<1	0-1	0-1	0-1	0-1	...
Epidote	0-1	<1	1-2	<2	<2	0-1	0-2
Calcite	0-2	0-1	<1	<1	0-1	0-2	0-1
Sericite	<1	<1	<1	<1	0-1	0-1	0-1
Rutile/titanite	tr	tr	tr	tr	tr	tr	...
Accessory Minerals							
Apatite	<2	1-2	<2	<2	1-2	1-3	<1
Titanite	<2	<1	0-1	<1	0-1	<1	<1
Zircon	tr	...	tr	tr	tr	tr	tr
Sulphide minerals[c]	tr	tr	tr	tr	tr	tr	tr
Plag. Composition			An_{16-18}		An_{30-34}		An_{10-15}
Color Index (CI)[d]	22±9	53±4	38±12	46±8	68±8	>85	>85

NOTE.-Modal ranges are based on 1000 counts per thin section in conjunction with visual estimation techniques for coarse-grained samples. tr = trace amounts.

[a] Rock units as follows: AS, alkali-feldspar syenite; MAS, melanocratic alkali-feldspar syenite; MS, melasyenite; MM, melamonzodiorite; MD, meladiorite; CP, clinopyroxenite; HB, hornblendite.

[b] Secondary amphibole varieties include magnesian hastingsite, actinolite, tremolite, and magnesio-riebeckite. Terminalogy after Leake (1978).

[c] Primary sulphide minerals include pyrite, chalcopyrite, bornite and covellite.

[d] Color index (CI) = total mode - quartz, plagioclase, alkali-feldspar, apatite, calcite, and sericite (after Streckeisen 1976).

Major Elements.-Whole-rock major and trace element analyses for 37 unaltered samples from the various rock units comprising the Murdock Creek intrusion are reported in table 2. Low whole-rock volatile contents (H_2O and CO_2 or total LOI's generally < 2) reflect their anhydrous primary mineralogy (except for minor biotite) and the lack of subsolidus hydration and carbonatization noted during petrographic inspection.

All samples are slightly undersaturated in SiO_2, containing several wt.% nepheline (Ne) or more uncommonly olivine (Ol) plus hypersthene (Hy) in the norm (table 3). Since normative nepheline is also diagnostic of alkaline igneous rocks (e.g., Sorensen 1974), its presence is consistent with respect to the alkalis vs. SiO_2 diagram (fig. 3a) that shows all Murdock Creek rock types within Myashiro's (1978) alkaline rock field. High normative magnetite (Mt) contents (up to 12.79%) indicate abundant Fe^{3+} which agrees with ferromagnesian silicate and opaque oxide evidence of high magmatic oxygen fugacity (f_{O_2}) throughout pluton evolution ($\approx 10^{-12}$ bars; Rowins et al., in prep.). However, these high normative magnetite contents are slightly misleading since calculation of the CIPW norm involves assigning all Fe^{3+} to magnetite unlike the observed mineralogy, where Fe^{3+} is contained in minerals other than magnetite (e.g., diopside and biotite). Normative leucite (Lc) and potassium metasilicate (Kp) in several biotite-rich clinopyroxenite and hornblendite samples is consistent with their classification as ultrapotassic igneous rocks sensu stricto (refer to discussion on petrogenesis).

TABLE 2

Major and Trace Element Analyses of Rocks of the Murdock Creek Intrusion

ROCK UNIT[a] / SAMPLE	AS 87101	AS 87102	AS 87103	AS 87104	AS 87105	AS 87108	AS 87117	AS 87118	AS 87119	AS 87120	AS 87121	AS 87134	AS 89218	MAS 88216	MAS 88217
SiO_2	56.3	56.8	56.6	55.5	56.8	57.8	56.7	57.2	56.1	58.5	57.2	55.0	54.7	50.3	49.5
TiO_2	0.63	0.62	0.56	0.76	0.52	0.56	0.67	0.61	0.81	0.54	0.65	0.65	0.67	0.98	1.15
Al_2O_3	14.5	15.8	16.4	13.0	14.1	14.5	14.9	15.3	12.7	14.5	15.0	14.7	14.7	10.6	10.6
Fe_2O_3	3.9	4.1	4.1	4.2	3.9	3.7	3.6	4.1	3.3	3.5	5.1	4.0	2.8	5.1	6.4
FeO	3.3	2.8	2.3	3.4	2.9	2.6	3.3	2.6	2.9	2.8	2.2	3.6	4.3	5.7	6.0
(FeO_T)	6.8	6.4	5.9	7.1	6.4	5.9	6.5	6.2	5.8	5.9	6.7	7.2	6.8	10.2	11.7
MnO	0.14	0.11	0.13	0.14	0.13	0.13	0.12	0.13	0.16	0.13	0.13	0.15	0.14	0.23	0.23
MgO	3.88	2.65	2.87	4.59	3.59	3.15	3.52	3.26	4.35	3.15	3.29	4.30	5.68	7.62	7.35
CaO	4.70	3.67	4.96	6.83	5.34	4.71	4.61	5.03	6.64	5.10	3.60	6.39	5.84	10.58	10.50
Na_2O	4.4	4.2	4.3	3.4	4.0	4.2	4.3	4.3	3.4	4.3	4.2	4.3	4.3	2.5	2.9
K_2O	5.24	5.85	5.72	6.26	6.32	6.46	5.94	5.97	6.57	6.30	6.40	4.62	4.18	3.87	3.37
P_2O_5	0.54	0.51	0.46	0.66	0.55	0.46	0.56	0.50	0.58	0.53	0.48	0.49	0.48	0.84	1.02
H_2O	0.9	1.4	0.8	0.6	0.6	0.5	0.7	0.5	0.6	0.3	0.8	0.9	1.1[d]	0.7	0.7
CO_2	1.3	0.1	0.1	0.1	0.2	0.7	1.0	0.3	0.5	0.1	1.0	0.6	na	0.1	0.1
TOTAL	99.73	98.61	99.30	99.44	98.95	99.47	99.92	99.80	98.61	99.75	100.05	99.70	98.89	99.12	99.82
S	<50	<50	101	114	<50	155	377	<50	279	<50	132	<50	400	100	200
Sc	14.0	13.0	12.0	20.6	15.0	13.0	14.0	15.0	18.0	13.0	14.0	18.0	na	na	na
V	na	na	na	na	na	na	na	na	na	na	na	na	153	260	290
Cr	160	160	140	190	130	140	130	130	150	110	160	200	262	250	150
Co	27	28	20	31	23	21	29	29	27	24	25	29	na	44	44
Ni	32	28	21	33	33	20	34	33	26	22	32	38	63	62	39
Cu	na	na	na	na	na	na	na	na	na	na	na	na	na	52	35
Zn	160	180	160	200	140	130	130	150	200	140	160	140	135	120	120
As	3.0	5.2	2.9	1.6	3.4	1.7	4.0	5.3	2.7	3.4	4.3	2.3	na	na	na
Rb	119	120	150	185	168	216	152	146	189	194	124	97	94	83	78
Sr	1804	1952	2670	1869	1851	1739	1853	2133	1424	1727	1960	1861	1840	1934	1934
Y	64	61	64	61	50	72	67	54	34	51	48	61	21	36	78
Zr	158	195	192	174	201	150	182	193	172	176	161	145	75	205	139
Nb	<2.0	<2.0	<2.0	<2.0	<2.0	<2.0	<2.0	<2.0	13.0	<2.0	<2.0	<2.0	<2.0	10.0	14.0
Mo	2	2	2	1	1	2	4	1	1	2	1	1	na	na	na
Sb	0.8	0.5	0.2	0.1	0.3	0.2	0.5	0.4	0.4	0.4	1.6	0.2	na	na	na
Ba	2785	3030	2966	3262	2842	2981	2886	3221	3400	2695	3066	3176	3059	3039	3992
La	78	79	74	97	82	91	88	92	110	86	80	72	na	74	86
Ce	132	141	123	164	129	150	149	153	184	136	139	124	na	na	na
Sm	11.0	10.0	10.0	13.0	9.1	10.0	11.0	12.0	16.0	12.0	11.0	10.0	na	na	na
Eu	4.0	3.0	3.0	4.0	3.0	2.0	3.0	3.0	4.0	2.0	3.0	2.0	na	na	na
Tb	1.3	1.2	1.3	1.5	1.1	1.1	1.4	1.4	1.9	1.4	1.4	1.1	na	na	na
Yb	1	1	1	1	1	1	1	1	2	2	1	2	na	3	3
Lu	0.3	0.3	0.3	0.3	0.3	0.3	0.3	0.3	0.4	0.3	0.3	0.3	na	na	na
Hf	4	4	4	4	4	3	4	4	6	5	4	3	na	na	na
Ta	<0.5	<0.5	<0.5	<0.5	0.6	0.7	<0.5	0.7	1.1	<0.5	0.6	<0.5	na	na	na
Au (ppb)	1	4	1	4	1	4	7	1	5	5	5	4	na	na	na
Th	4.5	6.9	4.6	3.8	5.5	6.8	6.4	7.4	10.0	10.0	6.1	4.4	na	na	na
U	1.4	1.7	1.0	0.6	0.9	1.2	1.4	1.5	1.6	2.0	1.6	1.0	na	na	na
Agpaitic index[e]	0.89	0.84	0.81	0.95	0.95	0.96	0.91	0.88	1.00	0.96	0.92	0.82	0.80	0.78	0.79

NOTE.-Oxides reported in wt.%. Trace elements in ppm except for gold (ppb).
na = not analysed.
FeO_T = all iron recalculated as FeO.

[a] Rock units as in table 1.

[b] Average augite syenite composition from the Kirkland Lake syenite complex (Macassa mine) (from table 3 in Kerrich and Watson 1984). Note that Ba = 132 ppm (?) appears to be erroneous as all reported unaltered augite syenite analyses (10) in table 2 of Kerrich and Watson (1984) have Ba contents ranging between 1660-2200 ppm, average = 1850 ppm.

[c] Average felsic syenite composition from the Kirkland Lake syenite complex (Macassa mine) (from table 3 in Kerrich and Watson 1984).

[d] wt.% loss-on-ignition at 1000 °C.

[e] Agpaitic index = molecular ratio $(Na_2O+K_2O)/Al_2O_3$.

TABLE 2 - Continued

Major and Trace Element Analyses of Rocks of the Murdock Creek Intrusion

ROCK UNIT[a]	MS	MS	MS	MS	MS	MS	MM	MM	MD	MD	MD	MD	CP	CP	CP
SAMPLE	87131	87133	88289	88291	89292	89293	88295	89227	87132	88288	89142A	89248A	87115	87129	87130
SiO_2	54.0	52.7	54.3	52.9	53.8	53.9	46.1	53.2	46.4	49.2	46.7	50.1	46.0	43.8	41.7
TiO_2	0.80	0.82	0.73	0.71	0.69	0.69	1.19	0.88	1.03	0.90	1.05	0.91	1.04	1.36	1.56
Al_2O_3	14.1	13.8	13.8	13.5	13.4	13.7	9.5	13.0	12.4	11.4	12.2	11.5	10.6	7.5	5.3
Fe_2O_3	4.4	4.5	3.2	2.8	2.8	2.7	7.0	4.7	5.6	4.0	5.2	3.9	4.7	8.1	8.8
FeO	4.1	4.7	4.3	4.5	4.8	4.7	7.8	4.6	6.2	6.2	6.5	6.4	7.1	8.0	7.9
(FeO_T)	8.0	8.7	7.1	7.0	7.3	7.1	14.0	8.8	11.2	9.8	11.2	9.9	11.3	15.2	15.7
MnO	0.16	0.18	0.15	0.16	0.15	0.16	0.21	0.17	0.20	0.19	0.21	0.19	0.20	0.30	0.28
MgO	5.67	6.17	6.37	7.09	6.56	6.91	9.26	6.54	8.36	9.44	9.20	9.66	10.63	10.01	12.51
CaO	7.18	7.50	6.96	7.09	6.16	6.93	10.29	8.86	10.15	9.15	10.36	9.40	10.98	14.15	16.78
Na_2O	3.9	3.6	4.2	3.6	4.6	4.2	2.3	4.3	2.5	2.8	2.4	3.1	2.0	1.4	0.5
K_2O	4.09	3.84	3.58	3.98	3.41	3.73	3.15	2.18	2.89	3.50	3.20	3.49	2.87	2.02	1.75
P_2O_5	0.52	0.54	0.52	0.44	0.45	0.47	0.63	0.61	0.78	0.65	0.82	0.60	0.62	1.12	1.46
H_2O	1.1	1.3	1.0	1.4	2.6[d]	1.3[d]	1.3	0.9[d]	2.0	1.5	1.3[d]	1.1[d]	2.1	1.3	1.2
CO_2	0.1	0.1	0.1	0.8	na	na	0.7	na	0.9	0.3	na	na	0.8	1.0	0.3
TOTAL	100.12	99.75	99.21	98.97	99.42	99.39	99.43	99.94	99.41	99.23	99.14	100.35	99.64	100.06	100.04
S	<50	100	<50	<50	400	400	600	300	127	<50	200	400	777	674	214
Sc	22.6	24.8	na	na	na	na	na	na	28.5	na	na	na	39.7	50.5	64.5
V	na	na	180	160	171	163	370	218	na	230	284	250	na	na	na
Cr	300	320	300	360	319	323	310	242	450	460	394	468	690	280	440
Co	37	40	38	35	na	na	52	na	56	48	na	na	68	71	90
Ni	51	64	81	120	73	78	57	44	100	100	109	95	150	66	90
Cu	na	na	27	110	na	na	100	na	na	65	na	na	na	na	na
Zn	140	220	98	110	172	156	130	139	200	120	136	195	170	200	210
As	3.3	2.4	na	na	na	na	na	na	2.2	na	na	na	2.0	0.9	1.5
Rb	131	90	94	103	81	116	112	92	88	147	102	154	100	65	70
Sr	1587	2196	1994	1588	1412	1660	789	2801	3013	1546	2871	1614	1515	1123	669
Y	71	56	55	49	24	21	70	30	51	67	24	23	53	46	40
Zr	225	121	188	187	108	106	158	165	122	188	87	123	197	220	109
Nb	<2.0	11.0	17.0	25.0	<2.0	<2.0	19.0	2.0	<2.0	35.0	<2.0	4.0	<2.0	<2.0	<2.0
Mo	3	0.5	na	na	na	na	na	na	1	na	na	na	1	1	0.5
Sb	0.2	0.2	na	na	na	na	na	na	0.2	na	na	na	0.2	0.1	0.1
Ba	2159	3655	2783	2722	2300	2815	1850	1303	3208	1565	3302	1665	2519	2128	2141
La	75	64	54	40	na	na	44	na	61	61	na	na	48	74	74
Ce	121	106	na	na	na	na	na	na	112	na	na	na	91	146	147
Sm	10.0	11.0	na	na	na	na	na	na	11.0	na	na	na	10.0	16.0	18.0
Eu	2.0	3.0	na	na	na	na	na	na	3.0	na	na	na	3.0	4.0	5.0
Tb	1.4	1.2	na	na	na	na	na	na	1.4	na	na	na	1.5	2.3	2.5
Yb	3	1	2	1	na	na	3	na	1	2	na	na	2	4	3
Lu	0.4	0.3	na	na	na	na	na	na	0.2	na	na	na	0.3	0.6	0.5
Hf	5	2	na	na	na	na	na	na	0.5	na	na	na	3	4	3
Ta	0.6	<0.5	na	na	na	na	na	na	<0.5	na	na	na	0.5	0.6	<0.5
Au (ppb)	1	4	na	na	na	na	na	na	8	na	na	na	5	5	4
Th	11.0	1.7	na	na	na	na	na	na	1.1	na	na	na	2.2	1.6	2.1
U	2.5	0.1	na	na	na	na	na	na	0.1	na	na	na	0.5	0.3	0.3
Agpaitic index[e]	0.77	0.73	0.78	0.76	0.84	0.81	0.76	0.72	0.58	0.74	0.61	0.77	0.60	0.60	0.51

TABLE 2 - Continued

Major and Trace Element Analyses of Rocks of the Murdock Creek Intrusion

ROCK UNIT[a]	CP	CP	CP	CP	HB	HB	HB	AUG-S[b]	PEL-S[c]
SAMPLE	87135	88297	89221	89296	88329	89327	89509	P2	P1
SiO_2	42.7	44.1	43.6	43.0	47.8	51.0	47.9	48.2	56.6
TiO_2	1.48	1.37	1.34	1.25	0.81	0.60	0.83	0.90	0.61
Al_2O_3	6.1	9.5	7.5	6.2	7.5	10.3	7.4	12.6	18.9
Fe_2O_3	8.1	5.6	3.4	4.7	3.1	2.5	2.6	na	na
FeO	8.0	8.1	7.0	9.2	5.9	6.1	5.9	na	na
(FeO_T)	15.2	13.1	10.0	13.4	8.7	8.3	8.2	7.8	3.7
MnO	0.31	0.22	0.20	0.26	0.18	0.17	0.15	0.13	0.08
MgO	10.89	11.50	14.54	12.17	15.95	12.95	16.10	6.6	0.90
CaO	16.36	12.04	13.02	13.56	11.95	8.82	12.33	7.2	1.9
Na_2O	1.0	1.6	0.5	0.7	0.7	2.0	0.9	3.1	4.4
K_2O	2.14	3.04	4.38	3.09	3.01	2.98	3.15	5.5	7.5
P_2O_5	1.38	0.77	1.29	0.89	0.19	0.22	0.13	0.52	0.22
H_2O	1.3	1.6	1.0[d]	0.8[d]	1.8	1.9[d]	1.2[d]	5.2[d]	3.6[d]
CO_2	0.3	0.3	na	na	0.2	na	na	na	na
TOTAL	100.06	99.74	97.77	100.02	99.09	99.54	98.59	97.75	98.41
S	155	1300	300	1000	<50	400	200	121.6	119.7
Sc	50.4	na	na	na	na	na	na	28.3	8.1
V	na	340	214	379	180	161	202	367	91
Cr	290	460	819	534	1200	1078	1230	318	80
Co	73	56	na	na	53	na	na	50	24
Ni	53	92	256	94	230	271	262	96	18
Cu	na	120	na	na	15	na	na	19	16
Zn	230	280	163	161	69	105	70	99	56
As	2.3	na	na	na	na	na	na	8.7	3.5
Rb	96	111	196	124	113	59	112	166	206
Sr	735	785	424	224	316	485	277	692	562
Y	44	59	28	28	30	19	14	24	21
Zr	235	93	55	70	72	96	42	156	265
Nb	<2.0	25.0	7.0	2.0	4.0	5.0	<2.0	6	10
Mo	1	na	na	na	na	na	na	na	na
Sb	0.2	na	na	na	na	na	na	3.6	3.1
Ba	2355	2349	2117	1694	1094	1533	121	132	817
La	120	33	na	na	12	na	na	na	na
Ce	205	na	na	na	na	na	na	na	na
Sm	20.4	na	na	na	na	na	na	na	na
Eu	5.0	na	na	na	na	na	na	na	na
Tb	2.5	na	na	na	na	na	na	na	na
Yb	3	1.8	na	na	0.7	na	na	na	na
Lu	0.5	na	na	na	na	na	na	na	na
Hf	6	na	na	na	na	na	na	na	na
Ta	<0.5	na	na	na	na	na	na	na	na
Au (ppb)	5	na	na	na	na	na	na	6	17
Th	8.4	na	na	na	na	na	na	9	26
U	1.3	na	na	na	na	na	na	2.6	3.2
Agpaitic index[e]	0.65	0.62	0.74	0.74	0.59	0.64	0.65	na	na

TABLE 3

CIPW Norms Calculated in Weight Percent for Rocks of the Murdock Creek Intrusion

ROCK UNIT[a] SAMPLE	AS 87101	AS 87102	AS 87103	AS 87104	AS 87105	AS 87108	AS 87117	AS 87118	AS 87119	AS 87120	AS 87121	AS 87134	AS 89218	MAS 88216	MAS 88217
Or	30.96	34.58	33.80	36.98	37.34	38.17	35.10	35.27	38.81	37.22	37.82	27.29	24.69	22.86	19.91
Ab	37.24	35.56	35.52	24.79	31.04	33.99	34.64	34.69	24.69	35.11	35.55	33.03	34.42	17.25	20.02
An	4.34	6.98	8.55	1.72	1.85	1.63	3.81	4.81	...	1.66	3.17	7.16	8.19	6.27	5.95
Ne	...	...	0.47	2.16	1.52	0.84	0.95	0.92	2.20	0.70	...	1.81	1.20	2.11	2.45
Ac	...	...	...	...	...	...	...	...	0.02	...	...	...	...	...	...
Lc	...	...	...	...	...	...	...	...	...	...	...	...	...	...	...
Kp	...	...	...	...	...	...	...	...	...	...	...	...	...	...	...
Di	12.30	6.23	10.21	22.07	16.69	14.81	12.30	13.28	23.08	16.06	9.02	17.01	14.17	32.55	31.48
Hy	1.44	5.03	...	...	...	...	...	...	...	...	2.37	...	...	...	...
Ol	3.19	1.47	1.81	2.01	1.83	1.37	3.68	1.80	1.11	1.33	1.16	3.84	8.69	6.15	5.48
Mt	5.67	5.96	5.96	6.10	5.67	5.38	5.23	5.96	4.79	5.09	5.65	5.81	4.07	7.41	9.30
Il	1.20	1.18	1.07	1.45	0.99	1.07	1.28	1.16	1.54	1.03	1.24	1.24	1.28	1.87	2.19
Hm	...	...	...	...	...	...	...	...	...	...	1.22	...	...	...	...
Ap	1.19	1.12	1.01	1.45	1.21	1.01	1.23	1.10	1.28	1.17	1.06	1.08	1.06	1.85	2.24
TOTAL	97.53	98.11	98.40	98.74	98.15	98.27	98.22	99.00	97.51	99.35	98.25	98.28	97.76	98.32	99.02
F.I.[b]	68.20	70.13	69.79	63.93	69.90	73.00	70.69	69.96	65.72	73.03	73.37	62.13	60.31	42.22	42.38

TABLE 3 - continued

ROCK UNIT[a] SAMPLE	MS 87131	MS 87133	MS 88289	MS 88291	MS 89292	MS 89293	MM 88295	MM 89227	MD 87132	MD 88288	MD 89142A	MD 89240A	CP 87115	CP 87129	CP 87130
Or	24.16	22.68	21.15	23.51	20.14	22.03	18.60	12.88	17.07	20.67	18.90	20.61	16.94	11.93	5.20
Ab	31.65	29.52	34.36	27.97	35.10	30.79	11.37	35.96	14.93	16.45	11.31	15.88	8.43	6.98	...
An	8.89	10.15	8.23	8.92	6.01	7.22	6.29	9.95	14.08	8.20	12.79	7.11	11.46	8.21	7.05
Ne	0.73	0.51	0.63	1.35	1.97	2.75	4.38	...	3.37	3.92	5.01	5.65	4.60	2.63	2.29
Ac	...	...	...	...	...	...	...	...	...	...	...	...	...	...	...
Lc	...	...	...	...	...	...	...	...	...	...	...	...	...	...	4.03
Kp	...	...	...	...	...	...	...	...	...	...	...	...	...	...	...
Di	18.56	18.79	18.31	18.71	17.36	19.32	32.55	23.88	24.91	26.38	26.59	28.53	31.18	43.64	52.85
Hy	...	...	...	...	...	...	...	1.57	...	...	...	...	...	...	...
Ol	5.87	7.42	8.24	9.93	9.83	9.72	10.43	4.83	10.34	12.86	11.93	12.79	13.96	7.54	8.15
Mt	6.39	6.54	4.65	4.07	4.08	3.89	10.17	6.87	8.14	5.81	7.57	5.69	6.83	11.77	12.79
Il	1.52	1.56	1.39	1.35	1.31	1.31	2.26	1.68	1.96	1.71	2.00	1.73	1.98	2.59	2.97
Hm	...	...	...	...	...	...	...	...	...	...	...	...	...	...	...
Ap	1.14	1.19	1.14	0.97	0.99	1.03	1.39	1.34	1.72	1.43	1.80	1.32	1.36	2.46	3.21
TOTAL	98.92	98.35	98.11	96.77	96.80	98.08	97.43	98.95	96.51	97.43	97.90	99.30	96.74	97.76	98.54
F.I.[b]	56.54	52.71	56.14	52.83	57.21	55.57	34.35	48.84	35.37	41.04	35.22	42.14	29.97	21.54	11.52

TABLE 3 - Continued

ROCK UNIT[a] SAMPLE	CP 87135	CP 88297	CP 89221	CP 89296	HB 88329	HB 89327	HB 89509
Or	8.27	17.95	...	7.62	17.75	17.59	18.58
Ab	...	0.23	...	...	3.63	16.99	0.30
An	5.83	9.76	5.37	4.42	8.42	10.16	7.13
Ne	4.58	7.20	2.29	3.30	1.24	...	3.77
Ac	...	...	...	...	...	...	...
Lc	3.43	...	19.97	8.33	...	...	...
Kp	...	...	0.23	...	...	...	...
Di	52.84	35.97	40.49	45.91	39.34	25.67	42.19
Hy	...	...	...	...	...	5.19	...
Ol	5.89	14.29	18.14	14.22	20.25	16.66	19.75
Mt	11.77	8.13	4.90	6.84	4.50	3.62	3.76
Il	2.82	2.61	2.55	2.38	1.54	1.14	1.58
Hm	...	...	...	...	...	...	...
Ap	3.04	1.69	2.55	1.96	0.42	0.48	0.29
TOTAL	98.46	97.84	96.77	94.97	97.09	97.51	97.34
F.I.[b]	16.28	25.38	22.26	19.25	22.62	34.58	22.65

NOTE.-CIPW weight percent norms for the same rocks as in table 2.

[a] Rock units as in table 1.

[b] F.I. = normative whole-rock fractionation index (wt.% Or + Ab + Ne + Lc + Kp).

The agpaitic index $(Na_2O+K_2O)/Al_2O_3$ (mol. prop.) ranges from 0.51 in clinopyroxenite (87130) to 1.0 in a single alkali-feldspar syenite sample (87119) indicating Murdock Creek syenites are of the miaskitic variety (Sorensen 1974). Peralkaline or agpaitic varieties have ratios above 1.0 resulting in normative acmite (Ac) and/or sodium metasilicate (Ns) molecules. Accordingly, except for sample 87119, none of the Murdock Creek rock samples are peralkaline which agrees with their lack of modal aegirine (or alkali amphibole, e.g., arfvedsonite) and normative acmite, long regarded as the hall-marks of peralkalinity in igneous rocks (Bailey 1969; Sorensen 1974).

The SiO_2 content has been used throughout this study as a qualitative fractionation index given its continuous increase from clinopyroxenite through meladiorite, melamonzodiorite, and melasyenite to alkali-feldspar syenite, although several very melanocratic alkali-feldspar syenite samples (88216, 88217) are slightly displaced towards lower SiO_2 values. Data points in the Harker variation diagrams (figs. 3b-l) demonstrate the compositional continuity of the Murdock Creek rock suite with smooth linear trends for all major elements (except Fe_2O_3) over the entire range of SiO_2 concentration, from 42 to 59 wt.%. These well-correlated trends reinforce the conclusion drawn from field relations, petrography, and ferromagnesian mineral chemistry (Rowins et al. 1989; Rowins et al., in prep.), that the Murdock Creek rock units (except hornblendite) are related through

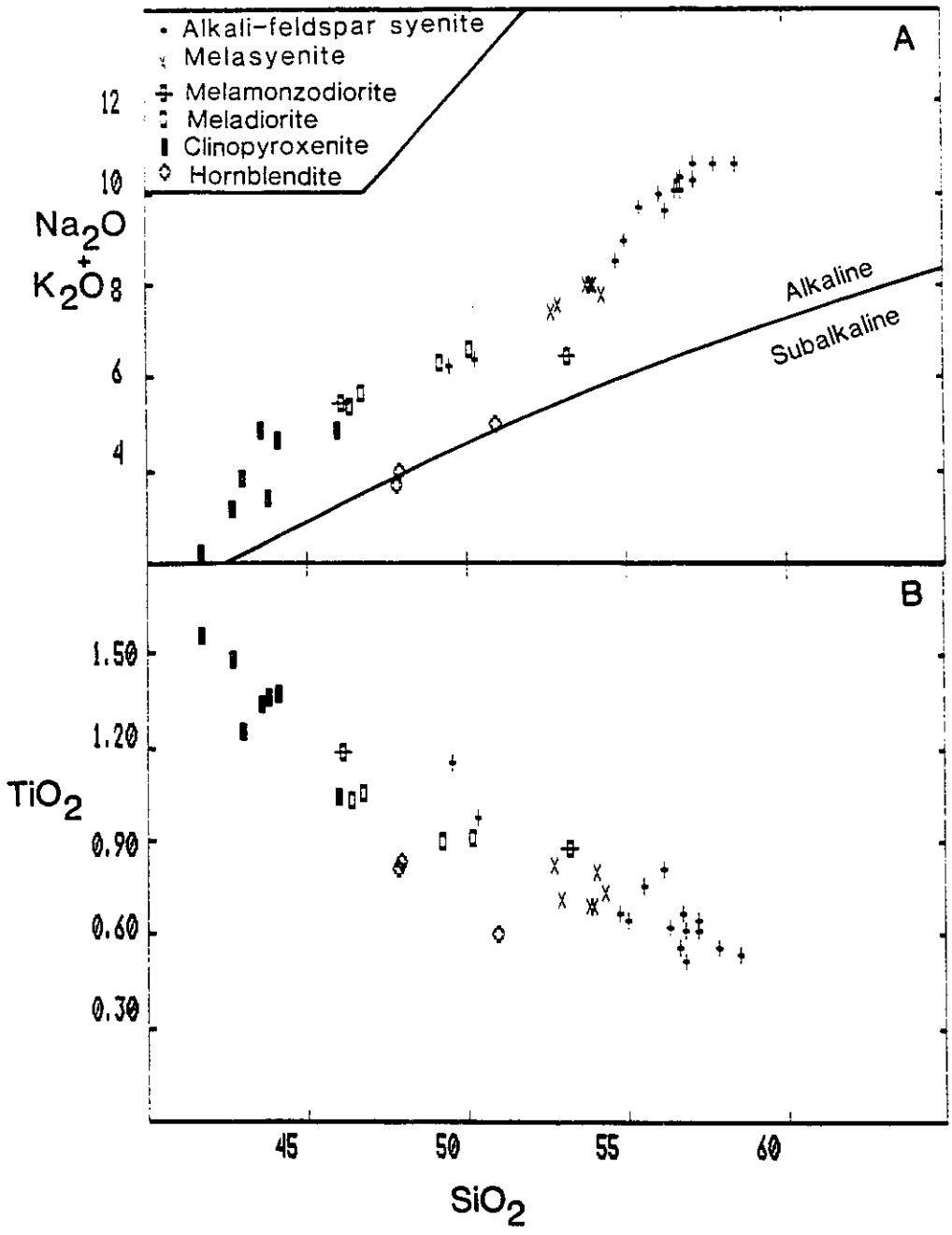

Fig. 3.-Major oxides plotted against SiO_2 (wt.%). Note that the highly melanocratic alkali-feldspar syenite samples 88216 and 88217 plot at SiO_2 values more typical of the less evolved rock types. Alkaline field boundary in fig. 3a from Myashiro (1978). The scatter in Fe_2O_3 contents (fig. 3d) results from post-magmatic oxidation processes (e.g., Boone 1969; Lalonde and Martin 1983). Boundaries in fig. 3k after Peccerillo and Taylor (1976) and Wheller et al. (1987). Slight scatter in P_2O_5 contents (fig. 3l) reflects variable apatite contents in analysed whole-rock samples.

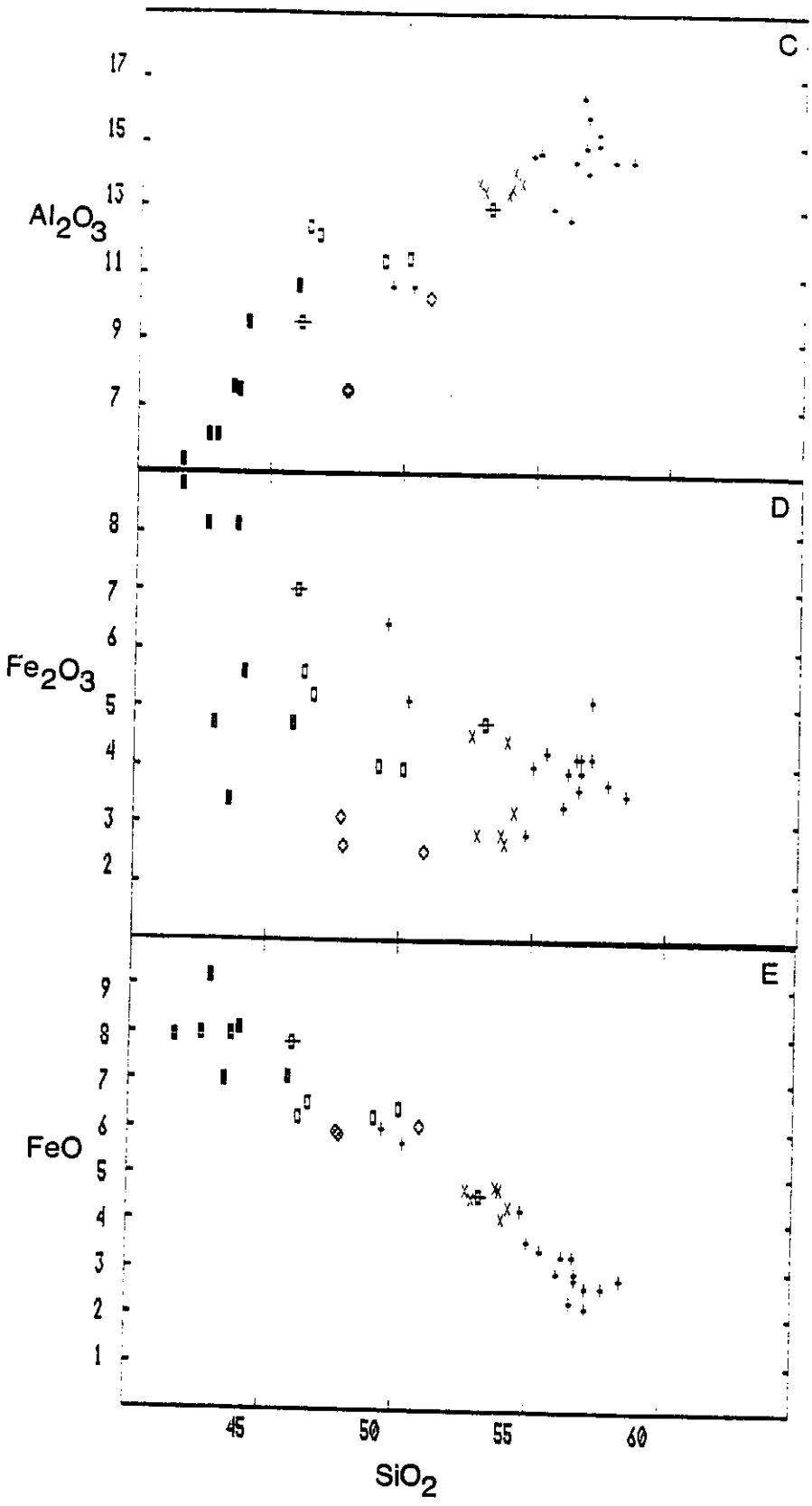
C
D
E
Al_2O_3
Fe_2O_3
FeO
SiO_2
17
15
13
11
9
7
8
7
6
5
4
3
2
9
8
7
6
5
4
3
2
1
45
50
55
60

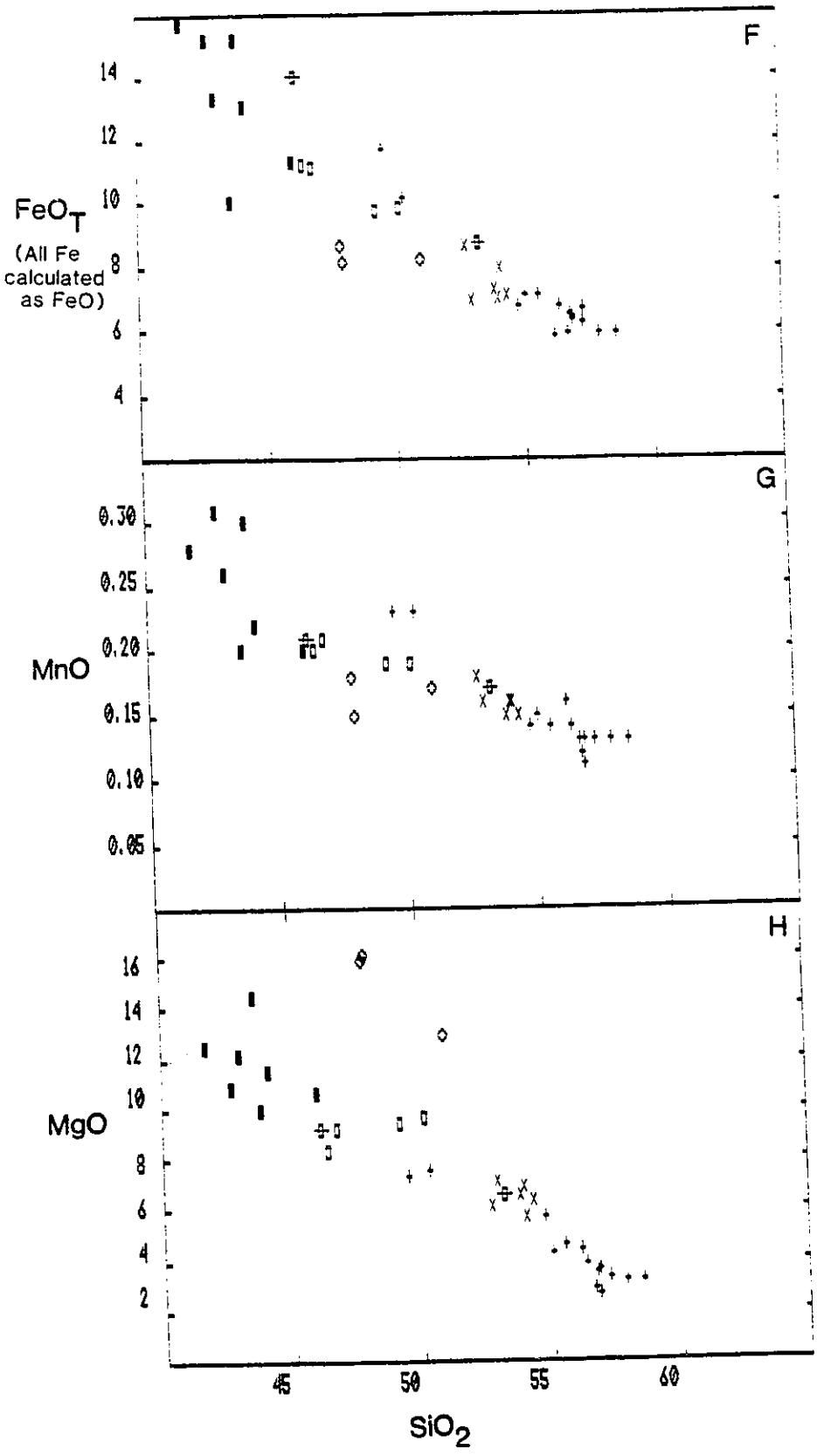
F
14
12
10
8
6
4
FeO$_T$
(All Fe calculated as FeO)
G
0.30
0.25
0.20
0.15
0.10
0.05
MnO
H
16
14
12
10
8
6
4
2
MgO
45
50
55
60
SiO$_2$

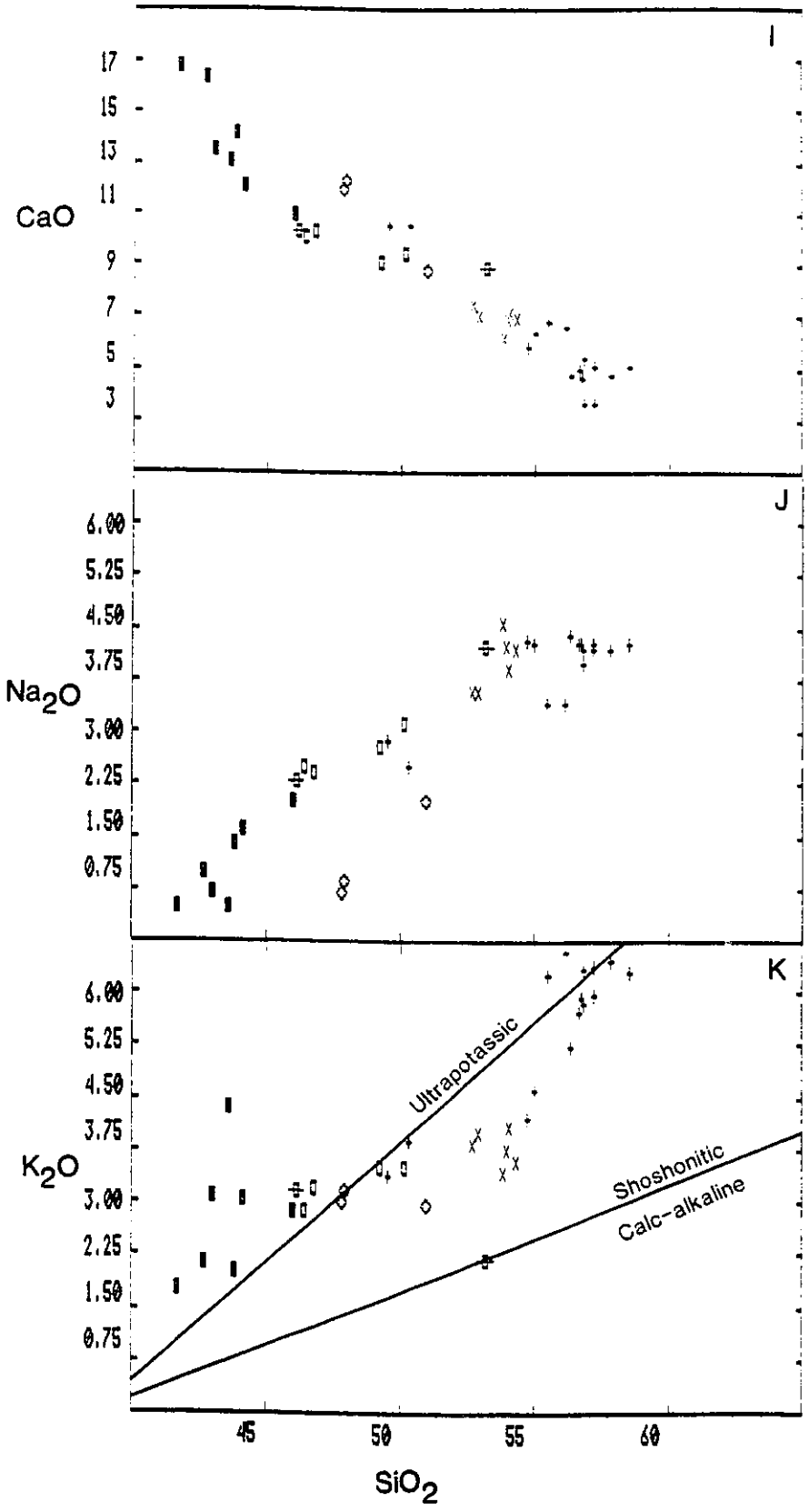
I
CaO
17
15
13
11
9
7
5
3
J
Na_2O
6.00
5.25
4.50
3.75
3.00
2.25
1.50
0.75
K
K_2O
Ultrapotassic
Shoshonitic
Calc-alkaline
45
50
55
60
SiO_2

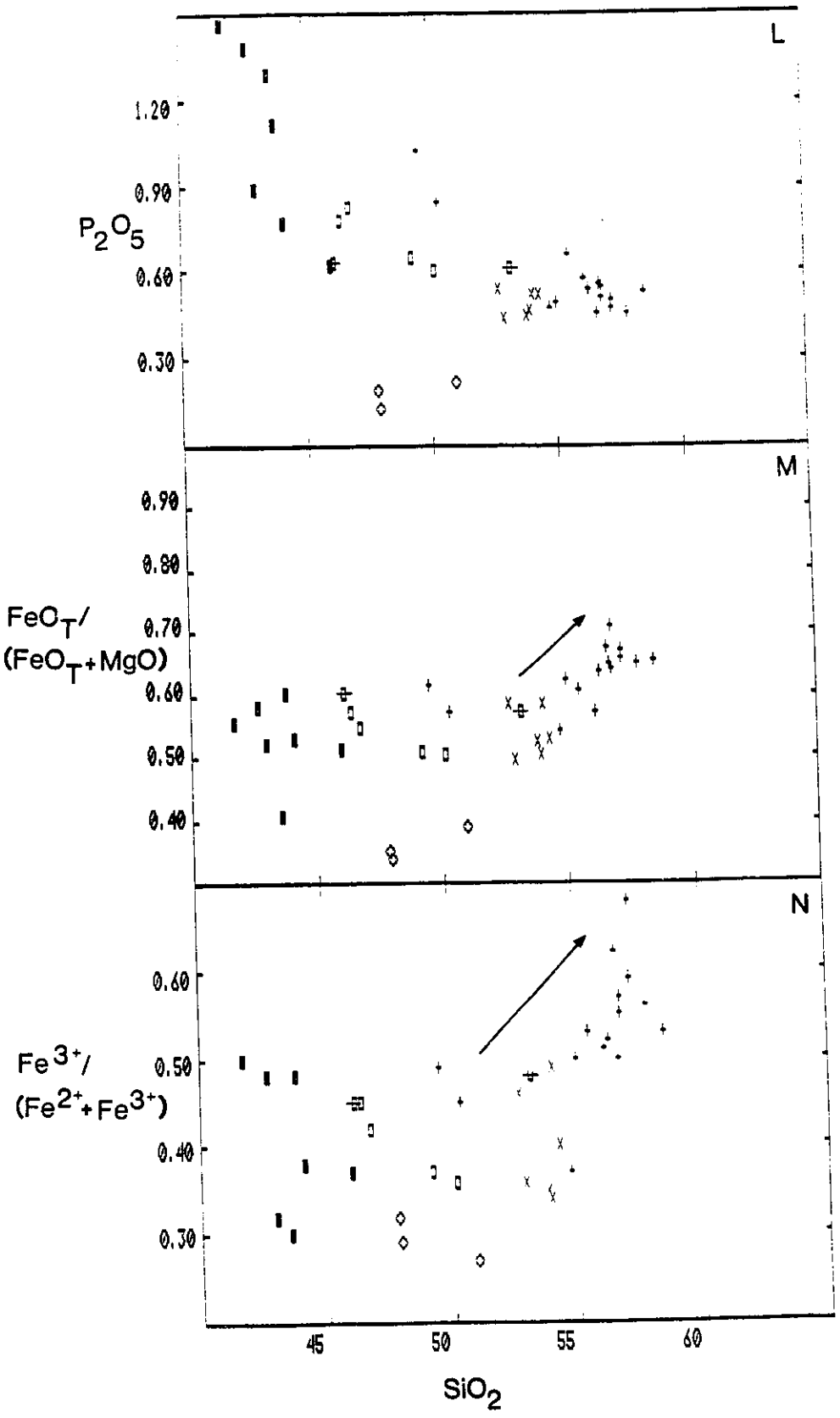
L
1.20
0.90
0.60
0.30
P_2O_5
M
0.90
0.80
0.70
0.60
0.50
0.40
$FeO_T/(FeO_T+MgO)$
N
0.60
0.50
0.40
0.30
$Fe^{3+}/(Fe^{2+}+Fe^{3+})$
45
50
55
60
SiO_2

differentiation of a single pulse of potassic mafic alkaline magma. The early crystallization of diopside, Mg-rich biotite, plagioclase (An_{30-34}) and accessory magnetite, apatite, and titanite (yielding mafic marginal rocks) caused progressive depletion of FeO_T, TiO_2, MnO, MgO, CaO and P_2O_5 in the residual melt. A concurrent buildup of Al_2O_3, K_2O and Na_2O was accomodated by the formation of increasingly larger quantities of K-feldspar which culminated in the crystallization of alkali-feldspar syenite.

The $FeO_T/(FeO_T+MgO)$ ratio (fig. 3m) is fairly constant throughout pluton evolution with values typically falling between 0.50 to 0.62. At the onset of alkali-feldspar syenite crystallization however, slight Fe enrichment occurs and values approach 0.70. This late Fe enrichment trend is readily explained by the removal of large quantities of Mg-rich mineral phases (i.e., diopside and biotite; see mineral compositions in Rowins et al., in prep.) during formation of the mafic marginal rocks.

Relatively high, though variable, $Fe^{3+}/(Fe^{2+}+Fe^{3+})$ ratios (average $\approx$ 0.44; fig. 3n) characterize all Murdock Creek rock units and are consistent with the maintenance of a high f_{O_2} during primary crystallization. Late Fe^{3+} enrichment in alkali-feldspar syenite mimicks the trend for total Fe. This is interpreted as resulting from an increased proportion of magnetite (in alkali-feldspar syenite) relative to coexisting ferromagnesian silicates which contain proportionally less Fe^{3+}.

The K_2O/Na_2O ratio generally exceeds unity, and together with

the K_2O vs. SiO_2 plot (fig. 3k) demonstrates the chemical affinity of Murdock Creek rock types with shoshonitic and ultrapotassic igneous rocks (Morrison 1980; Cullers and Graf 1984; Foley et al. 1987).

Trace Elements.-Abundances of the compatible transition metals Sc, V, Cr, Co, Ni are highest in the most mafic rock types of the intrusion and decrease fairly regularly with increasing SiO_2 content (figs. 4a-c). Such behaviour is consistent with the strong partitioning of transition metals into the early-crystallizing ferromagnesian silicates and Fe-Ti oxides (Gill 1981; Henderson 1982). Hornblendite samples possess the highest Cr (up to 1230 ppm) and Ni (up to 271 ppm) contents of any rock type in the intrusion. This, together with their high MgO contents (max 16.10 wt.%) and low $FeO_T/(FeO_T+MgO)$ ratios (fig. 3m) place them in the broad range considered characteristic of "primary" mantle-derived magmas (Rhodes 1981; Rock 1987), although Ni contents tend to be slightly low. These "mantle" characteristics indicate that the hornblenditic magmas were not greatly fractionated from liquids in equilibrium with mantle peridotite (c.f., Leat et al. 1988).

A wide range of incompatible element abundances are conveniently summarized on chondrite-normalized (cn) incompatible element plots (fig. 5) commonly refered to as spidergrams (Thompson et al. 1984). Spidergrams for all Murdock Creek rock types share remarkably similar geochemical features consistent with the hypothesis that they are genetically related to the same

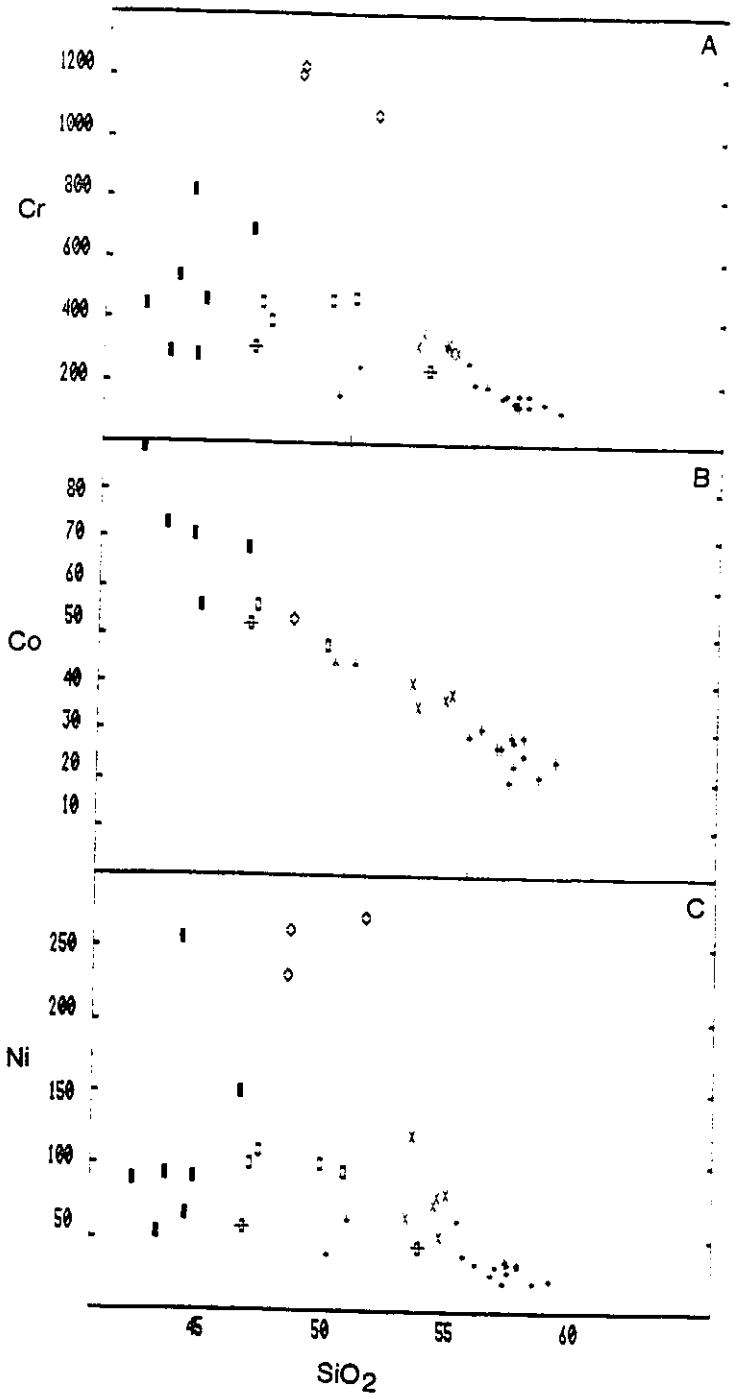

Fig. 4.-Selected trace elements plotted against SiO_2 (wt.%). The lack of clearly decreasing Cr (fig. 4a) and Ni (fig. 4c) abundances during evolution of the mafic marginal rocks is probably a consequence of fairly similar proportions of mafic minerals crystallizing during formation of these units (table 1). Only with advancing stages of pluton evolution, and significant decreases in the amounts of mafic minerals fractionating (crystallization of alkali-feldspar syenite), do Cr and Ni contents drop. Symbols as in fig. 3.

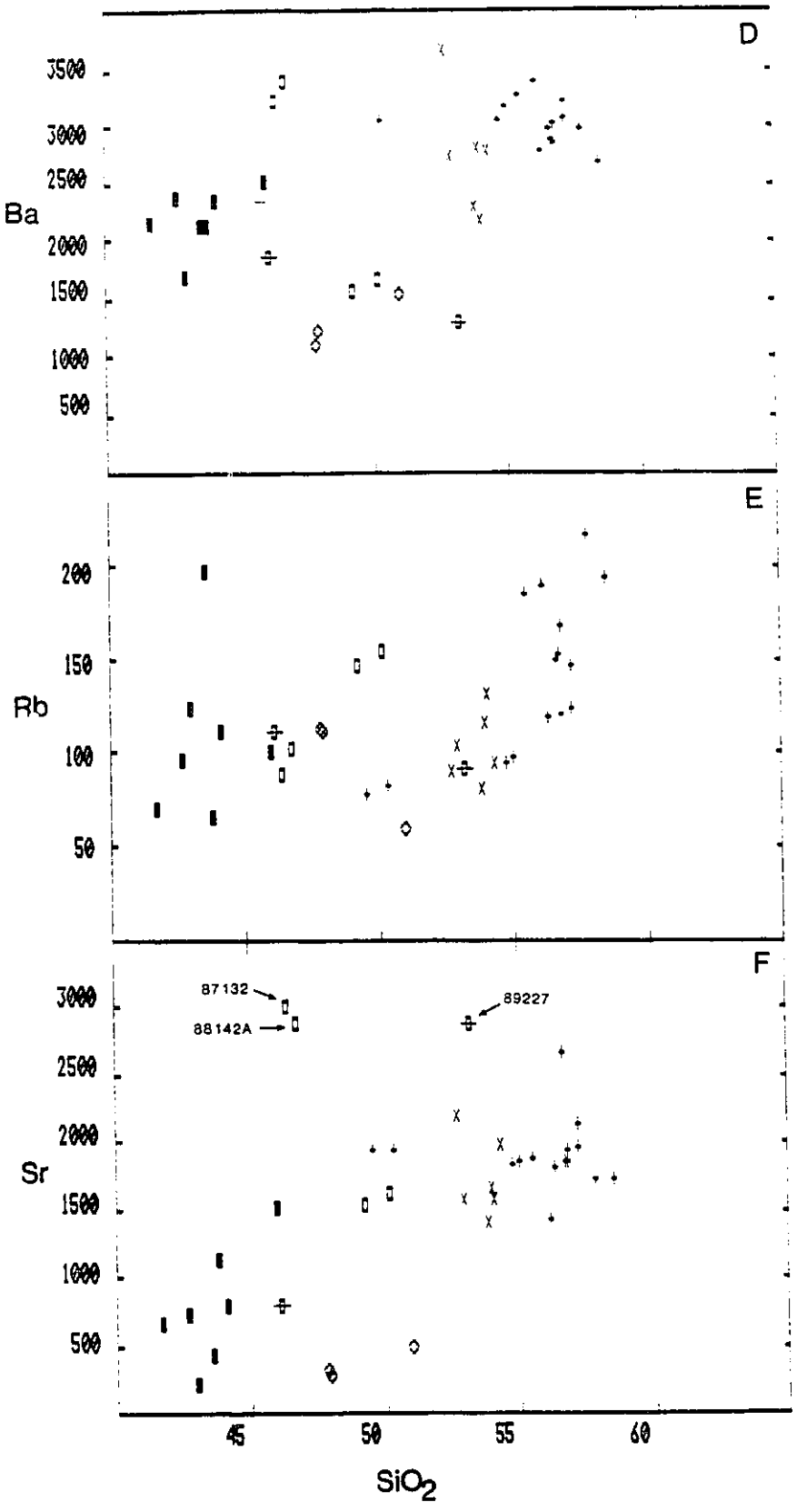
D
Ba
3500
3000
2500
2000
1500
1000
500
E
Rb
200
150
100
50
F
Sr
3000
2500
2000
1500
1000
500
87132
88142A
89227
45
50
55
60
SiO2

parental pulse of potassic mafic alkaline magma. Despite pre-emplacement evolution of the magma pulse (leaving denser mafic cumulate residuum below) and extensive post-emplacement fractional crystallization, many of the most important trace element characteristics have been inherited, almost unchanged, from the most primitive rock units to the most highly evolved. A consistent feature of Murdock Creek spidergrams are marked depletions at Nb, Ta, Ti, Th, and U, and enrichments in the other LILE's and LREE's. The tectonic implications of this distinctive pattern are addressed later.

High-field-strength elements (HFSE) such as Nb, Ta, Y, Zr, and Hf, lack systematic variation with increasing degrees of magmatic fractionation due to their concentration in accessory mineral phases which remained on the liquidus throughout crystallization; Nb and Ta in Fe-Ti oxides and Ti-silicates (Green 1981; Green and Pearson 1987; Ryerson and Watson 1987); and Zr and Hf in zircon (Watson 1979; Green 1981). The geochemical coherence of Zr and Hf is illustrated by the constancy of the Zr/Hf ratio over the entire compositional spectrum of Murdock Creek rock types. The average Zr/Hf ratio of about 45 is typical of syenites and alkali-basalt suites (Turekian and Wedepohl 1961; Gerasimovsky 1974; Weaver et al. 1987 and references therein). The Ca/Y ratio correlates negatively with SiO_2 (fig. 6), indicative of the dominant role clinopyroxene fractionation played during magma evolution. Lambert and Holland (1974) demonstrated that the fractionation of

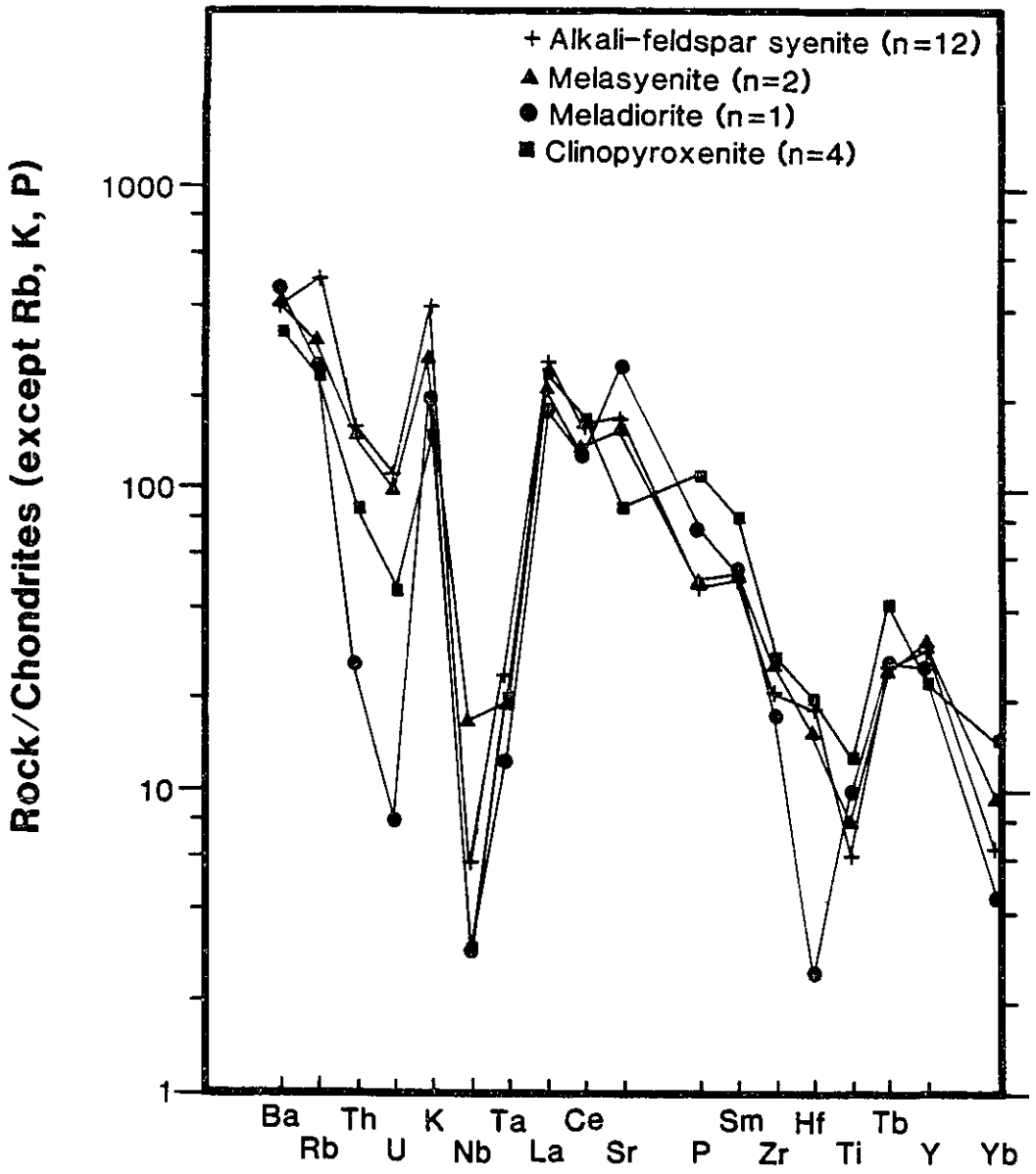

Fig. 5.-Chondrite-normalized incompatible element patterns (spidergrams) for rock units of the Murdock Creek intrusion. Normalizing factors are from Thompson (1982). Note that Rb, K, and P have been normalized to terrestrial rather than chondritic abundances. Pronounced negative anomalies at Nb, Ta, Ti, and lesser ones at Th and U, and positive anomalies at Ba, Rb, K, Sr, and La are characteristic of all Murdock Creek rock units (n = number of samples averaged).

clinopyroxene, as opposed to hornblende, reduces the Ca/Y ratio during progressive differentiation of felsic magmas. Because the clinopyroxene structure cannot accomodate Y, the residual melt is enriched in Y as Ca contents fall with fractionation of diopside. Plagioclase crystallization in the early stages of pluton evolution (meladiorite and melamonzodiorite produced) also diminishes the Ca/Y ratio in the residual melt because plagioclase cannot easily accomodate trivalent ions. Fractionation of biotite and K-feldspar has little effect on the ratio since they are essentially Ca- and Y-free minerals. Scatter in the Ca/Y versus SiO_2 plot may be attributed to the strong partitioning of Y into accessory minerals, particularly apatite and titanite (Nash 1972; Green 1981). However, the fairly good correlation in fig. 6 suggests that their effect on Y distribution was, by and large, subordinate to the extreme dominance of clinopyroxene fractionation.

Th and U tend to be most highly concentrated in alkali-feldspar syenite in compliance with their large ionic radii and resultant incompatibility. The Th/U ratio varies in a narrow range between 3.2 to 7.0, averaging about 4.9 (excluding two anomalously high values of 11.0 and 17.0 in samples 87132 and 87133 respectively), a value within the magmatic Th/U range (Maynard 1983) signifying that the absolute abundances are inherently a primary feature of the magma. The relative constancy of the ratio also concurs with the maintenance of uniform f_{O_2} during pluton crystallization because Th/U varies directly with

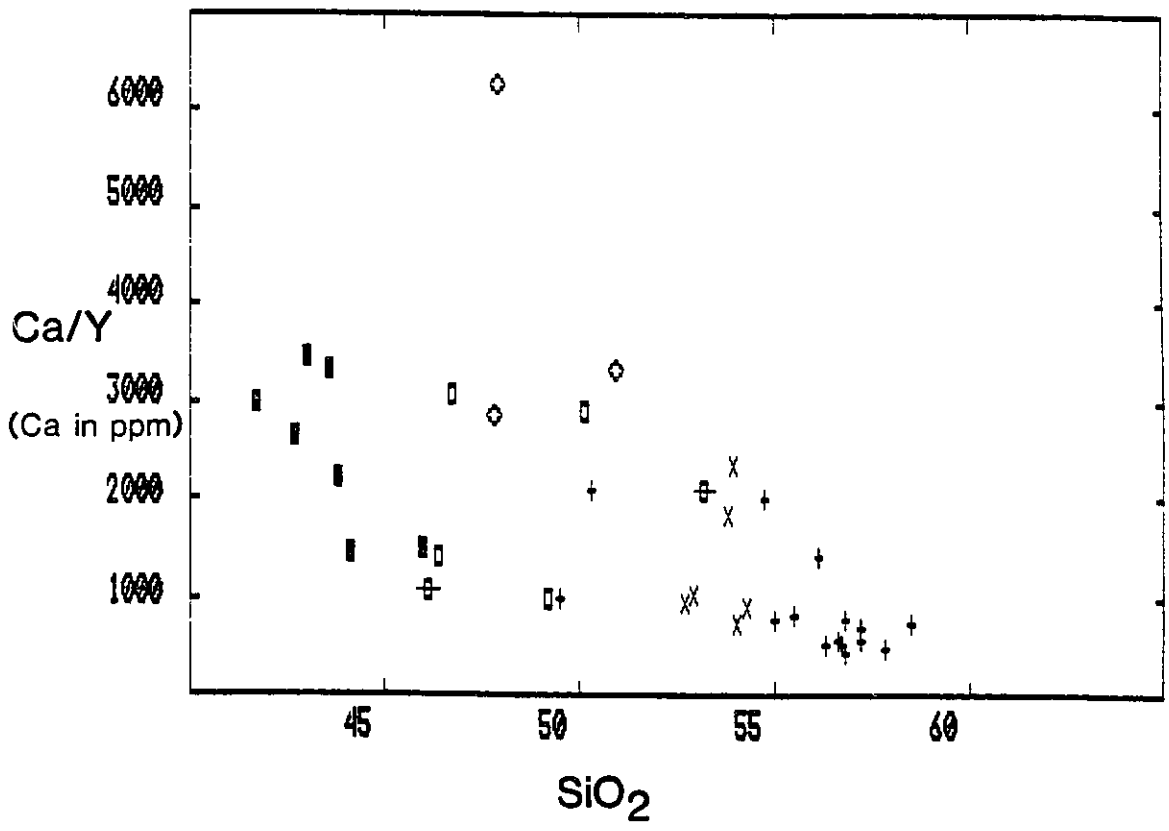

Fig. 6.-Ca/Y plotted against SiO_2 (wt.%). The negative correlation is consistent with the dominant role clinopyroxene fractionation is known to have played during pluton evolution (e.g., Lambert and Holland 1974). Symbols as in fig. 3.

magmatic f_{O_2} (Watkins and Haggerty 1967; Barbey and Cuney 1982).

The metallic elements Cu, Zn, As, Mo, Sb, and Au lack systematic variation with changing SiO_2 and their low concentrations are typical of syenitic rocks (Turekian and Wedpohl 1961; Gerasimovsky 1974; Sorensen 1974). Such incompatible behavior is congruent with the chalcophile nature of these elements (Brownlow 1979) and the uniformly low whole-rock S contents, manifested mineralogically by the scarcity of primary sulphide minerals.

Abundances of Ba, Rb, and Sr are higher than is the case for most rocks of syenitic composition (Turekian and Wedepohl 1961; Gerasimovsky 1974). Despite some scatter (likely due to the mobility of the LILE's during low temperature alteration; Clague and Frey 1982) in the chemical variation diagrams (figs. 4d-f), LILE abundances generally follow K_2O contents and correlate positively with SiO_2 in compliance with their exclusion from clinopyroxene, the main mineral component of the early-crystallized mafic differentiates. Barium and Rb are localized primarily in K-feldspar and biotite, common mineral phases in the late fractionation assemblage, where they substitute for K. Strontium replaces Ca in plagioclase (and in apatite to a lesser extent, e.g., Edgar 1989) hence the highest Sr contents would be expected in the most plagioclase-rich rocks of the intrusion. This prediction holds for meladiorite samples 88142A and 87132 and the melamonzodiorite 89227, but not for meladiorite samples 88288 and 88248A and one melamonzodiorite,

88295 (fig. 4f). The reason for this discrepency is not clear, but the high Sr contents in the more evolved plagioclase-poor felsic differentiates may derive from the substitution of Sr for K in K-feldspar, the dominant mineral component of these rocks (e.g., K_D (mineral-melt distribution coefficient) for Sr in K-feldspar in felsic melts = 3.55; Mittlefehldt and Miller 1983).

The highest K/Rb ratios are found in melasyenite and alkali-feldspar syenite (fig. 7), which is opposite to Shaw's (1968) predicted main trend for K/Rb variation during magmatic differentiation. The normal trend of decreasing K/Rb values with progressive differentiation is usually attributed to an increase in the amount of biotite (or sometimes leucite in volcanic rocks, e.g., Barbieri et al. 1968) because biotite preferentially concentrates Rb to a greater degree than other rock-forming minerals (Mittlefehldt and Miller 1983). A reverse trend such as displayed by the Murdock Creek intrusion is unusual but has been reported in the Kûngnât syenite complex, Greenland (Upton 1960), and the Blue Mountain nepheline syenite, Canada (Payne and Shaw 1967). Possible explanations for the K/Rb ratio reversal include: (a) the <u>early</u> crystallization of biotite which is enriched in Rb relative to K, leaving residual magma impoverished in Rb (Payne and Shaw 1967), (b) late crystallization or accumulation in the liquid of K-feldspar crystals impoverished in Rb relative to K (K/Rb ratio of biotite is about 1/3 that of coexisting K-feldspar; Beswick and Eugster 1969), and (c) selective leaching of Rb relative to K from K-feldspars into an escaping fluid (or

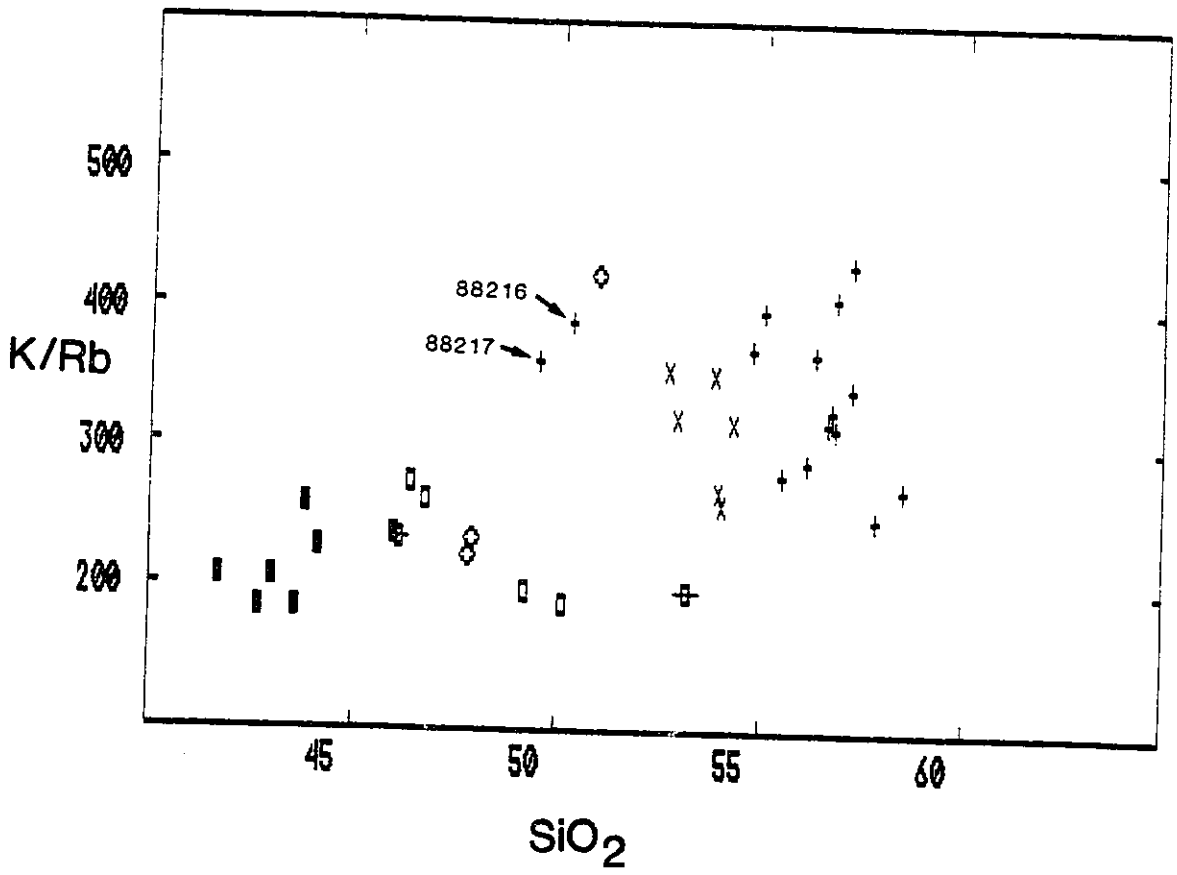

Fig. 7.-K/Rb plotted against SiO_2 (wt.%). Early biotite fractionation in combination with late K-feldspar fractionation appear to have resulted in higher K/Rb ratios in melasyenite and alkali-feldspar syenite samples (see text for further discussion). The very melanocratic alkali-feldspar syenite samples 88216 and 88217 have respective K/Rb ratios of 387 and 359, both values substantially higher than those found in samples of similar SiO_2 content but containing much less K-feldspar, thus demonstrating the large degree of control K-feldspar has on the ratio. Symbols as in fig. 3.

gas) phase (Heier and Brooks 1966; Arth et al. 1978). Explanations (a) and (b) seem most appropriate in the case of the Murdock Creek intrusion. The paucity of pegmatites and absence of miarolitic cavities argues against (c). Evidence that K-feldspar was indeed a primary influence on the K/Rb ratio is shown in fig. 7; two very melanocratic alkali-feldspar syenite samples, 88216 and 88217, have K/Rb ratios of 387 and 359 respectively, both values significantly higher than those found in samples of similar SiO_2 content but containing much less K-feldspar (e.g., meladiorite and melamonzodiorite).

The K/Sr, K/Ba, Rb/Sr, and Rb/Ba ratios remain fairly constant throughout pluton crystallization. Aberrant values usually reflect atypical proportions of biotite, plagioclase, and K-feldspar in specific samples from the various rock units. For example, clinopyroxenites 89221 and 89296 are enriched in biotite (up to 27 mode%) and devoid of feldspar. Consequently, they have very high Rb/Sr and K/Sr ratios. Similarly high ratios are found in hornblendite samples 87329 and 89509 which consist mainly of hornblende and biotite with only minor feldspar.

Ba/Sr ratios are highest in clinopyroxenite and lowest in meladiorite and melamonzodiorite; intermediate values occur in melasyenite and alkali-feldspar syenite. This irregular trend (fig. 8) is readily explainable in terms of mineral phases dominating the fractionation assemblage at the various stages of pluton crystallization; Ba substitutes readily for K in K-feldspar and presumably would be consumed rapidly by the first

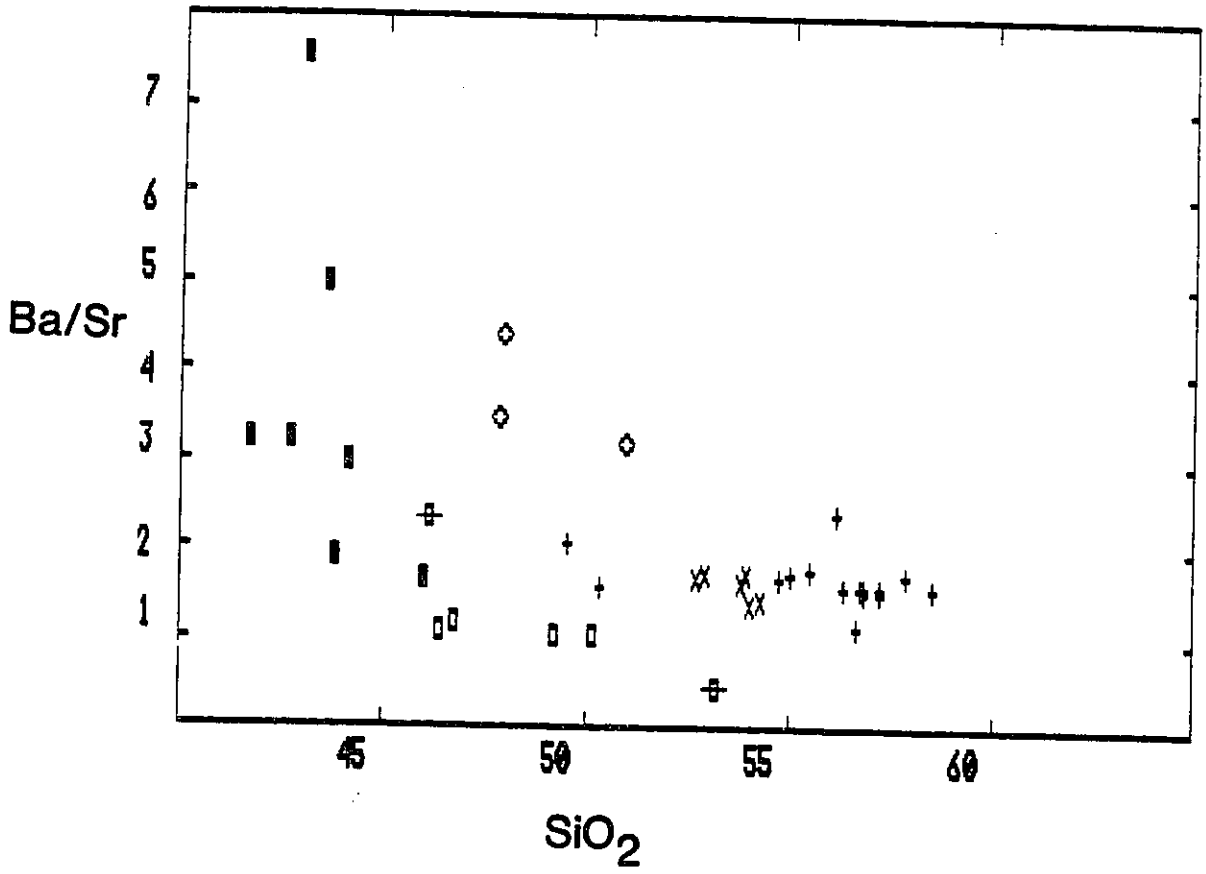

Fig. 8.-Ba/Sr plotted against SiO_2 (wt.%). The irregular trend demonstrates the influence of K-feldspar and plagioclase over Ba and Sr distribution in Murdock Creek rocks. See text for further discussion. Symbols as in fig. 3.

K-feldspars to crystallize, e.g., Philpotts and Schnetzer (1970), Long (1978), and Mittlefehldt and Miller (1983) have all measured K_D's for Ba in K-feldspar between 6.12 and 14.0 in felsic melts. Thus, early-crystallized mafic marginal rocks will have high Ba/Sr ratios even though they contain very little K-feldspar. In several clinopyroxenite samples devoid of K-feldspar, Ba is very likely sequestered in biotite (K_D = 3.21 for Ba in biotite in felsic melts; Mittlefehldt and Miller 1983). The lowest Ba/Sr ratios recorded in the plagioclase-rich intermediate rocks result from their high Sr contents (Sr substituting for Ca in plagioclase). The sudden reversal in the Ba/Sr ratio with advancing stages of evolution can be attributed to both decreasing plagioclase (and hence Sr) and increasing K-feldspar contents (and hence Ba).

Rare Earth Elements.-Rare earth element patterns (fig. 9) are remarkably similar for all Murdock Creek rock types, with chondrite-normalized La abundances between 150 and 350, and the heavy rare earth elements (HREE) about 5 to 20 times chondritic. Alkali-feldspar syenite typically dislpays slight LREE enrichment (La content between 70 to 110 ppm) and HREE depletion (Yb content 1 or 2 ppm) relative to the earlier formed mafic differentiates. This results in higher $(La/Yb)_{cn}$ ratios (max 59) and REE curves with slightly steeper negative slopes. The overall similarity of REE spectra in conjunction with the systematic steepening of profiles accompanying progressive crystallization, suggests a common parental magma and a cogenetic relationship through

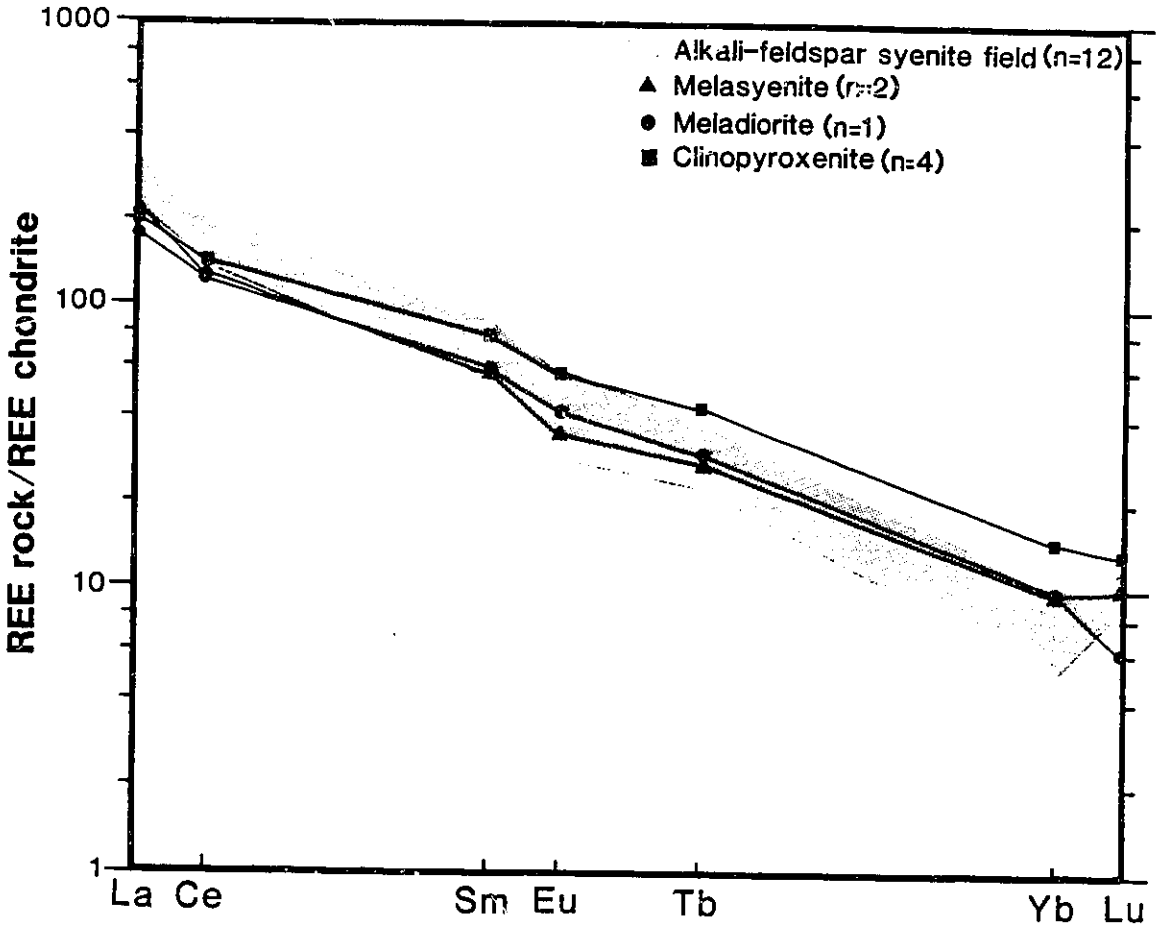

Fig. 9.-Average chondrite-normalized REE patterns for rock units of the Murdock Creek intrusion. Chondrite normalization factors are those of Haskin et al. (1968).

fractional crystallization of the main rock-forming minerals; clinopyroxene, which dominates the early fractionation assemblage, preferentially incorporates the HREE (Schnetzler and Philpotts 1970; Cullers and Graf 1984), whereas biotite and feldspar have only minor effect on the REE pattern of the melt, except possibly for Eu in the feldspars (Arth and Hansen 1975; Hanson 1980).

REE contents in the felsic members of the intrusion closely approximate those of typical Archean syenites (see fig. 5-17 in Condie 1981) except for slightly lower $(La/Yb)_{cn}$ ratios in response to mildly elevated HREE abundances. This slight HREE enrichment probably results from a greater abundance of clinopyroxene in these rocks, hence the more melanocratic character of the melasyenite and alkali-feldspar syenite compared to "average" syenites (Sorensen 1974; Lemaitre 1976; Condie 1981). REE patterns for Murdock Creek rock units also closely match REE profiles of; (1) felsic and augite syenite from the Kirkland Lake syenite complex (KLSC), although Murdock Creek rocks tend to possess higher $LREE_{cn}$ abundances; and (2) trachytic flows and tuffs belonging to the Timiskaming Group which are frequently postulated as extrusive equivalents to the Kirkland Lake syenite suite (Cooke and Moorehouse 1968; Ridler 1970), although La abundances are about 400 to 600 times chondrite or about twice that of the most evolved Murdock Creek alkali-feldspar syenite sample (Kerrich and Watson 1984; fig. 4). These closely corresponding REE patterns suggest consanguinity

between alkaline rocks in the Kirkland Lake area, a topic addressed in the next section.

Negligible or very small negative Eu anomalies in Murdock Creek REE profiles concur with the general lack of Eu anomalies in Archean alkaline igneous rocks (Condie 1981; Cullers and Graf 1984), and are consistent with a mantle origin for the pluton because in a crustal melt, feldspar would almost certainly have been a significant restite phase, generating large negative Eu anomalies in any equilibrated liquid (i.e. Eu^{2+} substituting for Ca^{2+} in plagioclase; Hansen 1980). Lack of pronounced Eu anomalies in the more evolved felsic members of the Murdock Creek rock suite might also seem to suggest that plagioclase fractionation, contrary to petrographic evidence, was not important in pluton evolution. However, the lack of substantial Eu anomalies is best explained by the uniformly high magmatic f_{O_2} under which all Murdock Creek rock units crystallized. This would have restricted the necessary reduction of Eu^{3+} to Eu^{2+} and inhibited anomaly formation (Weill and Drake 1973; Drake 1975; Drake and Weill 1975).

ΣREE contents remain at approximately the same level throughout the compositional spectrum of Murdock Creek rock types. In some instances, mafic differentiates possess slightly higher ΣREE abundances than the more evolved felsic differentiates, a feature seemingly contrary to simple generalizations about REE incompatibility during processes of magmatic fractionation. However, ΣREE constancy or even relative

depletion in more fractionated members of a differentiated intrusion is not uncommon and has frequently been attributed to the early crystallization of accessory mineral phases with high partition coefficients for the REE (e.g., Nagasawa and Schnetzler 1971; Miller and Mittlefehldt 1979, 1982; Mittlefehldt and Miller 1983; Cullers and Graf 1984). This explanation applies equally well to the Murdock Creek intrusion where titanite, apatite, and zircon are early crystallizing phases which remained on the liquidus throughout pluton evolution (table 1), although the steepening of REE profiles with progressive crystallization would seem to indicate that their effect on individual REE abundances did not appreciably exceeded those of the common rock-forming minerals, especially clinopyroxene; K_D's for the REE in clinopyroxene dominate the bulk distribution coefficients for the REE even when a significant amount of feldspar is involved (e.g., Simmons and Hodge 1978; Henderson 1984).

CONSANGUINITY OF LATE ARCHEAN POTASSIC ALKALINE IGNEOUS ROCKS IN THE KIRKLAND LAKE AREA

The possibility that the compositionally diverse suite of potassic alkaline igneous rocks in the Kirkland Lake district are related to a common tectono-magmatic event in the Late Archean (e.g., Colvine et al. 1988; Card 1989) has important implications, not only for reconstructing the geological history of this part of the Abitibi belt, but also from an economic standpoint given the close spatial and possible temporal

association between gold mineralization and alkaline intrusions, most notably the Kirkland Lake syenite complex (KLSC).

Late Archean (≈ 2680 Ma) composite syenitic plutons within and adjacent to the KLF exhibit many field, petrographic, and mineralogical similarities to one another (comparative descriptions can be found in Burrows and Hopkins 1923, Thomson 1950, Thomson et al. 1950, Lovell 1972, Ploeger and Crocket 1980, Kerrich and Watson 1984, Cameron and Carrigan 1987, Hicks and Hattori 1988, Smith and Sutcliffe 1988, Lévesque 1989; Rowins et al. 1989 and Rowins et al., in prep.). There is however surprisingly little geochemical data available in the literature for direct comparison of the Murdock Creek intrusion with other proximal syenitic intrusions. One exception is the KLSC, which has been the subject of numerous studies detailing the gold mineralizing event which has made this celebrated intrusion the centre of mining activity in the Kirkland Lake camp since the early part of this century. Comparison of the average abundances of major and trace elements in felsic and augite syenite from the KLSC (two of it's four main plutonic units) with melasyenite and alkali-feldspar syenite from the Murdock Creek intrusion, reveals a close geochemical resemblance (see samples P1 and P2 from Kerrich and Watson (1984) in table 2). The slightly elevated Al_2O_3 and K_2O, and lower FeO_T, MgO, and CaO content of the KLSC felsic syenite relative to the Murdock Creek alkali-feldspar syenite are a result of its more leucocratic character (e.g., more alkali-feldspar and less clinopyroxene than Murdock Creek

units). K_2O/Na_2O ratios in unaltered KLSC felsic and augite syenite samples typically exceed unity, matching those in Murdock Creek melasyenite and alkali-feldspar syenite samples, a clear indication of chemical affinity with ultrapotassic and shoshonitic igneous rocks. Trace element abundances and inter-element ratios are also very similar; corresponding rock types are LILE-enriched, Murdock Creek rocks slightly more so than their KLSC counterparts; low and similar Nb and Zr contents result in high Ti/Zr ratios in both the KLSC felsic and augite syenite (13 to 35), and in equivalent syenitic units from the Murdock Creek intrusion (16 to 30); and Nb/Y ratios of 0.2 to 0.5 in the KLSC syenites and 0.1 to 0.6 in the comparable Murdock Creek rock types. Zr/Y, Ti/V, K/Rb, and Rb/Sr ratios closely match in equivalent units from the two intrusions, and are somewhat lower than is the case for most rocks of syenitic composition (Turekian and Wedepohl 1961; Gerasimovsky 1974). The average Th/U ratio of Murdock Creek melasyenite and alkali-feldspar syenite samples (4.7 and 4.9 respectively) are not far off the average ratios for augite syenite and felsic syenite from the KLSC (3.5 and 7.9 respectively). Likewise, Cr/Ni ratios in the rock units under consideration are very similar (KLSC, 3.3-4.4; Murdock Creek, 4.1-5.1) and higher than in most syenitic rocks.

This geochemical similarity also extends to trachytic flows and tuffs belonging to the Timiskaming Group, and to calc-alkaline lamprophyres as shown through REE profiles (Kerrich

and Watson 1984) and spidergrams (Wyman and Kerrich 1988) (also see fig. 2 in Ujuke 1985 for REE profiles of Timiskaming trachytes).

PETROGENESIS

Theories on the petrogenesis of potassic mafic alkaline igneous rocks, and of mafic alkaline magmas in general, have had to reconcile large incompatible element enrichments (most notably the LILE's) and derivation, by partial melting, from supposedly normal garnet/spinel lherzolite mantle; the high Mg, Cr, and Ni contents of mafic alkaline rocks among other evidence (i.e., isotopic), appear to necessitate a mantle source (Sorensen 1974; Cullers and Graf 1984; Lloyd et al. 1985; Foley et al. 1987). Models have attempted to explained this incompatible element enrichment by a variety of processes including; (1) high degrees of crystal fractionation from more normal basaltic melts originating by partial melting of garnet peridotite mantle (O'Hara and Yoder 1967; Kay and Gast 1973); (2) assimilation of crustal material rich in these incompatible elements (refer to discussion in Gittens 1979); (3) zone refining operating over a large vertical distance in the mantle (Harris 1957; Harris and Middlemost 1969); and (4) low degree partial melting of a depleted or "modified" mantle peridotite metasomatically enriched in K and LILE's (Varne 1970; Dawson 1972; Lloyd and Baily 1975). These petrogenetic models have been reviewed in detail by Gupta and Yagi (1980) and more recently by Foley et al. (1987), but a

general concensus now exists that metasomatic processes (option #4) are most likely responsible for the selective LILE enrichments (Bailey 1982, 1987; Cullers and Graf 1984; Fitton and Upton 1987 and references therein; Foley et al. 1987; Menzies et al. 1987).

Consideration of the field, petrographic, mineralogical and geochemical data (this paper; Rowins et al. 1989; Rowins et al. in prep.) suggest that the Murdock Creek intrusion has evolved via a two-stage process. In the first stage, primitive mafic alkaline melt (probably potassic or shoshonitic basalt in composition) is produced by partial melting of metasomatically enriched mantle as suggested above. Partial melting was initiated by mantle upwelling during lithosphere extension which permitted mantle peridotite solidus boundaries to be crossed as explained in McKenzie and Bickle's (1988) model for the generation of basaltic magma. Partial melting may also have been facilitated by mantle degassing of CO_2 (Newton et al. 1980; Baily 1982) focussed up the KLF, given the widespread evidence for carbonatization associated with this structure. In the second stage following mantle fusion, a pulse of this primitive mafic alkaline partial melt differentiated, at mantle depths, and also during ascent within the KLF. Upon final emplacement at mid-crustal levels (Rowins et al., in prep.), the pluton underwent <u>in situ</u> fractional crystallization, yielding in order, clinopyroxenite, meladiorite, melamonzodiorite, melasyenite, and alkali-feldspar syenite.

Hornblendite, though not directly related to the specific pulse of potassic mafic alkaline magma which crystallized as the Murdock Creek intrusion, nonetheless has major and trace element abundances, and inter-element ratios similar to the least-evolved mafic plutonic members suggesting derivation from the same mantle source region. Hornblendite compositions also bear a remarkably close geochemical and mineralogical resemblance to lamprophyric rocks, specifically spessartites of the calc-alkaline lamprophyre clan (Rock 1984). Application of the various screens constructed for the classification of calc-alkaline lamprophyres (table 2 in Rock 1984) to the hornblendites, reveal complete agreement except for a greater proportion of mafic minerals in hornblendite than the calc-alkaline lamprophyre limit of 67% (e.g., colour index of Murdock Creek hornblendites > 67). A by-product of this relative mafic mineral enrichment are higher whole-rock MgO contents in hornblendites than are normal for calc-alkaline lamprophyres (Rock 1984). Highly mafic or even ultramafic K-rich rocks of this nature have been referred to as melaspessartites (Rock 1987 and references therein) and kentallenites (Macdonald et al. 1986) elsewhere, but in the Kirkland Lake area could simply be regarded as hornblende-cumulate members of a potassic basalt or lamprophyric magma suite which also includes calc-alkaline lamprophyres plus the highly differentiated syenites and trachytes. A similar intrusive hornblendite unit has also been identified, along with minette lamprophyres in the syenitic Otto stock (Smith and Sutcliffe 1988) lying just south of the Murdock

Creek intrusion (fig. 1). Lamprophyres, hornblendites and so called "appinites" in Scotland (Wright and Bowes 1979; Rock 1984 and references therein) are very commonly associated together (either within individual plugs, or in adjacent but separate plugs) in the vicinity of felsic (syenitoid, granitoid) plutons, and it appears that a similar igneous environment exists at Kirkland Lake. Syenitic magmas derived by fractionation of lamprophyric magmas have now been widely established (Macdonald et al. 1986; Thompson and Fowler 1986; Esperenca and Holloway 1987; Rock 1987; Boualdli et al. 1988; Fowler 1988; Nemec 1988; Leat et al. 1989).

TECTONIC IMPLICATIONS

Recent opinion favours the origin of the Superior Province as an accretionary terrane of continental fragments, arc complexes, and oceanic plateaux formed in plate tectonic regimes comparable to those of the Phanerozoic (Card 1989; Ludden 1989). East-trending elongate belts (subprovinces) of metavolcanic and granitic rocks (greenstone belts) that alternate with metasedimentary belts comprise the southern part of the Superior Province. Major subprovince contacts are complex zones of metamorphic and structural transition, and were commonly the loci for crustal-scale faults or "breaks" believed to be, in part, related to strike-slip movement during oblique convergence (Corfu and Stott 1986; Percival and Williams 1989). Hubert et al. (1984) have interpreted the Porcupine-Destor and the Larder

Lake-Cadillac faults, major faults in the Abitibi belt, to be sinistral strike-slip faults formed during oblique convergence.

It has been suggested that Archean alkaline igneous rocks in the Superior Province, and in particular, the potassic alkaline rocks associated with the KLF, formed from subduction-like processes at destructive plate margins, analogous to plate motions in the Phanerozoic (McNeil and Kerrich 1986; Wyman and Kerrich 1988). Cited in support of this interpretation are spidergrams displaying marked Nb, Ta, Ti, and sometimes P depletions in conjunction with LILE and LREE enrichments, a chemical signature typical of shoshonitic and ultrapotassic volcanic rocks formed in modern subduction-related island-arc complexes (Perfit et al. 1980; Pearce 1983; Macdonald et al. 1985; Varne et al. 1985; Thompson and Fowler 1986; Foley et al. 1987; Wheller et al. 1987; Stolz et al. 1988). Many authors, including most of those above, attribute this distinctive spidergram pattern to LILE and LREE enrichment in a previously Nb-Ta-Ti depleted mantle source by aqueous fluids or partial melts driven from subducted oceanic crust, the enriched elements being those which tend to be mobilized by aqueous fluids.

Despite the tectonic inferences drawn from these "spiked" spidergrams, the cause of the Ti-group depletion is controversial. It is usually attributed to either, (1) the presence of a residual titanate or perhaps a Fe-Ti oxide phase (into which Nb and Ta partition) after partial melting in the mantle (Saunders et al 1980; Green 1981; Morris and Hart 1983;

Brophy and Marsh 1986) or (2) that depletion is an inherent property of the source region, brought about by a previous episode of melt extraction, zone refining or equilibration with a percolating melt or fluid. The former hypothesis was rejected by Ryerson and Watson (1987) on the basis of experimental studies showing that Ti saturation over a range of physical conditions in melt compositions varying from basaltic to rhyolitic, was unlikely. Recent work has also suggested that Nb and Ta anomalies in some orogenic magmas are derived independently from a Ti-rich phase (Smalley et al. 1983; Briqueu et al. 1984). In any case, the studies of Watson and Ryerson (1987) among others (Gill 1981; Leat et al. 1988) have demonstrated that whatever the mechanism (or mechanisms) responsible for the Ti-group depletion, it must be able to operate in circumstances more general than subduction zones alone. Thus, the chemical signature of LILE and LREE enrichment coupled with Nb-Ta-Ti depletion, although characteristic, is <u>not unique</u> of magmas generated in Phanerozoic subduction zones. If one ascribes to the "residual Ti-rich accessory phase" model to explain the pronounced Ti-group depletions in Murdock Creek rocks, then titanite is probably the most likely candidate given the oxidized nature of the pluton's mantle source region (Rowins et al., in prep) and the relatively shallow level of mantle fusion (due to lithosphere extension and mantle upwelling), conditions which favour titanite stability (Hellman and Green 1979; Green 1980, 1981). A residual magnetite phase is also possible, but its ability to accommodate Nb, Ti,

and Ta is much less than that of titanite (Green and Pearson 1987).

Foley et al. (1987) have recently divided ultrapotassic mafic rocks into three principal groups according to their geochemistry and tectonic setting. Using their chemical classification criteria, two biotite clinopyroxenite samples (89221 and 89296) and two hornblendite samples (88329 and 89509) from the Murdock Creek intrusion are ultrapotassic *sensu stricto* ($K_2O/Na_2O \geq 2$, K_2O and $MgO \geq 3$) and most closely approximate their group II rocks. These occur dominantly in extensional environments. The large Nb, Ta, and Ti troughs in Murdock Creek spidergrams might seem to suggest an association with Foley et al.'s group III rocks; however, as discussed previously, depletion of these elements is not restricted to subduction zones, a point also noted by Foley et al. given the observed Ti-group depletion in spidergrams of group II rocks from the San Venanzo and Cupaello occurrences in Italy. These are not believed to be related to subduction (Cundari 1979, 1980).

Cameron (in press) has suggested an alternative to subduction processes for the generation of Archean potassic alkaline rocks associated with the KLF. He proposed that the alkaline rocks within the KLF occur in deep, narrow basins formed by sinistral strike-slip extension during a period of oblique convergence. This permitted mantle upwelling and low degree partial melting as in McKenzie and Bickle's (1988) model. We agree with this interpretation and note that a CO_2-rich melting environment is

consistent with the field evidence of extensive carbonatization, and with the classification of Murdock Creek ultrapotassic rocks as Foley et al.'s group II type since complexing with CO_2 readily explains this groups distinctly high CaO and Sr contents. The presence of a free CO_2 fluid or vapour phase is consistent with mantle enrichment under relatively oxidizing conditions (Cameron 1988), as implied by the intrinsically oxidized nature of syenitic intrusions in the Kirkland Lake area (Cameron and Carrigan 1987; Rowins et al., 1989; Rowins et al., in prep.) and ore fluids rising in the KLF (Cameron and Hattori 1987).

CONCLUSIONS

Major and trace element variation in the compositional continuum of rock types consitituting the Murdock Creek intrusion support a fractional crystallization model for pluton evolution, with incompatible elements (LILE's and LREE's) and the ratios K/Rb, La/Yb increasing, compatible elements (Sc, V, Cr, Co, Ni) and Ca/Y decreasing, and coherent ratios such as Th/U, Zr/Hf, Cr/Ni, and the LILE ratios K/Sr, K/Ba, Rb/Sr, Rb/Ba remaining relatively constant. Non-standard or irregular trends such as that displayed by the K/Rb and Ba/Sr ratios are explained in terms changing proportions of crystallizing mineral phases with different K_D's for these elements. The control of primary mineralogy over element distribution is well-illustrated in chemical variation diagrams, REE patterns, and chondrite-normalized incompatible element plots (spidergrams).

Consideration of all the geochemical data leads to a model of pluton petrogenesis in which (1) a mantle source region, which may already be depleted in Ti-group elements, is modified by volatiles rich in the LILE's and LREE's; (2) it is subjected to partial melting initiated by mantle upwelling via lithosphere extension, possibly facilitated by mantle degassing of CO_2, leading to a liquid of shoshonitic or potassic mafic alkaline character; and (3) a pulse of this partial melt then ascended to mid-crustal levels, differentiating en route and upon final emplacement, generated the evolved rock compositions prinicipally by in situ crystal fractionation of clinopyroxene, biotite, plagioclase and K-feldspar.

The many petrographic, mineralogical, and geochemical similarities between the Murdock Creek intrusion and the Kirkland Lake syenite complex (KLSC), and also with proximal syenitic plutons, Timiskaming Group trachytes, calc-alkaline lamprophyres, and hornblendite intrusions, suggest derivation via a common tectono-magmatic event in the late Archean, an interpretation in accord with current models on the origin of the Superior Province craton (Corfu 1987; Colvine et al. 1988). In the specific case of the Kirkland Lake syenite suite, repetitive episodes of small degrees of partial melting of the same metasomatically enriched upper mantle source region could produce numerous partial melt pulses (syenitic plutons) of slightly variable trace element character, yet the overall geochemical coherence is not lost.

ACKNOWLEDGEMENTS

We thank Ron Hartree (University of Ottawa) and members of the Geochemistry subdivision of the Geological Survey of Canada who carried out much of the analytical work. The assistance of John Loop in the University of Ottawa Geochemistry Laboratory is gratefully acknowledged. Jean-Francois Tardif is thanked for the preparation of thin sections. We are grateful to N.M.S. Rock for comments on the hornblendite-lamprophyre association. This research was funded by an NSERC grant to E.M.C.

REFERENCES CITED

Arth, J.G., and Hansen, G.N., 1975, Geochemistry and origin of the early Precambrian crust of northeastern Minnesota: Geochim. Cosmochim. Acta, v. 39, p. 325-362.

_____; Barker, F.; Peterman, Z.E.; and Friedman, I., 1978, Geochemistry of the gabbro-diorite-tonalite-trondhjemitic suite of southwest Finland and its implications for the origin of tonalitic and trondhjemitic magmas: Jour. Petrol., v. 19. p. 289-316.

Bailey, D.K., 1969, The stability of acmite in the presence of H_2O: Amer. Jour. Sci., Shairer Vol. 267-A, p. 1-16.

_____ 1982, Mantle metasomatism - continuing chemical change within the earth: Nature, v. 296, p. 525-530.

_____ 1987, Mantle metasomatism - perspective and prospect, in Fitton, J.G., and Upton, B.G.J., eds., Alkaline igneous rocks: Geol. Soc. London Spec. Publ., v. 30, p. 1-13.

Barbeiri, M.; Fornaseri, M.; and Penta, A., 1968, Rubidium and potassium relationship in some volcanoes of central Italy: Chem. Geol., v. 3, p. 189-197.

Barbey, P., and Cuney, M., 1982, K, Rb, Sr, Ba, U, and Th geochemistry of Lapland granulites (Ferroscandia). LILE fractionation controlling factors: Contrib. Mineral. Petrol., v. 81, p. 304-316.

Beswick, A.E., and Eugster, H.P., 1969, The distribution of potassium and rubidium between sanidine and phlogopite: Geol. Soc. Amer. Spec. Pap. 121, p. 25-26.

Bouabdli, A.; Dupuy, C.; and Dostal, J., 1988, Geochemistry of Mesozoic alkaline lamprophyres and related rocks from the Tamazert massif, High Atlas (Morocco): Lithos, v. 22, p. 43-58.

Boone, G.M., 1969, Origin of clouded red feldspars: Petrologic contrasts in a granite porphyry intrusion: Amer. Jour. Sci., v. 267, p. 633-668.

Briqueu, L.; Bougault, H.; and Joron, J.L., 1984, Quantification of Nb, Ta, Ti, and V anomalies in magmas associated with subduction zones: Petrologic implications: Earth Planet. Sci. lett., v. 68, p. 297-308.

Brophy, J.G., and Marsh, B.D., 1986, On the origin of high alumina arc basalt and the mechanics of melt extraction: Jour. Petrol., v. 27, p. 763-790.

Brownlow, A.H., 1979, Geochemistry: New York, Prentice-Hall Inc., 498 p.

Burrows, A.G., and Hopkins, P.E., 1923, Kirkland Lake gold area: Ont. Dept. Mines Ann. Rep. 1923, v. 32, pt. 4, 96 p.

Cameron, E.M., Gold at Kirkland Lake, Ontario: Product of strike-slip orogenesis ?: Geol. Surv. Can. Pap., in press.

_____ 1988, Archean gold: Relation to granulite formation and redox zoning in the crust: Geology, v. 16, p. 109-112.

_____, and Carrigan, W.J., 1987, Oxygen fugacity of Archean felsic magmas: Relationship to gold mineralization, in Current research. Part A: Geol. Surv. Can. Pap. 87-1A, p. 281-298.

_____, and Hattori, K., 1987, Archean gold mineralization and oxidized hydrothermal fluids: Econ. Geol., v. 82, p. 1177-1191.

Card, K.D., 1989, The Superior Province of the Canadian Shield: A product of Archean plate tectonics: Geol. Assoc. Can. Ann. Meet. Prog. with Abs., v. 14, p. A36.

Clague, D.A., and Frey, F.A., 1982, Petrology and trace element geochemistry of the Honolulu volcanics, Oahu: Implications for the oceanic mantle below Hawaii: Jour. Petrol., v. 23, p. 447-504.

Colvine, A.C.; Andrews, A.J.; Cherry, M.E.; Durocher, M.E.; Fyon, A.J.; Lavigne, M.J.; Macdonald, A.J.; Marmont, S.; Poulsen, K.H.; Springer, J.S.; and Troop, D.G, 1984, An integrated model for the origin of Archean lode gold deposits: Ont. Geol. Surv. Open File Rep. 5524, 98 p.

_____; Fyon, A.J.; Heather, K.B.; Marmont, S.; Smith, P.M.; and Troop, D.G., 1988, Archean lode gold deposits in Ontario: Ont. Geol. Surv. Misc. Pap. 139, 210 p.

Condie, K.C., 1981, Archean greenstone belts: Developments in Precambrian Geology, v. 3, 434 p.

Cooke, D.L., and Moorehouse, W.W., 1969, Timiskaming volcanism in the Kirkland Lake area, Ontario, Canada: Can. Jour. Earth Sci., v. 6, p. 117-132.

Corfu, F., 1987, Inverse age stratification in the Archean crust of the Superior Province: Evidence for infra- and subcrustal accretion from high resolution U-Pb zircon and monazite ages:

Precambrian Res., v. 36, p. 259-275.

_____, and Stott, G.M., 1986, U-Pb ages for late magmatism and regional deformation in the Shebandowan belt, Superior Province: A U-Pb zircon and titanite study: Jour. Geol., v. 95, p. 87-105.

_____; Krogh, T.E.; Kwok, Y.Y.; and Jensen, L.S., 1989, U-Pb zircon geochronology in the southwestern Abitibi greenstone belt, Superior Province: Can. Jour. Earth Sci., v. 26, p. 1747-1763.

Cullers, R.L., and Graf, J.L., 1984, Rare earth elements in igneous rocks of the continental crust: Predominantly basic and ultrabasic rocks, in Henderson, P., ed., Rare earth element geochemistry: Amsterdam, Elsevier, p. 237-274.

Cundari, A., 1979, Petrogenesis of leucite-bearing lavas in the Roman Volcanic Region, Italy: Contrib. Mineral. Petrol., v. 70, p. 9-21.

_____ 1980, Role of subduction in the genesis of leucite-bearing rocks: Facts or fashion: Contrib. Mineral. Petrol., v. 73, p. 432-434.

Dawson, J.B., 1972, Kimberlites and their relationship to the upper mantle: Phil. Trans. Royal Soc. London, v. A271, p. 297-311.

Drake, M.J., 1975, The oxidation state of europium as an indicator of oxygen fugacity: Geochim. Cosmochim. Acta, v. 39, p. 55-64.

_____, and Weill, D.F., 1975, Partition of Sr, Ba, Ca, Y,

Eu^{2+}, Eu^{3+}, and other REE between plagioclase feldspar and magmatic liquid: An experimental study: Geochim. Cosmochim. Acta, v. 39, p. 689-712.

Edgar, A.D., 1989, Barium- and strontium-enriched apatite in lamproites from West Kimberly, Western Australia, v. 74, p. 889-895.

Esperanca, S., and Holloway, J.R., 1987, On the origin of some mica-lamprophyres: Experimental evidence from a mafic minette: Contrib. Mineral. Petrol., v. 95, p. 207-216.

Fitton, J.G., and Upton, B.G.J., 1987, Introduction, in Fitton, J.G., and Upton, B.G.J., eds., Alkaline igneous rocks: Geol. Soc. London Spec. Publ., v. 30, p. ix-xiv.

Foley, S.F.; Venturelli, G.; Green, D.H.; and Toscani, L., 1987, The ultrapotassic rocks: Characteristics, classification, and constraints for petrogenetic models: Earth Sci. Rev., v. 24, p. 81-134.

Fowler, M.B., 1988, Ach'uaine hybrid appinite pipes: Evidence for mantle-derived shoshonitic parent magmas in Caledonian granite genesis: Geology, v. 16, p. 1026-1030.

Gerasimovsky, V.I., 1974, Trace elements in selected groups of alkaline rocks, in Sorensen, H., ed., The alkaline rocks: New York, Wiley, p. 402-412.

Gill, J., 1981, Orogenic andesites and plate tectonics: New York, Springer-Verlag, 390 p.

Gittens, J., 1979, The feldspathoidal alkaline rocks, in Yoder, H.S., ed., The evolution of the igneous rocks: Fiftieth

anniversary perspectives; Princton, Princeton University Press, p. 352-390.

Grabowski, G.; Lovell, H.L.; Guindon, D.; and Bath, A., 1987, Kirkland Lake resident geologists area: Ont. Geol. Surv. Misc. Pap. 138, p. 251-284.

Green, T.H., 1980, Island arc and continent-building magmatism -A review of petrogenic models based on experimental petrology and geochemistry: Tectonophysics, v. 63, p. 367-385.

_____ T.H., 1981, Experimental evidence for the role of accessory phases in magma genesis: Jour. Volcanol. Geotherm. Res., v. 10, p. 405-422.

_____, and Pearson, N.J., 1986, Ti-rich accessory phase saturation in hydrous mafic-felsic compositions at high P, T: Chem. Geol., v. 54, p. 185-201.

_____, and _____, 1987, An experimental study of Nb and Ta partitioning between Ti-rich minerals and silicate liquids at high pressure and temperature: Geochim. Cosmochim. Acta, v. 51, p. 55-62.

Gupta, A.K., and Yagi, K., 1980, Petrology and genesis of the leucite-bearing rocks: Berlin, Springer-Verlag, 252 p.

Hansen, G.N., 1980, Rare earth elements in petrogenetic studies of igneous systems: Ann. Rev. Earth Planet. Sci., v. 8, p. 371-406.

Harris, P.G., 1957, Zone refining and the origin of potassic basalts: Geochim. Cosmochim. Acta, v. 12, p. 195-208.

_____, and Middlemost, E.A.K., 1969, The evolution of

kimberlites: Lithos, v. 3, p. 77-88.

Haskin, L.A.; Haskin, M.A.; and Frey, F.A., 1968, Relative and absolute terrestrial abundances of the rare earths, in Ahrens, L.H., ed., Origin and distribution of the elements: Oxford, Pergamon, p. 889-912.

Heier, K.S., and Brooks, C., 1966, Geochemistry and genesis of the Heemskirk granite, west Tasmania: Geochim. Cosmochim. Acta, v. 30, p. 633-643.

Hellman, P.L., and Green, T.H., 1979, The role of sphene as an accessory phase in the high-pressure partial melting of hydrous mafic compositions: Earth Planet. Sci. Lett., v. 42, p. 191-201.

Henderson, P., 1982, Inorganic geochemistry: Oxford, Pergamon, 353 p.

_____ 1984, Rare earth element geochemistry: Amsterdam, Elsevier, 378 p.

Hewitt, D.F., 1963, The Timiskaming series in the Kirkland Lake area: Can. Mineral., v. 7, p. 497-523.

Hicks, K.D., and Hattori, K., 1988, Magmatic-hydrothermal and wall rock alteration petrology at the Lake Shore gold deposit, Kirkland Lake, Ontario, in Milne, V.G., ed., Geoscience research grant program, summary of research 1987-1988: Ont. Geol. Surv. Misc. Pap. 140, p. 192-204.

Hodgson, C.J., and MacGeehan, P.J., 1982, A review of the geological characteristics of "gold-only" deposits in the Superior Province of the Canadian Shield, in Geology of

Canadian gold deposits: Can. Inst. Min. Metal. Spec. Vol. 24, p. 211-229.

Hubert, C.; Trudel, P.; and Gelinas, L., 1984, Archean wrench fault tectonics and structural evolution of the Blake River Group, Abitibi belt, Quebec: Can. Jour. Earth Sci., v. 21, p. 1024-1032.

Hyde, R.S., 1980, Sedimentary facies in the Archean Timiskaming Group and their tectonic implications, Abitibi greenstone belt, northeastern Ontario, Canada: Precambrian Res., v. 12, p. 161-195.

Jensen, L.S., 1978, Archean komatiitic, tholeiitic, calc-alkaline and alkalic volcanic sequences in the Kirkland Lake area, in Currie, A.L., and Mackasey, W.O., eds., Toronto '78 field trips guidebook: Geol. Assoc. Can., p. 327-359.

_____, and Langford, F.F., 1985, Geology and petrogenesis of the Archean Abitibi belt in the Kirkland Lake area, Ontario: Ont. Geol. Surv. Misc. Pap. 123, 130 p.

Jolly, W.T., 1974, Regional metamorphic zonation as an aid in the study of Archean terrains: Abitibi regions, Ontario: Can. Mineral., v. 12, p. 499-508.

Kay, R.W., and Gast, P.W., 1973, Rare earth content and origin of alkali-rich basalts: Jour. Geol., v. 81, p. 653-682.

Kerrich, R., and Watson, G.P., 1984, The Macassa mine Archean lode gold deposit, Kirkland Lake, Ontario: Geology, patterns of alteration, and hydrothermal regimes: Econ. Geol., v. 79, p. 1104-1130.

Lalonde, A.E., and Martin, R.F., 1983, The Baie-des-Moutons syenitic complex, La Tabatière, Quebec. I. Petrography and feldspar mineralogy: Can. Mineral., v. 21, p. 65-79.

Lambert, R. St. J., and Holland, J.G., 1974, Yttrium geochemistry applied to petrogenesis utilizing calcium-yttrium relationships in minerals and rocks: Geochim. Cosmochim. Acta, v. 38, p. 1393-1414.

Leat, P.T.; Thompson, R.N.; Morrison, M.A.; Hendry, G.L.; and Dickin, A.P., 1988, Silicic magmas derived by fractional crystallization from Miocene minette, Elkhead Mountains, Colorado: Mineral. Mag., v. 52, p. 577-585.

LeMaitre, R.W., 1976, The chemical variability of some common igneous rocks: Jour. Petrol., v. 17, p. 589-637.

Lévesque, G., 1989, The Kirkland Lake intrusive complex: A petrographical and chemical approach: Unpublished B.Sc. thesis, University of Ottawa, 83 p.

Lloyd, F.E., and Baily, D.K., 1975, Light element metasomatism of the continental mantle: The evidence and the consequences: Phys. Chem. Earth, v. 9. p. 389-416.

_____; Arima, M.; and Edgar, A.D., 1985, Partial melting of a phlogopite-clinopyroxenite nodule from south-west Uganda: An experimental study bearing on the origin of highly potassic continental rift volcanics: Contrib. Mineral. Petrol., v. 91, p. 321-329.

Long, P.E., 1978, Experimental determination of partition coefficients for Rb, Sr, and Ba between alkali-feldspar and

silicate liquid: Geochim. Cosmochim. Acta, v. 42, p. 833-846.

Lovell, H.L., 1972, Geology of the Eby and Otto area, District of Timiskaming: Ont. Dept. Mines Northern Affairs Geol. Rep. 99, 79 p.

Ludden, J.L., 1989, Geochemical contraints on the origin of late Archean magmas: Examples from the Superior Province of Canada: Geol. Assoc. Can. Ann. Meet. Prog. with Abs., v. 14, p. A8.

Macdonald, R.; Thorpe, R.S.; Gaskarth, J.W.; and Grindrod, A.R., 1985, Multi-component origin of Caledonian lamprophyres of northern England: Mineral. Mag., v. 49, p. 485-494.

_____; Rock, N.M.S.; Rundle, C.C.; and Russell, O.J., 1986, Relationships between late Caledonian lamprophyric, syenitic, and granitic magmas in a differentiated dyke, southern Scotland: Mineral. Mag., v. 50, no. 358, p. 547-557.

Marmont, S., and Corfu, F., 1988, Timing of gold mineralization in the late Archean tectonic framework of the Canadian Shield: Evidence from U-Pb zircon geochronolgy of the Abitibi Sub-Province, in Goode, A.D.T., and Bosma, L.I., eds., Bicentennial gold '88 extended abstracts and oral programs: Geol. Soc. Australia Abs. Ser. no. 22, p. 45-50.

Maynard, J.B., 1983, Geochemistry of sedimentary ore deposits: New York, Springer-Verlag, 305 p.

McKenzie, D., and Bickle, M.J., 1988, The volume and composition of melt generated by extension of the lithosphere: Jour. Petrol., v. 29, p. 625-679.

McNeil, A.M., and Kerrich, R., 1986, Archean lamprophyre dykes and gold mineralization, Matheson, Ontario: The conjunction of LIL-enriched mafic magmas, deep crustal structures and Au concentration: Can. Jour. Earth Sci., v. 23, p. 324-343.

Menzies, M.; Rogers, N.; Tindle, A.; and Hawkesworth, C., 1987, Metasomatic and enrichment processes in lithospheric peridotites, an effect of asthenosphere-lithosphere interaction, in Menzies, M., ed., Mantle metasomatism: London, Academic Press Inc., p. 313-361.

Miller, C.F., and Mittlefehldt, D.W., 1979, Rare earth element depletion accompanying differentiation of felsic plutonic rocks: Geol. Soc. Amer. Abs. with Prog., v. 11, p. 479-480.

_____, and _____, 1982, Light rare earth element depletion in felsic magmas: Geology, v. 10, p. 129-133.

Mittlefehldt, D.W., and Miller, C.F., 1983, Geochemistry of the Sweetwater Wash pluton, California: Implications for "anomalous" trace element behaviour during differentiation of felsic magmas: Geochim. Cosmochim. Acta, v. 47, p. 109-124.

Morris, J.D., and Hart, S.R., 1983, Isotope and compatible element constraints on the genesis of island arc volcanics from Cold Bay and Amak Island, Aleutians, and implications for mantle structure: Geochim. Cosmochim. Acta, v. 47, p. 2015-2030.

Morrison, G.W., 1980, Characteristics and tectonic setting of the shoshonitic rock association: Lithos, v. 13, p. 97-108.

Myashiro, A., 1978, Nature of alkalic volcanic rock series:

Contrib. Mineral. Petrol., v. 66, p. 91-104.

Nagasawa, H., and Schnetzler, C.C., 1971, Partitioning of rare earth, alkali and alkaline earth elements between phenocrysts and acidic igneous magma: Geochim. Cosmochim. Acta, v. 35, p. 953-968.

Nash, W.P., 1972, Apatite-calcite equilibria in carbonatites: Chemistry of apatite from Iron Hill, Colorado: Geochim. Cosmochim. Acta, v. 36, p. 1313-1319.

Nemec, D., 1988, Origin of syenitic porphyries in the Central Bohemian pluton: Neues Jahrbuch Miner. Abh., v. 159, p. 59-71.

Newton, R.C.; Smith, J.V.; and Windley, B.F., 1980, Carbonic metamorphism, granulites and crustal growth: Nature, v. 288, p. 45-49.

Nunes, P.D., and Jensen, L.S., 1980, Geochronology of the Abitibi metavolcanic belt, Kirkland Lake area - progress report, in Pye, E.G., ed., Summary of geochronological studies 1977-1979: Ont. Geol. Surv. Misc. Pap. 92, p. 34-39.

O'Hara, M.J., and Yoder, H.S., 1967, Formation and fractionation of basic magmas at high pressures: Scottish Jour. Geol., v. 3, p. 67-117.

Payne, J.G., and Shaw, D.M., 1967, K-Rb relations in the Blue Mountain nepheline syenite: Earth Planet. Sci. Lett., v. 2, p. 290-292.

Pearce, J.A., 1982, Trace element characteristics of lavas from destructive plate boundaries, in Thorpe, R.S., ed.,

Andesites: Chichester, Wiley, p. 525-548.

Peccerillo, A., and Taylor, S.R., 1976, Geochemistry of Eocene calc-alkaline volcanic rocks from the Kastamonu area, northern Turkey: Contrib. Mineral. Petrol., v. 58, p. 63-81.

Percival, J.A., and Williams, H.R., 1989, The late Archean Quetico accretionary complex, Superior Province, Canada: Geology, v. 17, p. 23-25.

Perfit, M.R.; Gust, D.A.; Bence, A.E.; Arculus, R.J; and Taylor, S.R., 1980, Chemical characteristics of island-arc basalts: Implications for mantle sources: Chem. Geol., v. 30, p. 227-256.

Philpotts, J.A., and Schetzler, C.C., 1970, Phenocryst-matrix partition coefficients for K, Rb, Sr, and Ba, with applications to anorthosite and basalt genesis; Geochim. Cosmochim. Acta, v. 34, p. 307-322.

Ploeger, F.R., and Crockett, J.H., 1982, Relationship of gold to syenitic intrusive rocks in Kirkland Lake: Can. Min. Metal. Spec. Vol. 24, p. 69-72.

Rhodes, J.M., 1981, Characteristics of primary basaltic magmas, in BVSP. Basaltic volcanism on the terrestrial planets: Oxford, Pergamon, p. 409-452.

Ridler, R.H., 1970, Relationship of mineralization to volcanic stratigraphy in the Kirkland-Larder Lakes area, Ontario: Proc. Geol. Assoc. Can., v. 21, p. 33-42.

Rock, N.M.S., 1984, Nature and origin of calc-alkaline lamprophyres: Minettes, vogesites, kersantites and

spessartites: Trans. Royal Soc. Edinburgh Earth Sci., v. 74, p. 193-227.

_____ 1987, Nature of lamprophyres, in Fitton, J.G., and Upton, B.G.J., eds., Alkaline igneous rocks: Geol. Soc. London Spec. Publ., v. 30, p. 191-226.

Rowins, S.M.; Lalonde, A.E; and Cameron, E.M., 1989, Geology of the Archean Murdock Creek intrusion, Kirkland Lake, Ontario, in Current research. Part C: Geol. Surv. Can. Pap. 89-1C, p. 313-323.

_____; _____; and _____, Magmatic oxidation in the syenitic Murdock Creek intrusion, Kirkland Lake, Ontario: Evidence from the ferromagnesian silicates: in prep.

Ryerson, F.J., and Watson, E.B., 1987, Rutile saturation in magmas: Implications for Ti-Nb-Ta depletion in island-arc basalts: Earth Planet. Sci. Lett., v. 86, p. 225-239.

Saunders, A.D.; Tarney, J.; and Weaver, S.D., 1980, Transverse geochemical variations across the Antarctic Peninsula: Implications for the genesis of calc-alkaline magmas: Earth Planet. Sci. Lett., v. 46, p. 344-360.

Shaw, D.M., 1968, A review of K-Rb fractionation trends by covariance analysis: Geochim. Cosmochim. Acta, v. 32, p. 573-601.

Simmons, E.C., and Hedge, C.E., 1978, Minor-element and Sr-isotope geochemistry of Tertiary stocks, Colorado mineral belt: Contrib. Mineral. Petrol., v. 67, p. 379-396.

Smalley, P.C.; Field, D.; Lamb, R.C.; and Clough, P.W.L., 1983,

Rare earth, Th-Hf-Ta and large-ion-lithophile element variations in metabasites from the Proterozoic amphibolite-granulite transition zone at Arendal, south Norway: Earth Planet. Sci. Lett., v. 63, p. 446-458.

Sorensen, H., 1974, Alkali syenites, feldspathoidal syenites and related lavas, in Sorensen, H., ed., The alkaline rocks: New York, Wiley, p. 22-52.

Stolz, A.J.; Varne, R.; Wheller, G.E.; Foden, J.D.; and Abbott, M.J., 1988, The geochemistry and petrogenesis of K-rich alkaline volcanics from the Batu Tara volcano, eastern Sunda arc: Contrib. Mineral. Petrol., v. 98, p. 374-389.

Streckeisen, A., 1976, To each plutonic rock its proper name: Earth Sci. Rev., v. 12, p. 1-33.

Thompson, R.N., 1982, Magmatism of the British Tertiary Volcanic Province: Scottish Jour. Geol., v. 18, p. 50-107.

_____, R.N., and Fowler, M.B., 1986, Subduction-related shoshonitic and ultrapotassic magmatism: A study of Siluro-Ordovician syenites from the Scottish Caledonides: Contrib. Mineral. Petrol., v. 94, p. 507-522.

_____; Morrison, M.A.; Dickin, A.P; and Hendry, G.L., 1984, Continental flood basalts... Arachnids Rule OK ?, in Hawkesworth, C.J., and Norry, M.J., eds., Continental basalts and mantle xenoliths: Cheshire, Shiva, p. 158-185.

Thomson, J.E., 1950, Geology of Teck Township and the Kenogami Lake area, Kirkland Lake gold belt: Ont. Dept. Mines Ann. Rep. 1948, v. 57, pt. 5, p. 1-53.

_____; Charlewood, G.H.; Griffin, K.; Hawley, J.E.; Hopkins, H.; MacIntosh, C.G.; Ogrizlo, S.P.; Perry, O.S.; and Ward, W., 1950, Geology of the main ore zone at Kirkland Lake: Ont. Dept. Mines Ann. Rep. 1948, v. 57, pt. 5, p. 54-188.

Turekian, K.K., and Wedepohl, K.H., 1961, Distribution of the elements in some major units of the earth's crust: Geol. Soc. Amer. Bull., v. 7, p. 175-192.

Upton, B.G.J., 1960, The alkaline igneous complex of Kûngnât Fjeld South Greenland: Meddr. Groenl., v. 123, no. 4, p. 5-145.

Ujike, O., 1985, Geochemistry of Archean alkalic volcanic rocks from the Crystal Lake area, east of Kirkland Lake, Ontario, Canada: Earth Planet. Sci. Lett., v. 73, p. 333-344.

Varne, R., 1970, Hornblende lherzolite and the upper mantle: Contrib. Mineral. Petrol., v. 27, p. 45-58.

Watkins, N.D., and Haggerty, S.E., 1967, Primary oxidation and petrogenesis in a single lava: Contrib. Mineral. Petrol., v. 15, p. 251-271.

Watson, E.B., 1979, Zircon saturation in felsic liquids: Experimental results and applications to trace element geochemistry: Contrib. Mineral. Petrol., v. 70, p. 407-419.

Weaver, B.L.; Wood, D.A.; Tarney, J.; and Joron, J.L., 1987, Geochemistry of ocean island basalts from the South Atlantic: Ascension, Bouvet, St. Helena, Gough, and Tristan da Cunha, in Fitton, J.G., and Upton, B.G.J., eds., Alkaline igneous rocks: Geol. Soc. London Spec. Publ., v. 30, p. 253-267.

Weill, D.F., and Drake, M.J., 1973, Europium anomaly in plagioclase feldspar: Experimental results and semiquantitative model: Science, v. 180, p. 1059-1060.

Wheller, G.E.; Varne, R.; Foden, J.D.; and Abbott, M.J., 1987, Geochemistry of Quaternary volcanism in the Sunda-Banda Arc, Indonesia, and three-component genesis of island-arc basaltic magmas: Jour. Volcanol. Geotherm. Res., v. 32, p. 137-160.

Wilson, A.D., 1960, A modified scheme for the determination of ferrous iron in rocks: Analyst, v. 85, p. 823-827.

Wright, A.E., and Bowes, D.R., 1979, Geochemistry of the appinite suite, in Harris, A.L., ed., Caledonides of the British Isles - reviewed: Geol. Soc. London Spec. Publ., v. 8, p. 699-703.

Wyman, D., and Kerrich, R., 1988, Alkaline magmatism, major structures, and gold deposits: Implications for greenstone belt gold metallogeny: Econ. Geol., v. 83, p. 454-461.

APPENDIX 1.

Compositions and Structural Formulae of Clinopyroxene from the Murdock Creek intrusion.

Superscripts and abbreviations used in the tables are as follows:

The symbol "-" means less than 0.005, rounds to 0.00.

na = not analysed.

[a] Secondary aegirine-augite (all other analyses in the table are primary diopside).

[b] Rock units containing the analysed clinopyroxenes as follows: AS, alkali-feldspar syenite; MS, melasyenite; MM, melamonzodiorite; MD, meladiorite; CP, clinopyroxenite; HB, hornblendite.

[c] Number of analyses averaged.

[d] Total Fe calculated as FeO.

[e] Rock F.I. = host-rock normative fractionation index (wt.% Qtz + Ab + Or + Ne + Lc + Ns).

[f] Host-rock agpaicity index = molecular ratio (Na+K)/Al.

SAMPLE	108R3	111R2	118R3	118C3	119U1	134C2	10491[a]	10490	10495	10494[a]
ROCK UNIT[b]	AS	AS	AS	AS	AS	AS	AS	AS	AS	AS
#ANAL.[c]	1	1	1	3	1	1	2	2	2	2
SiO2	53.03	52.53	52.93	53.03	53.36	52.52	50.87	51.78	52.02	50.71
TiO2	0.13	0.22	0.54	0.42	0.12	0.17	0.60	0.51	0.50	0.75
Al2O3	1.42	1.16	2.41	1.92	0.94	1.63	2.38	2.21	2.03	2.26
Cr2O3	na	na	na	na	na	na	na	na	na	na
Fe2O3	6.67	4.97	3.25	3.09	5.03	3.70	9.19	6.70	7.00	9.06
FeO	6.79	4.50	3.90	3.74	6.03	3.97	4.17	1.33	1.25	4.24
MnO	0.53	0.35	0.32	0.27	0.40	0.47	0.39	0.31	0.38	0.34
MgO	9.66	13.40	13.07	13.75	12.11	13.86	10.34	13.24	13.49	10.40
CaO	18.77	21.68	21.49	21.88	21.17	21.57	19.54	21.24	21.52	19.50
Na2O	3.22	1.40	1.88	1.56	1.89	1.33	2.88	2.13	2.02	2.85
K2O	-	-	-	-	-	-	-	0.01	0.01	-
Tot.	100.22	100.21	99.79	99.66	101.05	99.22	100.36	99.47	100.22	100.08
FeOT[d]	12.79	8.97	6.82	6.52	10.56	7.30	12.44	7.36	7.55	12.39
Structural formulae based on 4 cations and 6 oxygens										
Si	1.99	1.95	1.96	1.96	1.97	1.96	1.91	1.92	1.92	1.90
AlIV	0.01	0.05	0.04	0.04	0.03	0.04	0.09	0.08	0.08	0.10
Fe3+IV	-	-	-	-	-	-	-	-	-	-
AlVI	0.05	-	0.06	0.04	0.01	0.03	0.01	0.02	0.01	-
Ti	-	0.01	0.01	0.01	-	-	0.02	0.01	0.01	0.02
Cr	na	na	na	na	na	na	na	na	na	na
Fe3+	0.19	0.14	0.09	0.09	0.14	0.10	0.26	0.19	0.19	0.26
Fe2+	0.21	0.14	0.12	0.12	0.19	0.12	0.13	0.04	0.04	0.13
Mn	0.02	0.01	0.01	0.01	0.01	0.01	0.01	0.01	0.01	0.01
Mg	0.54	0.74	0.72	0.76	0.67	0.77	0.58	0.73	0.74	0.58
Ca	0.75	0.86	0.85	0.87	0.84	0.86	0.78	0.84	0.85	0.79
Na	0.23	0.10	0.14	0.11	0.14	0.10	0.21	0.15	0.14	0.21
K	-	-	-	-	-	-	-	-	-	-
Fe/Fe+Mg	0.43	0.27	0.23	0.21	0.33	0.23	0.40	0.24	0.24	0.40
Fe3+/ΣFe	0.47	0.50	0.43	0.43	0.43	0.46	0.67	0.82	0.83	0.66
Na/Na+Ca	0.24	0.10	0.14	0.12	0.14	0.10	0.21	0.15	0.15	0.21
ROCK F.I.[e]	73.00	83.10	69.96	69.96	65.72	62.13	63.93	63.93	63.93	63.93
ROCK AGP[f]	0.96	0.94	0.88	0.88	1.00	0.82	0.95	0.95	0.95	0.95

SAMPLE	10536[a]	10816	10821	11105	11115	11114	11742	11852	11941	13474
ROCK UNIT[b]	AS	AS	AS	AS	AS	AS	AS	AS	AS	AS
#ANAL.[c]	2	3	2	3	2	2	4	2	2	2
SiO2	51.40	53.87	53.38	51.64	51.60	52.63	52.70	52.28	52.53	51.74
TiO2	0.52	0.44	0.45	0.26	0.22	0.27	0.42	0.58	0.81	0.39
Al2O3	2.67	1.62	1.87	1.01	1.16	0.85	2.44	2.41	0.88	1.87
Cr2O3	na	na	na	na	na	na	na	na	na	na
Fe2O3	8.36	2.34	2.94	5.81	5.91	3.51	3.21	3.58	5.82	5.32
FeO	4.76	5.32	5.76	4.95	3.83	3.66	4.70	4.12	5.11	2.55
MnO	0.31	0.36	0.38	0.46	0.47	0.22	0.37	0.37	0.45	0.44
MgO	9.78	13.41	12.36	12.39	12.88	14.83	12.71	12.95	12.19	14.23
CaO	18.83	21.61	21.05	21.49	21.53	22.34	21.43	21.50	21.08	21.80
Na2O	3.30	1.62	1.96	1.50	1.51	0.89	1.76	1.70	1.99	1.28
K2O	-	0.01	-	-	-	0.02	0.01	0.01	-	-
Tot.	99.93	100.60	100.15	99.51	99.12	99.23	99.75	99.50	100.86	99.61
FeOT[d]	12.28	7.43	8.41	10.18	9.15	6.82	7.59	7.34	10.35	7.34
Structural formulae based on 4 cations and 6 oxygens										
Si	1.93	1.98	1.98	1.94	1.94	1.96	1.95	1.94	1.95	1.92
AlIV	0.07	0.02	0.02	0.05	0.05	0.04	0.05	0.06	0.04	0.08
Fe3+IV	-	-	-	0.01	0.01	-	-	-	0.01	-
AlVI	0.05	0.05	0.06	-	-	-	0.06	0.05	-	-
Ti	0.02	0.01	0.01	0.01	0.01	0.01	0.01	0.02	0.02	0.01
Cr	na	na	na	na	na	na	na	na	na	na
Fe3+	0.24	0.06	0.08	0.15	0.16	0.10	0.09	0.10	0.15	0.15
Fe2+	0.15	0.16	0.18	0.16	0.12	0.11	0.15	0.13	0.16	0.08
Mn	0.01	0.01	0.01	0.01	0.01	0.01	0.01	0.01	0.01	0.01
Mg	0.55	0.73	0.68	0.69	0.72	0.82	0.70	0.72	0.67	0.79
Ca	0.76	0.85	0.84	0.87	0.87	0.89	0.85	0.86	0.84	0.87
Na	0.24	0.12	0.14	0.11	0.11	0.06	0.13	0.12	0.14	0.09
K	-	-	-	-	-	-	-	-	-	-
Fe/Fe+Mg	0.41	0.24	0.28	0.32	0.29	0.21	0.25	0.24	0.32	0.22
Fe3+/ΣFe	0.61	0.28	0.31	0.51	0.58	0.46	0.38	0.44	0.51	0.65
Na/Na+Ca	0.24	0.12	0.14	0.11	0.11	0.07	0.13	0.12	0.15	0.10
ROCK F.I.[e]	69.90	73.00	73.00	83.10	83.10	83.10	70.69	69.96	65.72	62.13
ROCK AGP[f]	0.95	0.96	0.96	0.94	0.94	0.94	0.91	0.88	1.00	0.82

SAMPLE	13471	13380	13382	13386	13381	13387	29525	29526	132R1	132C2
ROCK UNIT[b]	AS	MS	MS	MS	MS	MS	MM	MM	MD	MD
#ANAL[c]	2	1	2	1	2	2	2	1	1	2
SiO2	51.38	51.32	50.79	51.97	51.63	52.03	52.69	52.50	52.44	52.97
TiO2	0.24	0.28	0.41	0.24	0.23	0.16	0.12	0.15	0.16	0.14
Al2O3	1.74	1.79	2.31	1.70	1.65	1.54	1.19	1.29	1.98	1.96
Cr2O3	na	na	na	na	na	na	na	na	na	na
Fe2O3	6.08	5.93	5.84	5.21	5.02	5.44	3.22	4.01	1.32	1.84
FeO	2.29	2.62	3.66	3.55	3.18	3.07	5.66	5.43	6.93	6.57
MnO	0.44	0.43	0.48	0.45	0.40	0.38	0.37	0.39	0.28	0.35
MgO	14.14	13.87	12.88	14.04	14.08	14.64	13.42	13.41	13.29	13.51
CaO	21.65	22.59	22.28	21.92	22.60	21.70	22.72	22.57	22.11	22.22
Na2O	1.29	1.05	1.17	1.13	0.98	1.08	0.86	0.90	0.78	0.86
K2O	-	0.01	0.01	-	-	-	0.02	0.03	-	-
Tot.	99.24	99.89	99.83	100.21	99.97	100.04	100.27	100.68	99.29	100.42
FeOT[d]	7.76	7.96	8.91	8.24	7.70	7.96	8.56	9.04	8.12	8.23
Structural formulae based on 4 cations and 6 oxygens										
Si	1.92	1.91	1.90	1.92	1.92	1.93	1.96	1.95	1.96	1.96
AlIV	0.08	0.08	0.10	0.07	0.07	0.07	0.04	0.05	0.04	0.04
Fe3+IV	-	0.01	-	0.01	0.01	-	-	-	-	-
AlVI	-	-	-	-	-	-	0.01	-	0.05	0.04
Ti	0.01	0.01	0.01	0.01	0.01	0.01	-	-	-	-
Cr	na	na	na	na	na	na	na	na	na	na
Fe3+	0.17	0.16	0.16	0.13	0.13	0.14	0.09	0.11	0.04	0.05
Fe2+	0.07	0.08	0.11	0.11	0.10	0.10	0.18	0.17	0.22	0.20
Mn	0.01	0.01	0.02	0.01	0.01	0.01	0.01	0.01	0.01	0.01
Mg	0.79	0.77	0.72	0.77	0.78	0.81	0.74	0.74	0.74	0.75
Ca	0.87	0.90	0.89	0.87	0.90	0.86	0.90	0.90	0.89	0.88
Na	0.09	0.08	0.09	0.08	0.07	0.08	0.06	0.07	0.06	0.06
K	-	-	-	-	-	-	-	-	-	-
Fe/Fe+Mg	0.24	0.24	0.28	0.25	0.23	0.23	0.26	0.27	0.26	0.26
Fe3+/ΣFe	0.71	0.67	0.59	0.57	0.59	0.62	0.34	0.40	0.15	0.20
Na/Na+Ca	0.10	0.08	0.09	0.09	0.07	0.08	0.06	0.07	0.06	0.07
ROCK F.I.[e]	62.13	52.71	52.71	52.71	52.71	52.71	34.35	34.35	35.37	35.37
ROCK AGP[f]	0.82	0.73	0.73	0.73	0.73	0.73	0.76	0.76	0.58	0.58

SAMPLE	132R2	12933	13585	13589	13588	65B18	65B20	13522	13524	13525
ROCK UNIT[b]	MD	MD	CP	CP	CP	CP	CP	CP	CP	CP
#ANAL.[c]	1	3	2	3	3	2	2	2	2	2
SiO2	54.10	52.59	50.42	50.79	52.38	51.81	51.69	51.25	52.61	51.15
TiO2	0.12	0.19	0.47	0.52	0.21	0.25	0.30	0.49	0.24	0.37
Al2O3	1.16	1.64	2.38	2.91	1.91	1.92	1.78	2.90	2.26	2.47
Cr2O3	na	na	na	na	na	0.03	0.01	0.02	na	na
Fe2O3	0.56	2.63	6.05	5.71	4.67	4.91	3.91	5.28	3.63	5.40
FeO	6.59	4.98	2.76	3.74	2.75	5.17	5.13	4.26	4.21	3.42
MnO	0.33	0.26	0.35	0.29	0.27	0.34	0.03	0.33	0.31	0.32
MgO	14.21	14.65	13.23	12.61	14.31	11.84	12.77	12.34	13.29	13.36
CaO	23.06	22.63	22.52	22.75	22.64	21.90	22.60	22.44	22.46	22.00
Na2O	0.64	0.58	1.11	1.18	1.14	1.61	1.12	1.37	1.32	1.24
K2O	0.01	-	0.01	0.01	-	0.01	0.01	0.01	-	-
Tot.	100.78	100.14	99.30	100.53	100.28	99.79	99.35	100.69	100.33	99.73
FeOT[d]	7.09	7.35	8.20	8.88	6.95	9.34	8.65	9.01	7.48	8.28
Structural formulae based on 4 cations and 6 oxygens										
Si	1.99	1.94	1.89	1.88	1.93	1.94	1.94	1.90	1.94	1.90
AlIV	0.01	0.06	0.11	0.12	0.07	0.06	0.06	0.10	0.06	0.10
Fe3+IV	-	-	-	-	-	-	-	-	-	-
AlVI	0.04	0.01	-	0.01	0.01	0.03	0.02	0.03	0.04	0.01
Ti	-	0.01	0.01	0.01	0.01	0.01	0.01	0.01	0.01	0.01
Cr	na	na	na	na	na	0.00	na	0.00	na	na
Fe3+	0.01	0.07	0.17	0.16	0.13	0.14	0.11	0.15	0.10	0.15
Fe2+	0.20	0.15	0.09	0.12	0.08	0.16	0.16	0.13	0.13	0.11
Mn	0.01	0.01	0.01	0.01	0.01	0.01	-	0.01	0.01	0.01
Mg	0.78	0.81	0.74	0.70	0.79	0.66	0.71	0.68	0.73	0.74
Ca	0.91	0.90	0.90	0.90	0.89	0.88	0.91	0.89	0.89	0.88
Na	0.05	0.04	0.08	0.09	0.08	0.12	0.08	0.10	0.09	0.09
K	-	-	-	-	-	-	-	-	-	-
Fe/Fe+Mg	0.22	0.22	0.26	0.28	0.21	0.31	0.28	0.29	0.24	0.26
Fe3+/ΣFe	0.07	0.32	0.66	0.58	0.61	0.46	0.41	0.53	0.44	0.59
Na/Na+Ca	0.05	0.04	0.08	0.09	0.08	0.12	0.08	0.10	0.10	0.09
ROCK F.I.[e]	35.37	21.54	16.28	16.28	16.28	23.50	23.50	16.28	16.28	16.28
ROCK AGP[f]	0.58	0.60	0.65	0.65	0.65	0.84	0.84	0.65	0.65	0.65

SAMPLE	13523	115R2	115C1	13048	130C5	130C6	32928	32930
ROCK UNIT[b]	CP	CP	CP	CP	CP	CP	HB	HB
#ANAL.[c]	2	1	2	2	1	2	3	4
SiO2	50.95	52.74	53.80	50.65	53.82	53.69	53.87	54.18
TiO2	0.47	0.25	0.21	0.47	0.26	0.22	0.05	0.05
Al2O3	2.83	2.05	1.23	2.57	0.68	0.95	0.36	0.40
Cr2O3	na	na	na	na	na	na	0.05	-
Fe2O3	5.33	1.85	1.03	4.23	1.74	1.53	2.08	1.09
FeO	4.81	6.80	6.01	3.84	1.93	3.49	3.89	4.29
MnO	0.29	0.31	0.25	0.32	0.12	0.23	0.19	0.21
MgO	12.33	13.07	14.18	14.18	17.71	16.39	14.75	15.18
CaO	22.00	22.80	23.10	22.64	23.30	23.36	24.57	24.62
Na2O	1.31	0.79	0.73	0.55	0.24	0.33	0.53	0.36
K2O	-	-	-	-	-	-	0.05	0.02
Tot	100.32	100.66	100.54	99.45	99.80	100.19	100.39	100.40
FeOT[d]	9.61	8.46	6.94	5.93	3.50	4.87	5.76	5.27
Structural formulae based on 4 cations and 6 oxygens								
Si	1.90	1.95	1.98	1.89	1.96	1.96	1.98	1.99
AlIV	0.10	0.05	0.02	0.11	0.03	0.04	0.02	0.01
Fe3+IV	-	-	-	-	0.01	-	-	-
AlVI	0.02	0.04	0.03	-	-	-	-	-
Ti	0.01	0.01	0.01	0.01	0.01	0.01	-	-
Cr	na	na	na	na	na	na	-	-
Fe3+	0.15	0.05	0.03	0.12	0.04	0.04	0.06	0.03
Fe2+	0.15	0.21	0.19	0.12	0.06	0.11	0.12	0.13
Mn	0.01	0.01	0.01	0.01	-	0.01	0.01	0.01
Mg	0.68	0.72	0.78	0.79	0.96	0.89	0.81	0.83
Ca	0.88	0.90	0.91	0.91	0.91	0.92	0.97	0.97
Na	0.09	0.06	0.05	0.04	0.02	0.02	0.04	0.03
K	-	-	-	-	-	-	-	-
Fe/Fe+Mg	0.30	0.27	0.22	0.23	0.10	0.14	0.18	0.16
Fe3+/ΣFe	0.50	0.20	0.14	0.50	0.45	0.28	0.33	0.19
Na/Na+Ca	0.10	0.06	0.05	0.04	0.02	0.02	0.04	0.03
ROCK F.I.[e]	16.28	29.97	29.97	11.52	11.52	11.52	22.62	22.62
ROCK AGP[f]	0.65	0.60	0.60	0.51	0.51	0.51	0.59	0.59

APPENDIX 2.

Compositions and Structural Formulae of Biotite from the Murdock Creek intrusion.

Superscripts and abbreviations used in the tables are as follows:

The symbol "-" means less than 0.005, rounds to 0.00.

na = not analysed.

[a] FeO/Fe_2O_3 estimated from analyses of biotite in the same rock unit.

[b] Phlogopites according to the biotite-annite-siderophyllite-eastonite classification scheme of Deer et al. (1963).

[c] Rock units containing the analysed biotites as in Appendix 1 notes.

[d] Number of analyses averaged.

[e] H_2O calculated by assuming OH+F+Cl = 4.

[f] Rock F.I. = host-rock normative fractionation index (wt.% Qtz + Ab + Or + Ne + Lc + Ns).

SAMPLE	669U5	638U2	111U3[a]	119U1[a]	13477[a]	134U1[a]	105U3[a]	105U1	108U2	10823[a]
ROCK UNIT[c]	AS	AS	AS	AS	AS	AS	AS	AS	AS	AS
#ANAL.[d]	2	3	2	1	3	1	1	2	3	3
SiO2	38.12	38.39	37.99	38.37	36.27	36.67	37.63	37.34	38.29	39.10
TiO2	2.95	2.65	3.66	2.80	3.50	4.06	2.25	2.03	2.61	2.48
Al2O3	13.25	13.20	13.36	12.76	14.27	14.79	13.65	14.16	12.92	12.84
Cr2O3	-	-	-	-	-	-	-	-	-	-
Fe2O3	4.60	4.84	4.79	5.26	5.23	4.93	6.20	6.20	5.10	5.10
FeO	11.00	11.83	11.30	12.42	12.36	11.62	11.60	11.60	12.10	12.10
MnO	0.47	0.51	0.28	0.47	0.40	0.36	0.42	0.44	0.64	0.44
MgO	13.73	12.77	15.47	14.99	14.18	14.27	14.87	14.39	14.78	15.02
CaO	0.02	-	-	0.03	0.02	0.06	-	-	0.04	0.01
Na2O	0.05	0.05	0.08	0.07	0.06	0.10	0.05	0.09	0.09	0.10
K2O	10.01	10.23	9.38	9.83	9.75	9.62	10.46	10.48	9.27	10.05
H2O[e]	3.92	3.80	3.61	3.42	3.78	3.59	3.62	3.74	3.41	3.75
F	0.25	0.45	0.89	1.23	0.41	0.86	0.76	0.53	1.27	0.56
Cl	0.02	0.01	0.04	0.01	0.07	0.06	0.04	0.01	-	0.04
O=F	0.11	0.19	0.37	0.52	0.17	0.36	0.32	0.22	0.53	0.24
O=Cl	-	-	0.01	-	0.02	0.01	0.01	-	-	0.01
Tot.	98.28	98.55	100.47	101.14	100.12	100.62	101.22	100.79	99.98	101.34
Structural formulae based on 22 oxygens										
Si	5.75	5.80	5.60	5.67	5.43	5.42	5.57	5.55	5.70	5.74
Z=8 AlIV	2.25	2.20	2.32	2.22	2.52	2.58	2.38	2.45	2.27	2.22
Fe3+IV	-	-	0.08	0.11	0.06	-	0.05	-	0.04	0.03
AlVI	0.11	0.16	-	-	-	-	-	0.03	-	-
Ti	0.33	0.30	0.41	0.31	0.39	0.45	0.25	0.23	0.29	0.27
Cr	-	-	-	-	-	-	-	-	-	-
Fe3+	0.52	0.55	0.45	0.47	0.53	0.55	0.64	0.69	0.53	0.53
Fe2+	1.39	1.50	1.39	1.53	1.55	1.44	1.44	1.44	1.51	1.49
Mn	0.06	0.07	0.03	0.06	0.05	0.05	0.05	0.06	0.08	0.05
Mg	3.09	2.88	3.40	3.30	3.16	3.15	3.28	3.19	3.28	3.29
ΣY	5.50	5.45	5.68	5.68	5.68	5.63	5.65	5.63	5.69	5.63
Ca	-	-	-	-	-	0.01	-	-	0.01	-
Na	0.01	0.01	0.02	0.02	0.02	0.03	0.01	0.03	0.03	0.03
K	1.93	1.97	1.76	1.85	1.86	1.82	1.97	1.99	1.76	1.88
ΣX	1.94	1.99	1.79	1.88	1.88	1.85	1.99	2.01	1.79	1.91
F	0.12	0.22	0.41	0.57	0.19	0.40	0.36	0.25	0.60	0.26
Cl	0.01	-	0.01	-	0.02	0.02	0.01	-	-	0.01
Fe/Fe+Mg	0.38	0.42	0.36	0.39	0.40	0.39	0.39	0.40	0.39	0.38
Fe3+/ΣFe	0.27	0.27	0.28	0.28	0.28	0.28	0.32	0.32	0.27	0.27
ROCK F.I.[f]	69.79	68.20	65.72	65.72	62.13	62.13	69.90	69.90	73.00	73.00

SAMPLE	10818[a]	10497[a]	10400[a]	11110[a]	11739[a]	11744[a]	11850[a]	11854[a]	11938[a]	12017[a]
ROCK UNIT[c]	AS	AS	AS	AS	AS	AS	AS	AS	AS	AS
#ANAL.[d]	2	2	2	2	2	2	3	2	2	2
SiO2	38.76	36.67	37.31	37.74	37.31	37.84	37.63	37.78	38.65	38.13
TiO2	2.26	2.85	2.74	3.07	2.94	2.28	2.35	2.87	2.99	1.52
Al2O3	12.56	13.73	13.54	13.06	14.24	14.53	13.53	13.77	13.05	13.93
Cr2O3	-	-	-	-	-	-	-	-	-	-
Fe2O3	5.10	5.79	5.58	4.86	5.57	5.30	5.03	5.03	5.16	5.00
FeO	12.10	13.66	13.16	11.47	13.15	12.49	11.86	11.86	12.19	11.80
MnO	0.50	0.40	0.44	0.34	0.46	0.49	0.58	0.56	0.37	0.43
MgO	14.91	13.65	14.40	15.55	12.80	13.03	13.63	13.80	14.79	15.47
CaO	0.05	0.09	0.03	-	-	0.01	0.03	-	0.04	-
Na2O	0.06	0.17	0.11	0.09	0.09	0.12	0.14	0.05	0.05	0.04
K2O	9.82	9.16	9.34	9.65	10.31	10.10	9.78	10.39	9.41	9.63
H2O[e]	3.44	3.67	3.70	3.63	3.64	3.61	3.76	3.72	3.67	3.53
F	1.16	0.62	0.62	0.79	0.69	0.81	0.51	0.61	0.75	1.02
Cl	0.05	0.05	0.01	0.06	0.04	0.02	0.03	-	0.02	0.04
O=F	0.49	0.26	0.26	0.33	0.29	0.34	0.21	0.26	0.32	0.43
O=Cl	0.01	0.01	-	0.01	0.01	-	0.01	-	-	0.01
Tot.	100.27	100.24	100.72	99.97	100.94	100.29	98.64	100.18	100.82	100.10
Structural formulae based on 22 oxygens										
Si	5.76	5.50	5.55	5.61	5.56	5.64	5.69	5.63	5.69	5.66
Z=8 AlIV	2.20	2.43	2.37	2.29	2.44	2.36	2.31	2.37	2.27	2.34
Fe3+IV	0.04	0.07	0.08	0.10	-	-	-	-	0.04	-
AlVI	-	-	-	-	0.06	0.19	0.10	0.05	-	0.09
Ti	0.25	0.32	0.31	0.34	0.33	0.26	0.27	0.32	0.33	0.17
Cr	-	-	-	-	-	-	-	-	-	-
Fe3+	0.53	0.58	0.55	0.44	0.62	0.59	0.57	0.56	0.53	0.56
Fe2+	1.50	1.71	1.64	1.43	1.64	1.56	1.50	1.48	1.50	1.46
Mn	0.06	0.05	0.06	0.04	0.06	0.06	0.07	0.07	0.05	0.05
Mg	3.30	3.05	3.19	3.45	2.84	2.89	3.07	3.07	3.25	3.42
ΣY	5.65	5.72	5.74	5.70	5.56	5.55	5.58	5.56	5.66	5.76
Ca	0.01	0.01	-	-	-	-	-	-	0.01	-
Na	0.02	0.05	0.03	0.03	0.03	0.03	0.04	0.01	0.01	0.01
K	1.86	1.75	1.77	1.83	1.96	1.92	1.89	1.98	1.77	1.82
ΣX	1.89	1.82	1.81	1.86	1.99	1.96	1.93	1.99	1.79	1.83
F	0.55	0.29	0.29	0.37	0.33	0.38	0.24	0.29	0.35	0.48
Cl	0.01	0.01	-	0.01	0.01	0.01	0.01	-	-	0.01
Fe/Fe+Mg	0.39	0.44	0.41	0.36	0.44	0.43	0.40	0.40	0.39	0.37
Fe3+/ΣFe	0.27	0.28	0.28	0.28	0.28	0.28	0.28	0.28	0.28	0.28
ROCK F.I.[f]	73.00	63.93	63.93	65.72	70.69	70.69	69.96	69.96	65.72	73.03

	SAMPLE	13167	13169[a]	13378[a]	133U2[a]	29553[a]	29555[a]	13266[a]	129U1	13263[a]	130U3[a]
	ROCK UNIT[c]	MS	MS	MS	MS	MM	MM	MD	MD	MD	CP
	#ANAL.[d]	2	2	3	1	3	3	2	3	2	2
	SiO2	37.99	37.62	36.58	36.69	36.92	37.04	36.79	36.55	37.15	36.30
	TiO2	3.08	2.88	3.87	3.57	3.57	2.78	3.12	3.95	2.84	4.14
	Al2O3	14.39	14.54	14.26	14.45	13.54	13.42	14.53	15.35	14.89	15.04
	Cr2O3	-	-	-	-	0.07	0.03	-	-	-	-
	Fe2O3	5.90	5.90	6.20	6.17	6.42	6.32	5.68	4.10	5.66	5.60
	FeO	10.00	10.00	11.73	11.70	12.16	11.97	10.76	11.10	10.73	10.60
	MnO	0.34	0.32	0.32	0.37	0.27	0.29	0.22	0.30	0.31	0.06
	MgO	13.44	13.15	13.69	14.07	13.62	14.23	13.90	13.81	13.36	16.81
	CaO	0.03	-	-	-	-	0.03	-	-	0.06	-
	Na2O	0.09	0.09	0.05	0.07	0.16	0.15	0.12	0.29	0.10	0.40
	K2O	9.87	10.36	9.69	9.50	9.65	9.59	9.90	9.59	9.85	8.93
	H2O[e]	3.74	3.78	3.75	3.79	4.00	4.00	3.85	3.90	3.85	3.91
	F	0.57	0.45	0.51	0.44	na	na	0.35	0.30	0.35	0.31
	Cl	0.15	0.15	0.04	0.04	na	na	0.05	0.01	0.08	0.01
	O=F	0.24	0.19	0.21	0.19	-	-	0.15	0.13	0.15	0.13
	O=Cl	0.03	0.03	0.01	0.01	-	-	0.01	-	0.02	-
	Tot.	99.32	99.02	100.47	100.66	100.38	99.85	99.11	99.12	99.06	101.97
	Structural formulae based on 22 oxygens										
	Si	5.65	5.64	5.44	5.44	5.51	5.55	5.52	5.46	5.56	5.26
Z=8	AlIV	2.35	2.36	2.50	2.52	2.38	2.37	2.48	2.54	2.44	2.57
	Fe3+IV	-	-	0.06	0.04	0.11	0.09	-		-	0.17
	AlVI	0.18	0.20	-	-	-	-	0.08	0.16	0.19	-
	Ti	0.34	0.32	0.43	0.40	0.40	0.31	0.35	0.44	0.32	0.45
	Cr	-	-	-	-	0.01	-	-	-	-	-
	Fe3+	0.66	0.67	0.63	0.65	0.61	0.63	0.64	0.46	0.64	0.44
	Fe2+	1.24	1.25	1.46	1.45	1.52	1.50	1.35	1.39	1.34	1.28
	Mn	0.04	0.04	0.04	0.05	0.03	0.04	0.03	0.04	0.04	0.01
	Mg	2.98	2.94	3.04	3.11	3.03	3.18	3.11	3.07	2.98	3.63
	ΣY	5.45	5.42	5.60	5.65	5.60	5.66	5.56	5.56	5.52	5.82
	Ca	-	-	-	-	-	-	-	-	0.01	-
	Na	0.03	0.03	0.01	0.02	0.05	0.04	0.03	0.08	0.03	0.11
	K	1.87	1.98	1.84	1.80	1.84	1.83	1.89	1.83	1.88	1.65
	ΣX	1.90	2.01	1.85	1.82	1.88	1.88	1.93	1.91	1.92	1.76
	F	0.27	0.21	0.24	0.21	na	na	0.17	0.14	0.17	0.14
	Cl	0.04	0.04	0.01	0.01	na	na	0.01	-	0.02	-
	Fe/Fe+Mg	0.39	0.40	0.41	0.41	0.42	0.41	0.39	0.38	0.40	0.34
	Fe3+/ΣFe	0.35	0.35	0.32	0.32	0.32	0.32	0.32	0.25	0.32	0.32
	ROCK F.I.[f]	56.54	56.54	52.71	52.71	52.71	52.71	35.37	21.54	35.37	11.52

	SAMPLE	11514[a]	13527[a]	13596[a]	11506	32923[ab]	32945[b]
	ROCK UNIT[c]	CP	CP	CP	CP	HB	HB
	#ANAL.[d]	1	2	3	2	3	3
	SiO2	37.56	35.03	35.75	38.33	38.00	38.24
	TiO2	2.83	2.99	3.10	2.38	1.85	2.12
	Al2O3	14.11	15.03	15.19	14.60	14.34	14.52
	Cr2O3	-	-	-	-	0.26	0.29
	Fe2O3	6.00	7.70	7.70	6.00	4.85	4.80
	FeO	11.60	12.80	12.80	11.60	9.36	9.27
	MnO	0.13	0.31	0.26	0.14	0.12	0.09
	MgO	16.02	13.58	13.98	15.66	16.56	16.21
	CaO	0.02	0.01	-	-	-	-
	Na2O	0.13	0.19	0.20	0.12	0.09	0.17
	K2O	9.91	9.40	9.29	9.06	10.02	10.21
	H2O[e]	3.85	3.91	3.87	3.87	4.08	4.08
	F	0.31	0.10	0.21	0.32	na	na
	Cl	0.09	0.04	0.05	0.12	na	na
	O=F	0.13	0.04	0.09	0.13	-	-
	O=Cl	0.02	0.01	0.01	0.03	-	-
	Tot.	101.41	101.04	101.30	101.88	99.53	100.00
	Structural formulae based on 22 oxygens						
	Si	5.46	5.23	5.26	5.55	5.61	5.62
Z=8	AlIV	2.42	2.65	2.63	2.45	2.39	2.38
	Fe3+IV	0.12	0.12	0.11	-	-	-
	AlVI	-	-	-	0.04	0.11	0.13
	Ti	0.31	0.34	0.34	0.26	0.21	0.23
	Cr	-	-	-	-	0.03	0.03
	Fe3+	0.54	0.75	0.74	0.65	0.54	0.53
	Fe2+	1.41	1.60	1.57	1.41	1.16	1.14
	Mn	0.02	0.04	0.03	0.02	0.02	0.01
	Mg	3.47	3.03	3.06	3.38	3.64	3.55
	ΣY	5.75	5.75	5.76	5.76	5.70	5.63
	Ca	-	-	-	-	-	-
	Na	0.04	0.06	0.06	0.03	0.03	0.05
	K	1.84	1.79	1.74	1.67	1.89	1.91
	ΣX	1.88	1.85	1.80	1.71	1.91	1.96
	F	0.14	0.05	0.10	0.15	na	na
	Cl	0.02	0.01	0.01	0.03	na	na
	Fe/Fe+Mg	0.37	0.45	0.44	0.38	0.32	0.32
	Fe3+/ΣFe	0.32	0.35	0.35	0.32	0.32	0.32
	ROCK F.I.[f]	29.97	16.28	16.28	29.97	22.62	22.62

APPENDIX 3.

Compositions and Structural Formulae of Amphibole from the Murdock Creek intrusion.

Superscripts and abbreviations used in the tables are as follows:

The symbol "-" means less than 0.005, rounds to 0.000.

na = not analysed.

[a] FeO/Fe_2O_3 estimated from analyses of amphiboles in the same rock unit.

[b] Fe^{3+} contents were calculated on the basis of 23 oxygens and then adjustment of the total cations, excluding (Ca+Na+K), to 13 by varying $Fe^{3+}/(Fe^{2+}+Fe^{3+})$.

[c] Rock units containing the analysed amphiboles as in Appendix 1 notes.

[d] Amphibole classification according to the criteria of Leake (1978): 1, magnesian hastingsite; 2, actinolite; 3, pargasitic hornblende; 4, magnesian hastingsitic hornblende; 5, magnesio-riebeckite; 6, tremolite; 7, magnesio-hastingsitic hornblende; 8, edenitic hornblende.

[e] Number of analyses averaged.

[f] H_2O calculated by assuming OH+F+Cl = 2.

[g] Rock F.I. = host-rock normative fractionation index (wt.% Qtz + Ab + Or + Ne + Lc + Ns).

SAMPLE	63028[a]	63815[a]	63816[a]	64037[a]	66001	66811[a]	66814[a]	10529[a]	10861[a]	10856[a]
ROCK UNIT[c]	AS	AS	AS	AS	AS	AS	AS	AS	AS	AS
AMPH. TYPE[d]	1	1	1	1	1	1	1	2	2	2
#ANAL.[e]	2	1	1	2	1	1	1	1	2	1
SiO2	39.26	38.72	38.90	38.96	40.13	39.61	39.29	55.93	55.28	56.30
TiO2	1.67	2.01	1.89	1.66	2.63	2.45	2.27	0.08	0.08	0.09
Al2O3	10.75	10.81	10.95	10.51	11.07	11.11	10.96	0.55	0.45	0.26
Cr2O3	0.05	-	-	0.02	0.02	-	-	-	-	-
Fe2O3	6.72	6.34	6.53	6.56	5.27	5.52	6.31	5.17	5.40	3.40
FeO	13.92	13.13	13.51	13.58	10.92	11.42	13.05	6.48	6.76	5.01
MnO	0.41	0.38	0.50	0.49	0.42	0.43	0.54	0.50	0.67	0.72
MgO	9.13	9.28	9.21	9.18	11.05	10.65	9.20	17.26	16.39	18.44
CaO	10.19	10.04	9.88	10.13	10.99	10.45	9.82	10.41	10.58	11.51
Na2O	3.58	3.23	3.21	3.86	3.49	3.29	3.42	1.41	1.14	0.62
K2O	1.76	1.86	1.89	1.73	1.65	1.76	1.82	0.18	0.17	0.13
H2O[f]	1.74	1.63	1.61	1.71	1.64	1.73	1.86	2.05	1.98	1.83
F	0.41	0.59	0.65	0.44	0.71	0.47	0.16	0.16	0.17	0.58
Cl	0.03	0.02	0.03	0.02	0.02	0.03	0.02	-	0.15	0.05
O=F	0.17	0.25	0.27	0.19	0.30	0.20	0.07	0.07	0.07	0.24
O=Cl	0.01	-	0.01	-	-	0.01	-	-	0.03	0.01
Tot.	99.44	97.79	98.48	98.66	99.77	98.71	98.64	100.11	99.11	98.68
Structural formulae based on 23 oxygens										
SiIV	6.07	6.06	6.06	6.07	6.08	6.07	6.08	7.89	7.91	7.98
T=8 AlIV	1.93	1.94	1.94	1.93	1.92	1.93	1.92	0.09	0.08	0.02
Fe3+IV	-	-	-	-	-	-	-	0.02	0.01	-
AlVI	0.03	0.05	0.07	-	0.05	0.08	0.08	-	-	0.02
Fe3+	0.78	0.75	0.77	0.77	0.60	0.64	0.74	0.53	0.57	0.36
Ti	0.19	0.24	0.22	0.20	0.30	0.28	0.26	0.01	0.01	0.01
Cr	0.01	-	-	-	-	-	-	-	-	-
Mg	2.10	2.17	2.14	2.13	2.49	2.43	2.12	3.63	3.50	3.89
Fe2+	1.80	1.72	1.76	1.77	1.38	1.46	1.69	0.77	0.81	0.59
Mn	0.05	0.05	0.05	0.07	0.05	0.06	0.07	0.06	0.08	0.09
ΣC	4.97	4.98	5.00	4.94	4.88	4.95	4.96	5.00	4.97	4.96
Mn	-	-	0.01	-	-	-	-	-	-	-
Ca	1.69	1.68	1.65	1.69	1.78	1.72	1.63	1.57	1.62	1.75
Na	0.31	0.32	0.34	0.31	0.22	0.28	0.37	0.39	0.32	0.17
ΣB	2.00	2.00	2.00	2.00	2.00	2.00	2.00	1.96	1.94	1.92
Na	0.76	0.66	0.63	0.86	0.81	0.69	0.66	-	-	-
K	0.35	0.37	0.38	0.34	0.32	0.34	0.36	0.03	0.03	0.02
ΣA	1.11	1.03	1.01	1.20	1.13	1.03	1.02	0.03	0.03	0.02
F	0.20	0.29	0.32	0.22	0.34	0.23	0.08	0.07	0.08	0.26
Cl	0.01	0.01	0.01	0.01	0.01	0.01	0.01	-	0.04	0.01
Fe/Fe+Mg	0.55	0.53	0.54	0.54	0.44	0.46	0.53	0.27	0.28	0.20
Fe3+/ΣFe	0.30	0.30	0.30	0.30	0.30	0.30	0.30	0.42	0.42	0.38
ROCK F.I.[g]	68.20	68.20	68.20	70.13	69.79	69.79	69.79	69.90	73.00	73.00

SAMPLE	11447[a]	11443	11446[a]	10696[b]	10600[b]	10692[b]	11747	29533[a]	12952	13054[a]
ROCK UNIT[c]	AS	AS	AS	AS	AS	AS	AS	MM	MD	CP
AMPH. TYPE[d]	2	2	2	5	5	5	2	1	2	3
#ANAL.[e]	2	2	1	1	2	1	2	3	1	1
SiO2	52.32	52.79	53.15	55.49	55.46	55.78	56.23	41.85	56.82	42.12
TiO2	0.61	0.49	0.62	0.06	0.10	0.06	0.09	1.57	0.04	2.34
Al2O3	2.39	2.56	2.40	0.52	0.63	0.46	0.56	10.64	0.99	11.88
Cr2O3	-	-	-	-	-	-	-	0.02	-	-
Fe2O3	6.20	6.20	6.20	14.99	13.96	15.26	4.70	5.20	3.10	3.10
FeO	7.90	7.90	7.90	9.26	10.12	9.95	5.90	12.33	7.40	7.30
MnO	0.54	0.48	0.56	0.36	0.24	0.33	0.53	0.34	0.25	0.25
MgO	15.61	15.69	15.76	10.00	9.85	9.53	16.99	11.61	18.06	12.93
CaO	9.21	9.31	9.12	1.40	1.90	1.22	11.35	11.76	12.59	11.62
Na2O	3.02	2.62	2.48	6.68	6.24	6.75	0.91	2.49	0.31	2.28
K2O	0.66	0.70	0.71	0.11	0.14	0.06	0.14	1.26	0.06	1.49
H2O[f]	1.61	1.63	1.75	1.93	2.05	2.09	1.92	1.89	2.07	1.81
F	1.01	0.99	0.74	0.31	0.06	-	0.42	0.22	0.19	0.37
Cl	0.01	0.02	0.02	0.02	-	-	0.02	0.07	0.03	0.06
O=F	0.43	0.42	0.31	0.13	0.03	-	0.18	0.09	0.08	0.16
O=Cl	-	-	-	-	-	-	-	0.02	0.01	0.01
Tot.	100.66	100.96	101.10	101.00	100.72	101.50	99.58	101.14	101.82	97.38
Structural formulae based on 23 oxygens										
SiIV	7.51	7.53	7.56	7.98	8.00	8.00	7.95	6.23	7.87	6.31
T=8 AlIV	0.40	0.43	0.40	0.02	-	-	0.05	1.77	0.13	1.69
Fe3+IV	0.09	0.04	0.04	-	-	-	-	-	-	-
AlVI	-	-	-	0.07	0.11	0.08	0.04	0.10	0.03	0.41
Fe3+	0.58	0.63	0.63	1.62	1.52	1.65	0.50	0.58	0.32	0.35
Ti	0.07	0.05	0.07	0.01	0.01	0.01	0.01	0.18	-	0.26
Cr	-	-	-	-	-	-	-	-	-	-
Mg	3.34	3.34	3.34	2.14	2.12	2.04	3.58	2.58	3.73	2.89
Fe2+	0.95	0.94	0.94	1.11	1.22	1.19	0.70	1.54	0.86	0.91
Mn	0.07	0.04	0.02	0.04	0.03	0.04	0.06	0.03	0.03	0.03
ΣC	5.00	5.00	5.00	4.99	5.00	5.00	4.89	5.00	4.97	4.85
Mn	-	0.02	0.04	-	-	-	-	0.01	-	-
Ca	1.42	1.42	1.39	0.22	0.29	0.19	1.72	1.88	1.87	1.87
Na	0.58	0.56	0.57	1.78	1.71	1.81	0.25	0.11	0.08	0.13
ΣB	2.00	2.00	2.00	2.00	2.00	2.00	1.97	2.00	1.95	2.00
Na	0.26	0.17	0.12	0.08	0.04	0.07	-	0.61	-	0.53
K	0.12	0.13	0.13	0.02	0.03	0.01	0.03	0.24	0.01	0.28
ΣA	0.38	0.30	0.25	0.10	0.06	0.08	0.03	0.85	0.01	0.81
F	0.46	0.45	0.33	0.14	0.03	-	0.19	0.10	0.08	0.18
Cl	-	-	-	-	-	-	-	0.02	0.01	0.02
Fe/Fe+Mg	0.33	0.33	0.32	0.56	0.56	0.58	0.25	0.45	0.24	0.30
Fe3+/ΣFe	0.41	0.41	0.41	0.59	0.55	0.58	0.42	0.28	0.27	0.28
ROCK F.I.[g]	na	na	na	na	na	na	70.69	34.35	21.54	11.52

SAMPLE	13037	13524	13582[a]	13590[a]	65B48	11511[a]	115008[a]	115009[a]	11510[a]	11598
ROCK UNIT[c]	CP	CP	CP	CP	CP	CP	CP	CP	CP	CP
AMPH.TYPE[d]	3	1	1	1	2	1	7	4	1	4
#ANAL.[e]	1	1	2	2	3	1	2	1	2	2
SiO2	43.89	40.03	39.78	40.30	56.40	41.01	43.03	42.82	41.61	42.98
TiO2	2.02	2.31	2.29	2.16	-	1.86	1.41	1.57	1.66	1.53
Al2O3	10.94	12.06	12.01	12.09	0.36	11.56	10.34	10.30	11.16	10.83
Cr2O3	-	-	-	-	-	-	-	-	-	-
Fe2O3	3.10	5.26	5.31	5.37	2.78	4.81	4.40	4.69	4.84	4.69
FeO	7.30	12.35	12.47	12.61	7.76	10.49	9.59	10.22	10.57	10.22
MnO	0.20	0.33	0.33	0.30	0.50	0.26	0.25	0.24	0.27	0.20
MgO	13.47	10.65	10.62	10.60	17.41	12.21	13.42	13.02	12.04	12.49
CaO	11.64	11.46	11.29	11.42	11.28	11.42	11.50	11.64	11.59	11.52
Na2O	2.08	2.75	2.76	2.74	0.75	2.40	2.69	2.62	2.43	2.51
K2O	1.21	1.77	1.70	1.64	0.08	1.32	1.04	1.18	1.25	1.15
H2O[f]	1.86	1.92	1.81	1.86	2.10	1.97	1.94	1.91	1.70	1.94
F	0.33	0.11	0.34	0.26	-	-	0.14	0.21	0.57	0.14
Cl	0.02	0.11	0.09	0.09	0.07	0.10	0.07	0.08	0.12	0.09
O=F	0.14	0.05	0.14	0.11	-	-	0.06	0.09	0.24	0.06
O=Cl	-	0.02	0.02	0.02	0.02	0.02	0.02	0.02	0.03	0.02
Tot.	97.92	101.04	100.63	101.31	99.47	99.39	99.75	100.39	99.54	100.21
Structural formulae based on 23 oxygens										
SiIV	6.50	6.00	5.99	6.03	7.99	6.15	6.37	6.34	6.23	6.36
T=8 AlIV	1.50	2.00	2.01	1.97	0.01	1.85	1.63	1.66	1.77	1.64
Fe3+IV	-	-	-	-	-	-	-	-	-	-
AlVI	0.41	0.14	0.13	0.16	0.05	0.20	0.18	0.13	0.21	0.24
Fe3+	0.35	0.59	0.60	0.60	0.30	0.54	0.49	0.52	0.55	0.52
Ti	0.23	0.26	0.26	0.24	-	0.21	0.16	0.17	0.19	0.17
Cr	-	-	-	-	-	-	-	-	-	-
Mg	2.97	2.38	2.39	2.36	3.68	2.73	2.96	2.87	2.69	2.75
Fe2+	0.90	1.55	1.57	1.58	0.92	1.32	1.19	1.26	1.32	1.26
Mn	0.03	0.04	0.04	0.04	0.05	-	0.02	0.03	0.03	0.03
ΣC	4.89	4.96	4.99	4.98	5.00	5.00	5.00	4.98	4.99	4.98
Mn	-	-	-	-	0.01	0.03	0.01	-	-	-
Ca	1.85	1.84	1.82	1.83	1.71	1.84	1.83	1.85	1.86	1.83
Na	0.15	0.16	0.18	0.17	0.21	0.13	0.16	0.15	0.14	0.17
ΣB	2.00	2.00	2.00	2.00	1.93	2.00	2.00	2.00	2.00	2.00
Na	0.44	0.64	0.63	0.62	-	0.57	0.61	0.60	0.57	0.54
K	0.23	0.34	0.33	0.31	0.01	0.25	0.20	0.22	0.24	0.22
ΣA	0.67	0.98	0.96	0.93	0.01	0.82	0.81	0.82	0.81	0.76
F	0.16	0.05	0.16	0.12	-	-	0.07	0.10	0.27	0.07
Cl	0.01	0.03	0.02	0.02	0.02	0.03	0.02	0.02	0.03	0.02
Fe/Fe+Mg	0.30	0.47	0.48	0.48	0.25	0.41	0.36	0.38	0.41	0.39
Fe3+/ΣFe	0.28	0.28	0.28	0.28	0.24	0.29	0.29	0.29	0.29	0.29
ROCK F.I.[g]	11.52	16.28	16.28	16.28	23.50	29.97	29.97	29.97	29.97	29.97

SAMPLE	11509[b]	32939[b]	32940[b]
ROCK UNIT[c]	CP	HB	HB
AMPH.TYPE[d]	6	8	7
#ANAL.[e]	1	2	2
SiO2	57.92	46.33	45.13
TiO2	0.09	0.80	0.89
Al2O3	0.80	8.91	9.34
Cr2O3	-	0.21	0.19
Fe2O3	3.91	4.68	7.22
FeO	1.85	7.25	5.07
MnO	0.23	0.20	0.26
MgO	21.32	15.55	15.76
CaO	11.85	12.02	11.56
Na2O	0.70	2.26	2.56
K2O	0.12	0.84	0.85
H2O[f]	2.12	2.00	1.94
F	0.17	0.17	0.30
Cl	-	0.01	0.01
O=F	0.07	0.07	0.13
O=Cl	-	-	-
Tot.	101.01	101.16	100.95
Structural formulae based on 23 oxygens			
SiIV	7.89	6.65	6.49
T=8 AlIV	0.11	1.35	1.51
Fe3+IV	-	-	-
AlVI	0.02	0.16	0.08
Fe3+	0.40	0.51	0.78
Ti	0.01	0.09	0.10
Cr	-	0.02	0.02
Mg	4.33	3.33	3.38
Fe2+	0.21	0.87	0.61
Mn	0.03	0.02	0.03
ΣC	5.00	5.00	5.00
Mn	-	-	-
Ca	1.73	1.85	1.78
Na	0.19	0.15	0.22
ΣB	1.92	2.00	2.00
Na	-	0.48	0.50
K	0.02	0.15	0.16
ΣA	0.02	0.63	0.66
F	0.07	0.08	0.14
Cl	-	-	-
Fe/Fe+Mg	0.12	0.29	0.29
Fe3+/ΣFe	0.66	0.37	0.56
ROCK F.I.[g]	29.97	22.62	22.62